UNIVERSITÀ DEGLI STUDI DI PALERMO
FACOLTA' DI AGRARIA
DIPARTIMENTO DI SCIENZE AGRARIE E FORESTALI

Dottorato di ricerca in
"Tecnologie per la Sostenibilità ed il Risanamento Ambientale"
Ciclo XXIV
Triennio 2011-2013
SSD: AGR/13 – Chimica Agraria

CHARACTERIZATION OF CHEMICAL AND PHYSICAL PROPERTIES OF BIOCHAR FOR ENERGY PURPOSES AND ENVIRONMENTAL RESTORATION

TESI DI
Giulia Cimò

TUTOR
Prof. Pellegrino Conte

CO-TUTOR
Prof. Giuseppe Alonzo

COORDINATORE DEL DOTTORATO
Prof. Sebastiano Calvo

DOTTORATO

ACKNOWLEDGEMENTS

Without the support and the help received from several persons, this project would not have been possible.

I would like to express my gratitude to my supervisor **Prof. Pellegrino Conte** for providing me guidance, knowledge, support and time.

A special thanks to **Prof. Giuseppe Alonzo** for the opportunity he gave me to do this project and the financial support over the last years.

I am particularly indebted to **Prof. Gabriele E. Schaumann** and **Prof. Jiri Kucerik,** Department of Environmental and Soil Chemistry, University of Koblenz-Landau, for welcoming me into their working group, for the fruitful discussions, their kindness, support, and help during the project.

I would like to thank **Dr. Claudio De Pasquale, Prof. Eristanna Palazzolo, Dr. V. Armando Laudicina** and **Dr. Michele Panno** for their technical support and assistance in project trials, analyses and results interpretation.

Thanks to **Dr. Anne E. Berns,** Institute of Bio- and Geosciences, Jülich, for the helpfulness and analyses she did.

A special thanks to **Valentina, Zdenek** e **Farid,** both friends and co-workers, for their help, availability, affection and friendship, without whom I would not have succeeded.

I would like to thank all my colleagues, assistants and friends, from Palermo and Landau, for the help and all the nice moments we spent together, **Anna, Gabriella, Ewa, Anthi, Denis, Allan, Lucio, Melina, Vincenzo, Loredana, Rita, Filippo** and so on.

Finally, all my love and gratitude to my parents, **Gaetano e Virginia** and my brother **Giuseppe** for giving me their strength, encouragement and support, and to my boyfriend **Oscar** who helps me to face, with strength and confidence, all the obstacles that everyday life presents us.

I count myself lucky to have met all of you.

TABLE OF CONTENTS

LIST OF FIGURES

CHAPTER 4 : EFFECT OF PYROLYSIS CONDITIONS ON THE SURFACE PROPERTIES OF CHARS FROM POULTRY MANURE

CHAPTER 5 : EVALUATION OF INORGANIC CONTAMINANT REMOVAL FROM AQUEOUS SOLUTIONS USING BIOCHAR FROM CHICKEN MANURE, CONIFER AND POPLAR WOOD AS ADSORBENT

LIST OF TABLES

CHAPTER 1 : INTRODUCTION

Climate change is one of the most important challenges the modern world is facing (Lehmann et al., 2006). It is now commonly accepted that the increase in the greenhouse gases concentration (mainly carbon dioxide, methane and various nitrous oxides) in the atmosphere affects Earth's climate system (Lehmann et al., 2006). One of the main reasons for this concentration is the use of fossil fuels, a practice that can only be reduced through international efforts. In recent decades, the industrialized countries lifestyle has significantly changed the scenario and the energy prospects worldwide (Hubacek et al., 2007). Indeed, the increasing energy demand, coupled with the high cost of conventional fuels, the uncertainty of their supply and the problems related to global warming, stresses the importance of this resource that may no longer be undervalued and regarded as something for granted (Strategia Energetica Nazionale, 2012).

At present, interest in the search for alternative and renewable energy sources has increased dramatically (Zhang et al., 2010). These can in fact complement and partly replace fossil fuels, allowing both the diversification of energy supply and the reduction of greenhouse gases emissions. In the perspective of climate mitigation strategies, a possible and viable alternative to fossil fuels is the use of bioenergy alternatives.

Bioenergy is a renewable and clean energy source derived from biomasses (Zhang et al., 2010). Different kinds of waste materials (such as food residuals, agricultural crops, animal and municipal solid wastes) have the potential to be converted into energy and bio-products, which can be applied for power generation, transportation, as well as the production of biomaterials. For example, biomasses can be easily processed into higher-value fuels, such as methanol (C_2H_5OH) and hydrogen (H_2) (Zhang et al., 2010).

The modern industrial systems for the production of bioenergy include thermo-chemical processes, such as pyrolysis and gasification (Bridgewater, 2001). These practices involve the heating of various types of biomass (feedstock), under controlled conditions, to produce synthesis gas (or syngas) and oil (or bio-oils), commonly used as fuel. Both products can be burned to produce heat, power or a combination of the two. The third combustible produced by pyrolysis is a carbon-rich solid residue referred to as biochar, char or charcoal. This material is a highly porous fine grained substance, really similar in appearance to the coal produced by natural burning.

First considered as an industrial waste, in recent years, the interest in this material has grown enormously due to its ability to improve physical, chemical, biological and mechanical properties of soils, when used as a soil amendment (Glaser et al., 2002; Lehmann et al., 2003; Day et al., 2005; Liang et al., 2006; Polmehier et al., 2009; Sohi et al., 2010; Uchimiya et al., 2010; Yuan et al., 2011). Its application to soils (still banned in Italy) is practiced to achieve two main objectives: increase soil fertility and contribute to climate change mitigation through carbon sequestration in soils (Ogawa et al., 2006; Laird, 2008; Matthews, 2008; Lehmann et al., 2009).

Recently, char has also been used (unmodified or further activated) for remediation purposes due to its adsorption properties (Franz et al., 2000; Machida et al., 2006; Uchimiya et al., 2011). Biochar can be applied in wastewaters treatment for the removal of heavy metals or other chemicals released from industrial activities (Liu and Zhang, 2009), but also directly on soils to uptake organic and inorganic contaminants, thereby sequestering and rendering them unavailable for plants (Beesley et al., 2010; Namgay et al., 2010; Uchimiya et al., 2010; 2011; Fellet et al., 2011; Karami et al., 2011).

The properties and the effects of biochars widely vary since they are produced by various processes (i.e., gasification, pyrolysis) and from any kind of natural or synthetic organic material (de Jong et al., 2003; Shinogi et

al., 2003; Yaman, 2004; Erlich et al., 2006; Mohan et al., 2011). Both the chemical composition and the physical structure of biochar are influenced by feedstock nature (Fushimi et al., 2003; Demirbas, 2004; Vassilev et al., 2010), the technique used for its production (Antal and Gronli, 2003; Erlich et al., 2006; Basu, 2010), and process conditions (e.g., charring temperature and residence time) (Czimczik et al., 2002; Gundale and DeLuca, 2006; Brown, 2009). Since these properties greatly influence biochar effects and its interactions with the environment, we can infer that understanding char chemical and physical properties is crucial in order to address it to correct agronomical and environmental uses and allow meaningful pre-application quality assessments.

1.1 Motivation and objectives of the study

Biochar production processes as well as its various applications provide numerous benefits to both environment and economy (Lehmann et al., 2006; Basu, 2010). However, understanding the physicochemical structure of this valuable product has to be improved in order to be able to obtain the aforementioned benefits and to avoid environmental costs.

In this study, chicken or poultry manure (PM) was chosen as feedstock for biochar preparation. This biomass is traditionally used by farmers as an effective organic fertilizer (Chan et al., 2008). Indeed, it is considered a valuable source for readily available plant nutrients, such as N, P, K and other micronutrients (Huang et al., 2011). Notwithstanding the advantages of PM for increasing soil fertility, there are food safety and environmental concerns about its application in agricultural sites in its unmodified form (Wilkinson et al., 2003; Chan et al., 2008). In fact, the misuse of chicken manure as fertilizer may result in serious environmental problems (Gay et al., 2003), such as human and animal health risks, odors, and leaching of nitrates

and other pollutants into groundwater (Fan et al., 2000). For this reason, conversion of chicken manure to char has been proposed as an attractive methodology to reduce PM volume and weight, and its stink (Shinogi and Kanri, 2003; Popov et al., 2004). Some studies have already examined PM biochar characteristics (Uchimiya et al., 2010). Further studies must be performed to evaluate the possibility to use poultry manure chars either as soil amendments or for remediation purposes in order to avoid environmental damages. As already stressed, char characteristics and properties are greatly affected by pyrolysis process and its parameters (mainly process temperature and residence time). These factors are particularly important in determining the nature of the final product and, consequently, its potential value in terms of carbon sequestration, agronomic performance and/or environmental remediation.

The project has two main objectives. Firstly, it aims to report about the changes occurring in the chemical properties and in the physical structure of biochars produced from poultry manure when it is obtained at different pyrolysis temperatures and heating times, and how these changes can influence its agronomic or remediation potential. This topic is discussed in Chapters 3 and 4.

The second objective of the project is to investigate the potential of three different kinds of biochars, produced from poultry manure, conifer and poplar wood residues, as adsorbents for inorganic contaminants (i.e., heavy metals) for wastewater treatment. In chapter 5, biochar adsorption qualities are evaluated using kinetic (pseudo-first order, pseudo-second-order), equilibrium and isotherms (Langmuir, Freundlich, Toth and Redlich-Peterson) models, used to fit experimental data.

References

Antal MJ, Grønli M (2003) The Art, Science, and Technology of Charcoal Production. Ind Eng Chem Res 42(8):1619-1640

Basu P (2010) Biomass gasification and pyrolysis: practical design and theory. Elsevier. 365 pp

Beesley L, Moreno-Jimenez E, Gomez-Eyles JL (2010) Effects of biochar and green waste compost amendments on mobility, bioavailability and toxicity of inorganic and organic contaminants in a multi-element polluted soil. Environ Pollut 158:2282–2287

Bridgewater AV (2001) Thermal conversion of biomass and waste: the status. Birmingham (UK): Bio-Energy Research Group, Aston University

Brown R (2009) Biochar Production Technology. In: Lehmann J, Joseph S (eds) Biochar for Environmental Management: Science and Technology. Earthscan, London

Chan KY, Van Zwieten L, Meszaros I, Downie A, Joseph S (2008) Using poultry litter biochars as soil amendments. Aust J Soil Res 46:437-444.

Czimczik CI, Preston CM, Schmidt MWI, Werner RA, Schulze ED (2002) Effect of charring on mass, organic carbon, and stable carbon isotope composition of wood. Org Geochem 33:1207–1223

Day D, Evans RJ, Lee JW, Reicosky D (2005) Economical CO_2, SO_x, and NO_x capture from fossil-fuel utilization with combined renewable hydrogen production and large-scale carbon sequestration. Energy 30:2558-2579

Demirbas A (2004) Effects of temperature and particle size on bio-char yield from pyrolysis of agricultural residues. J Anal Appl Pyrol 72(2):243-248

de Jong W, Pirone A, Wòjtowicz MA (2003) Pyrolysis of Miscanthus giganteus and wood pellets: TG-FTIR analysis and reaction kinetics. Fuel 82:1139-1147

Erlich C, Björnbom E, Bolado D, Giner M, Fransson TH (2006) Pyrolysis and gasification of pellets from sugar cane bagasse and wood. Fuel 85(10-11):1535-1540

Fan ZJ, Ai YW, Li JM, Li GW (2000) Discussion of controlling N loss from volatilization in animal manure. J Sichuan Normal Univ 23(5):548–550

Fellet G, Marchiol L, Delle Vedove G, Peressotti A (2011) Application of biochar on mine tailings: effects and perspectives for land reclamation. Chemosphere 83:1262-1297

Franz M, Arafat HA, Pinto NG (2000) Effect of chemical surface heterogeneity on the adsorption mechanism of dissolved aromatics on activated carbon. Carbon 38:1807–1819

Fushimi C, Araki K, Yamaguchi Y, Tsutsumi A (2003) Effect of Heating Rate on Steam Gasification of Biomass. 2. Thermogravimetric-Mass Spectrometric (TG-MS) Analysis of Gas Evolution. Ind Eng Chem Res 42:3929-3936

Gay SW, Schmidt DR, Clanton CJ, Janni KA, Jacobson LD, Weisberg S (2003) Odor, total reduced sulfur and ammonia emissions from animal housing facilities and manure storage units in Minnesota. Appl Eng Agric 19(3):347–360

Gundale MJ, DeLuca TH (2006) Temperature and source material influence ecological attributes of Ponderosa pine and Douglas-fir charcoal. For Ecol Manag 231:86–93

Huang G, Wang X, Han L (2011) Rapid estimation of nutrients in chicken manure during plant-field composting using physicochemical properties. Bioresource Technol 102:1455–1461

Hubacek K, Guan D, Barua A (2007) Changing lifestyles and consumption patterns in developing countries: A scenario analysis for China and India, Futures 39(9):1084-1096

Karami N, Clemente R, Moreno-Jiménez E, Lepp NW, Beesley L (2011) Efficiency of green waste compost and biochar soil amendments for reducing lead and copper mobility and uptake to ryegrass. J Hazard Mater 191:41–48

Laird AD (2008) The charcoal vision: A win-win-win scenario for simultaneously producing bioenergy, permanently sequestering carbon, while improving soil and water quality. Agron J 100:178-181

Lehmann J, Gaunt J, Rondon M (2006) Bio-char sequestration in terrestrial ecosystems – A review. Mitig Adapt Strat GL 11:403–427

Lehmann J, Czimczik C, Laird D, Sohi S (2009) Stability of biochar in the soil. In: Lehmann J, Joseph S (Eds.), Biochar for environmental management: science and technology. Earthscan, London. 416 pp.

Liang B, Lehmann J, Solomon D, Kinyangi J, Grossman J, O'Neill B, Skjemstad JO, Thies J, Luizao FJ, Petersen J, Neves EG (2006) Black Carbon increases cation exchange capacity in soils. Soil Sci Soc Am J 70:1719-1730

Liu Z, Zhang FS (2009) Removal of lead from water using biochars prepared from hydrothermal liquefaction of biomass. J Hazard Mater 167:933–939

Machida M, Mochimaru T, Tatsumoto H (2006) Lead(II) adsorption onto the graphene layer of carbonaceous materials in aqueous solution. Carbon 44:2681–2688

Matthews JA (2008) Carbon negative biofuels. Energ Policy 36:940-945

Mohan D, Rajput S, Singh VK, Steele PH, Pittman Jr CU (2011) Modeling and Evaluation of Chromium Remediation from Water using Low Cost Bio-Char, a Green Adsorbent. J Hazard Mater 188(1-3):319-333

Namgay T, Singh B, Singh BP (2010) Influence of biochar application to soil on the availability of As, Cd, Cu, Pb, and Zn to maize (*Zea mays* L.). Aust J Soil Res 48:638-647

Ogawa M, Okimori Y, Takahashi F (2006) Carbon sequestration by carbonization of biomass and forestation: three case studies. Mitig Adapt Strat GL 11:429-444

Pohlmeier A, Haber-Pohlmeier S, Stapf S (2009) A fast field cycling nuclear magnetic resonance relaxometry study of natural soils. Vadose Zone J 8:735-742

Popov V, Itoh H, Brebbia CA, Kungoles A (2004) Waste management and the environment II. WIT Press: Boston

Shinogi Y, Yoshida H, Koizumi T, Yamaoka M, Saito T (2003) Basic characteristics of low-temperature carbon products from waste sludge. Adv Environ Res 7:661–665

Shinogi Y, Kanri Y (2003) Pyrolysis of plant, animal and human waste: physical and chemical characterization of the pyrolytic products. Bioresource Technol 90(3):241-247

Sohi SP, Krull E, Lopez-Capel E, Bol R (2010) A review of biochar and its use and function in soil. Adv Agron 105:47-82

Strategia Energetica Nazionale: per un'energia più competitiva e sostenibile (2012) Documento per consultazione pubblica. http://www.sviluppoeconomico.gov.it/images/stories/documenti/20121016 SEN- Documento_di_consultazione.pdf

Uchimiya M, Lima IM, Klasson KT, Chang S, Wartelle LH, Rodgers JE (2010) Immobilization of Heavy Metal Ions (Cu^{II}, Cd^{II}, Ni^{II}, and Pb^{II}) by Broiler Litter-Derived Biochars in Water and Soil. J Agr Food Chem 58:5538–5544

Uchimiya M, Wartelle LH, Klasson KT, Fortier CA, Lima IM (2011) Influence of pyrolysis temperature on biochar property and function as a heavy metal sorbent in soil. J Agr Food Chem 59:2501–2510

Vassilev SV, Baxter D, Andersen LK, Vassileva CG (2010) An overview of the chemical composition of biomass. Fuel 89(5):913–933

Wilkinson KG, Harapas D, Tee E, Tomkins RB, Premier R (2003) Strategies for the Safe Use of Poultry Litter in Food Crop Production. Horticulture Australia Ltd, Sidney

Yaman S (2004) Pyrolysis of biomass to produce fuels and chemical feedstocks. Energ Convers Manage 45:651-671

Yuan JH, Xu RK, Wang N, Li JY (2011) Amendment of Acid Soils with Crop Residues and Biochars. Pedosphere 21(3):302–308

Zhang L, Xu C, Champagne P (2010) Overview of recent advances in thermo-chemical conversion of biomass. Energ Convers Manage 51:969–982

CHAPTER 2 : LITERATURE REVIEW

2.1 Biomass

The term biomass refers to non-fossil organic biodegradable substances which are obtained by plant and animal residues, directly or indirectly produced by photosynthesis (Loppinet-Serani et al., 2008). Biomass can be considered as a stored source of solar energy in the form of chemical energy contained in the chemical bonds between adjacent oxygen, carbon, nitrogen and hydrogen atoms (Zhang et al., 2010). When these bonds are broken, by biological and/or thermo-chemical processes, this stored energy is released. The use of biomass fuels provides substantial environmental benefits: unlike fossil fuels, biomass is a renewable resource and its combustion generates lower emissions of environmentally detrimental gases, such as carbon dioxide (CO_2), sulphur dioxide (SO_2) and nitrogen oxides (N_xO_y) with respect to fossil fuels (Jenkins et al., 1998; McKendry, 2002a). Biomass absorbs carbon dioxide during growth and emits it during combustion (Demirbas, 2004a). Therefore, biomass contributes to the atmospheric carbon dioxide recycling and does not increase the greenhouse effect since, during its growth, it uptakes the same amount of atmospheric CO_2 which is released during its combustion (C neutral). However, it should be noticed that in comparison with solid fossil fuels, biomass contains less carbon, more oxygen, larger amount of moisture and has a lower heating value (Jenkins et al., 1998; Demirbas, 2004a; Zhang et al., 2010). Nevertheless, biomasses can be effectively employed for energy production, used directly or after having been processed in a solid (charcoal), liquid (ethanol, biodiesel, methanol, vegetable oil or pyrolysis oil) or gaseous (CH_4, CO, CO_2, H_2) fuel (Basu, 2010). The conversion of biomass materials has the precise objective to transform a carbonaceous solid material (originally difficult to handle, bulky

and with a low energy concentration) into a fuel having physicochemical characteristics which allow its economic storage and transferability through pumping systems (Demirbas, 2004a).

The biomasses used for energy purposes are available in various forms, and can be classified according to their origin: forestry and agro-forestry, agriculture, zootechnical or industrial wastes (Singh et al., 2000; Zhang et al., 2010) (Fig. 1).

The biomass resulting from forestry or agroforestry activities is made mainly by wood-like materials. Conversely, biomass from agriculture is made by residues from agricultural activities (e.g., cereal straw, vine shoots, branches pruning) or energy crops (e.g., sunflower, rapeseed, linseed, soybean, coconut palm). Both forestry and agricultural biomasses are generally composed of cellulose, hemicellulose, lignin, lipids, proteins, simple sugars and starches (Mohan et al., 2006). But, among these compounds, cellulose ($(C_6H_{10}O_5)_x$), hemicellulose (e.g., xylan $(C_5H_8O_4)_m$), and lignin ($[C_9H_{10}O_3(OCH_3)_{0.9\text{-}1.7}]_n$) are the three main constituents (Tab. 1) (Demirbas and Balat, 2007). Biomass also contains inorganic constituents and a fraction of water (Jenkins et al., 1998; Mohan et al., 2006).

Component	**Percent Dry Weight**
Cellulose	40-60
Hemicellulose	10-30
Lignin	20-30
Physical and Energetic Characteristics	
Humidity	25-60%
Bulk density	800-1120 kg m^{-3}
Net calorific value	3600-3800 kcal kg^{-1}

Table 1 – Main characteristics of woody biomass.

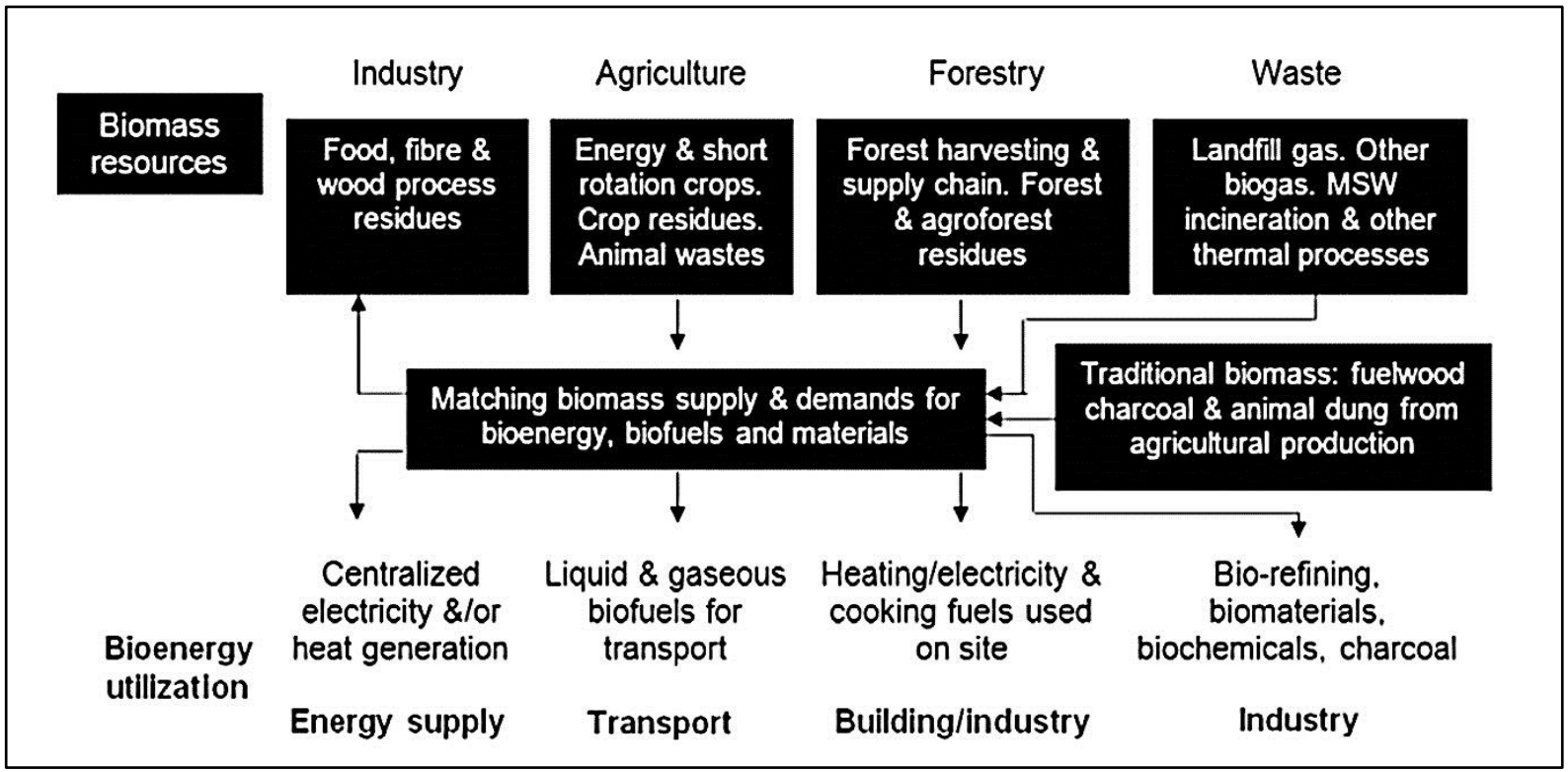

Figure 1 – Biomasses and their energetic utilization (Reprinted from Energy Conversion and Management, vol. 51, Zhang et al., Overview of recent advances in thermo-chemical conversion of biomass, 969–982, Copyright 2010, with permission from Elsevier).

The zootechnical industry provides animal biomasses, mainly livestock manures. These are composed by all the waste products and the wastewaters coming from herds (e.g., feces, urine, litter and food wastes). The manures have a highly variable composition depending on their origin and on the different types of farming to which animals are subjected. According to their specific characteristics, these wastes should undergo different treatment to be used as energy sources. Finally, food processing wastes (e.g., whey, meat or fish slaughter residues), sewage sludge, municipal solid waste (MSW) and pulping by-products (e.g., black liquor) are produced by industrial activities.

From the statistical report published by the Italian GSE (Gestore dei Servizi Energetici - Manager of Energy Services) in 2010, biomass and wastes represented only 11% of the national energy production. Among these, the main input came from wood materials (37%) and biogas (29%) whereas wastes and biofuels contributed respectively to 21% and 13% of the total biomass energetic production (Fig. 2).

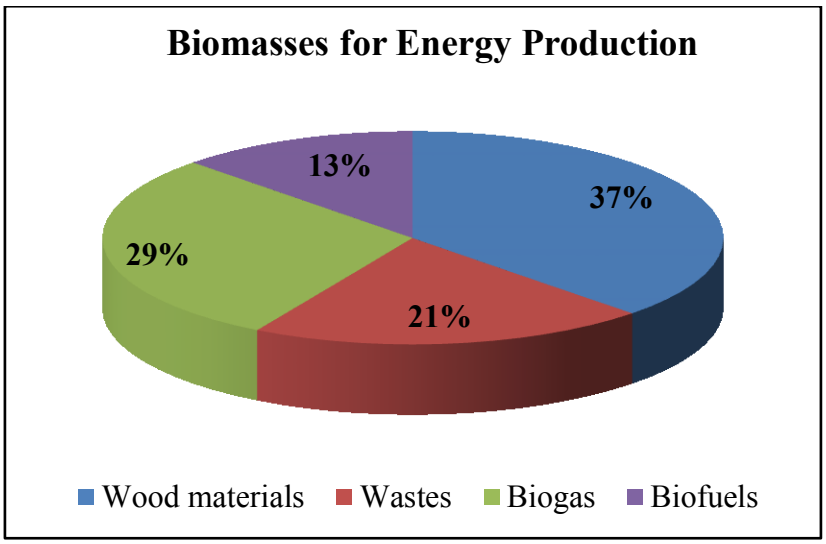

Figure 2 – Biomasses used for the Italian bioenergy production in 2010 (GSE data).

Unfortunately, in Italy, biomasses are still considered more as wastes than as energy sources. Farmers, breeders and agro-food industries generally tend to burn these by-products or to dispose them in the environment, thereby creating serious environmental and economic damages. Instead, the use of these materials to produce renewable energy could lead to several benefits. From an environmental point of view, biomass conversion to energy would reduce greenhouse gases emissions and, from an economic point of view, it would cut the cost of agricultural waste disposing and increase the companies income.

2.2 Biomass energy conversion technologies

The conversion of biomass to energy can be achieved through two different pathways: thermochemical and biochemical/biological processes (Ni et al., 2006; Basu, 2010) (Fig. 3).

The processes based on thermochemical conversion are settled on the transformation of the original biomass through the action of heat (i.e., combustion) directly into thermal energy or other products (solid, liquid or gas) that can be subsequently used for energy purposes. Conversely, biochemical processes exploit chemical reactions produced by enzymes, fungi or microorganisms that break down biomass particles into smaller molecules producing energy (Basu, 2010).

The choice of the most appropriate conversion process depends on the physical, chemical and energetic properties of the biomass. As an example, lignin is a non-fermentable material which cannot be completely decomposed via biological approaches. For this reason, lignin must be degraded via thermochemical approaches (Jenkins et al., 1998; Williams et al., 2003). Also ligno-cellulosic biomasses which show low moisture contents (i.e., less than 30%) and high C/N ratios (i.e., C/N ratios exceeding the value of 30) are directed to thermochemical conversion. Conversely, if the C/N ratio is lower

than 30, and moisture content is higher than 30% of the total biomass weight, the biomass is addressed towards biochemical conversion.

Although biochemical processes have the advantage to require little external energy (Basu, 2010), thermochemical ones have higher efficiency. Indeed, the latter require a lower reaction time (few seconds to minutes vs. several days to weeks) and produce a larger amount of cracked organic compounds than biochemical pathways (Bridgewater, 2001).

In the next paragraphs, a brief description of biochemical processes and an overview of the principles and applications of the main four thermochemical biomass conversion approaches (combustion, pyrolysis, gasification and liquefaction) (Fig. 3) will be provided.

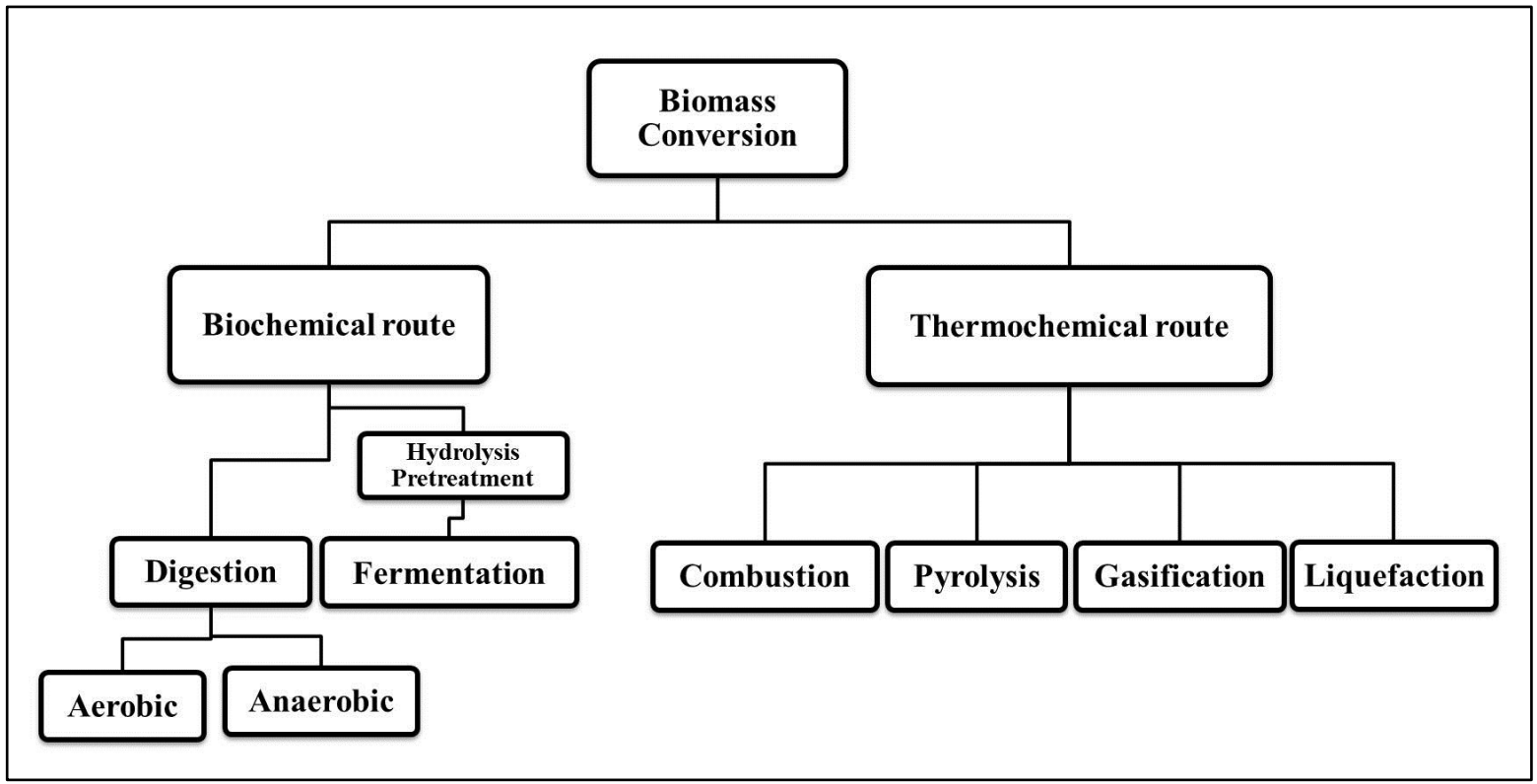

Figure 3 – Thermochemical and biochemical pathways for the conversion of biomass to energy.

2.2.1 Biochemical conversion

Biochemical conversion approaches involves three main processes: 1) anaerobic or aerobic digestion, 2) fermentation, 3) enzymatic or acid hydrolysis (Fig. 3).

Anaerobic digestion is the process by which microorganisms break down biodegradable material in the absence of oxygen (National Non-Food Crops Centre, 2011). Anaerobic bacteria do not need oxygen from the air because they process the one included inside the biomass (Basu, 2010).

The main products of anaerobic digestion are biogas (made by 60% methane, 40% carbon dioxide and traces of other gases) and digestate (an inert and sterile solid residue containing valuable plant nutrients and organic humus) (National Non-Food Crops Centre, 2011). Biogas can be combusted to generate heat, power or transport fuel while digestates can be applied to soils as fertilizer or be marketed as a peat substitute (Dagnall, 1995). Digestate fiber may also be used as feedstock for ethanol production (Yue et al., 2010) or subjected to secondary processing in order to make low-grade building products, such as fiberboard (Dagnall, 1995).

Aerobic digestion or composting also provides a biochemical breakdown of biomass, but it takes place in the presence of oxygen. Aerobic bacteria carry out chemical processes to convert the starting biomass into heat, carbon dioxide, water and ammonium. The ammonium is further converted into plant-nourishing nitrites and nitrates through nitrification (Trautmann and Olynciw, 2000). The solid residue, called compost, is rich in nutrients and can be used as soil conditioner, fertilizer and/or as a natural pesticide for soil.

Fermentation process involves two stages. In the first step, part of the biomass is converted into fermentable sugars using acids or enzymes. Then, the sugar is decomposed by yeasts to produce heat, ethanol, carbon dioxide and other chemicals (Basu, 2010). The liquid fermentation product (i.e., ethanol) can be efficiently used as biofuel for transport (Farrell et al., 2006).

Since lignin is not completely decomposed via fermentation, ligno-cellulosic feedstock require an hydrolysis pretreatment (acid, enzymatic, or hydrothermal) before fermentation (Fig. 3). Hydrolysis is needed to break down cellulose and hemicellulose molecules into simple sugars which can then be decomposed by yeast and bacteria. For this reason, fermentation is preferably used for starch and sugar-based feedstock (e.g., corn and sugarcane) while it is not efficient for cellulosic biomasses (Basu, 2010).

2.2.2 Thermochemical conversion

Combustion, pyrolysis, gasification and liquefaction are the four thermochemical pathways for biomass thermochemical conversion.

Combustion determines the release of all the energy stored within the biomass producing heat and gases with low heating value (Basu, 2010). Conversely, pyrolysis, liquefaction, or gasification processes transform biomass energy into solid (e.g., biochar), liquid (e.g., bio-oils), or gaseous (e.g., syngas) fuels ready to various applications (Zhang et al., 2010). Besides, the purpose of combustion is the merely conversion of chemical energy into heat while gasification and pyrolysis also produce valuable chemical by-products.

The main process conditions of the four different pathways are summarized in Table 2. These processes differ for several parameters, such as the maximum temperature reached, the maximum pressure applied, the use of catalysts and the biomass pre-treatments.

Process	Temperature (°C)	Pressure (MPa)	Catalyst	Drying
Combustion	700-1400	> 0.1	Not required	Not essential
Pyrolysis	380-530	0.1-0.5	Not required	Necessary
Gasification	700-1400	> 0.1	Not essential	Necessary
Liquefaction	250-330	5-20	Essential	Not required

Table 2 – Comparison of the four major thermochemical conversion processes (redrawn from Demirbas, 2009).

Combustion

Combustion represents the oldest and the most widely used process for biomass conversion, responsible for over 97% of the world's bio-energy production (Zhang et al., 2010).

From a chemical point of view, combustion is an exothermic reaction occurring in the presence of oxygen. Biomass is completely converted into water (H_2O), carbon dioxide (CO_2) and heat (more than 90% of biomass energy) (Basu, 2010). Generally, the chemical equation for stoichiometric combustion of a generic hydrocarbon in oxygen is:

$$C_xH_y + zO_2 \rightarrow xCO_2 + \frac{y}{2} H_2O$$

where z = x + (¼)y.

Combustion process consists of three main stages: drying, pyrolysis/reduction, and combustion of volatile gases and solid char (Demirbas and Balat, 2007). More than 70% of the overall heat generation comes from the combustion of volatiles gases (Zhang et al., 2010).

Combustion has the advantage to be a well understood, highly reliable and low cost technology although it is going to be replaced by more advanced and environmentally friendly technologies, such as pyrolysis and gasification.

Pyrolysis

Pyrolysis is a thermal decomposition process taking place at elevated temperatures, in absence or limited presence of oxygen. It aims to convert biomass into solid (charcoal), liquid (tar or bio-oil), and gaseous (CH_4, CO, CO_2, H_2, C_2H_4, C_2H_6) products, which are then applied as sources for energy production or basis for the synthesis of new chemicals (Yaman, 2004). Pyrolysis is usually employed for the thermochemical conversion of biomasses that are not suitable for biochemical conversion (e.g., low moisture herbaceous and woody materials) (Demirbas and Balat, 2007).

A typical pyrolysis process can be divided into four main stages (Maschio et al., 1992; Basu, 2010). The first stage is biomass drying which occurs at around 100°C. At this temperature, free moisture and loosely bound water molecules evaporate. The second step occurs between 100 and 300°C and is referred to as pre-pyrolysis. It consists in a slight weight loss due to biomass internal rearrangements (i.e., bond breakage, appearance of free radicals, formation of carbonyl groups) which lead to a release of small amounts of water (H_2O) and low-molecular-weight gases (CO and CO_2). The intermediate stage is the main pyrolysis process during which solid decomposition occurs, accompanied by a significant weight loss from the initially fed biomass. It takes place between 200 and 600°C and it involves the breakdown of large biomass particles into char, condensable and non-condensable gases. The final stage involves the continuous char devolatilization, caused by the further cleavage of C–H and C–O bonds, and the secondary cracking of volatiles into char and non-condensable gases.

The overall process can be represented by a generic reaction such as:

$$C_nH_mO_p \text{ (biomass)} + \text{heat} \rightarrow \Sigma_{liquid}\, C_xH_yO_z + \Sigma_{gas}\, C_aH_bO_c + H_2O + C \text{ (char)}$$

Pyrolysis products can be divided into three main classes: solid (charcoal), liquid (tars, heavier hydrocarbons and water) and gases (e.g., CH_4, CO, CO_2, H_2, C_2H_4, C_2H_6). The relative amounts of these products depend on several

factors, but they are mainly affected by the heating rate and the final temperature reached by the biomass.

The solid product is named char. It is composed mainly by carbon (around 85%) but it also contains oxygen, hydrogen and inorganic components. The liquid product, also indicated as tar or bio-oil, is a black tarry fluid containing up to 20% of water. It consists of a complex mixture of oxygenated aromatic and aliphatic compounds, i.e. phenols, carbohydrates, carboxylic acids, aromatics, hydroxyaldehydes, hydroxyketones, their condensation products and other derivatives (Piskorz et al., 1988; Mohan et al., 2006). Finally, pyrolysis produces both condensable (vapor) and non-condensable gases (primary gas). The vapors are made of heavier molecules and condense after cooling, becoming part of the liquid yield of pyrolysis. Conversely, the non-condensable mixture contains low-molecular-weight gases, such as carbon dioxide, carbon monoxide, methane, ethane, and ethylene (Basu, 2010).

Pyrolysis process can be adapted in order to allow the production of charcoal, pyrolytic oil or gas. Depending on its operating parameters, pyrolysis can be subdivided into three different processes: 1) fast, 2) mild or conventional, and 3) slow (Bridgwater et al., 1999). These processes are usually carried out in the absence of a medium whereas other two, hydropyrolysis and hydrous pyrolysis, take place in H_2 and H_2O, respectively (Basu, 2010).

Table 3 summarizes the reaction conditions and the product yields for various pyrolysis processes by comparing each of them with the gasification process.

Mode	Residence Time	Heating Rate	Final Temperature (°C)	Liquid (%)	Char (%)	Gas (%)
Fast	< 2s	very high	500	70-80	10-15	10-15
Conventional	5-30 min	low	600	40-50	20-30	30-40
Slow	days	very low	400	30	35	35
Hydro	< 10 s	high	< 500	30-50	10-20	30-40
Gasification	seconds to minutes	very high	> 800	5	10	85

Table 3 – Reaction conditions and product yields for various pyrolysis processes, in comparison with gasification.

Fast pyrolysis is a process providing high heating rates (hundreds °C s^{-1}) and extremely short residence times (1-2s) (Tab. 3). The biomass is heated so rapidly that it reaches the maximum temperature before its decomposition (Pütün, 2002). Fast pyrolysis aims to maximize the production of liquids or bio-oils while it inhibits the formation of solid by-products (Maschio et al., 1992; Bridgewater et al., 1999; Yanik et al., 2007). The liquid product comes from the condensation of volatile organic matter generated by heating the biomass. Bio-oil appears as a black viscous fluid, composed by 20-25% of water, 20-25% of water insoluble lignin, 25-30% of organic acids, 5-12% of non-polar hydrocarbons, 5-10% of anhydrosugars and 10-25% of other oxygenated compounds (Piskorz et al., 1988; Mohan et al., 2006). It is a potential liquid fuel that can be easily stored and transported. But, due to its low calorific value (approximately 55% than that of normal diesel), it is mainly used for the production of electrical energy rather than for the transport industry. Bio-oil also contains high-valuable biochemical, relevant for food and pharmaceutical industries.

To maximize liquid yield, several factors must be accounted for. These include: a fine particle size (<1mm), a careful control of the temperature (450-550°C), a high heating rate (>200°C s^{-1}), a short hot vapor residence time (~2s), and a rapid cooling of the vapors (Maschio et al., 1992;

Bridgwater et al., 1999; Pütün, 2002; Uzun et al., 2007; Yanik et al., 2007). In addition to bio-oil production, at higher temperatures (700-1000°C), fast pyrolysis also generate H_2 hydrogen gas (Marquevich et al., 1999; Czernik and Bridgewater, 2004).

Conventional or mild pyrolysis is characterized by moderate reaction temperatures (<600°C) and low heating rate (~20°C s^{-1}), with residence times ranging from seconds to minutes (Tab. 3). This kind of pyrolysis produces a slightly greater yield of liquids compared to solid or gaseous products.

Conversely, the main goal of slow pyrolysis or carbonization is the production of a solid material indicated as charcoal or char. This is the oldest form of pyrolysis and it has been used for thousands of years to produce charcoal (Mohan et al., 2006; Yanik et al., 2007).

Slow pyrolysis is carried out with a long vapor residence time, low heating rate and relatively low temperatures (Tab. 3). During the process, the biomass is heated slowly to a relatively low temperature (~400°C) in the absence of oxygen, and over a long period of time (in the ancient times even for several days). The long residence time is necessary to allow the conversion of condensable vapors into char and non-condensable gases. In contrast to fast pyrolysis, slow pyrolysis does not necessarily require a fine feedstock particle size (smaller than 1 mm). Indeed, also raw materials that are not available as powders or fine particles can be used (Maschio et al., 1992). As reported by Mok et al. (1992), a higher yield of charcoal can be obtained from biomass feedstock containing large lignin and low hemicellulose content.

The pyrolytic charcoal can be applied in a wide range of areas, from domestic cooking and heating to metallurgical or chemical uses (Laird et al., 2011). It can also be used as a raw material for the production of chemicals, activated carbon, fireworks, absorbents, soil conditioners, and pharmaceuticals (Karaosmanoglu and Tetik, 1999).

While normal pyrolysis is conducted in the absence of a medium, hydropyrolysis and hydrous pyrolysis are carried out in H_2 and H_2O, respectively.

During hydropyrolysis, the biomass is decomposed in a high-pressure hydrogen atmosphere. The presence of H_2 allows the hydrogenation of free radical fragments of volatiles in order to stabilize them in a gaseous form before they repolymerize to form char (Probstein and Hicks, 2006). The result is a high yield of volatiles and low-molecular-weight hydrocarbons (Rocha et al., 1997).

Hydrous pyrolysis is a two stage process in which the biomass is decomposed in high-temperature water. In the first step, the biomass is subjected to water at 200-300°C, under high pressure to produce hydrocarbons. Then, in the second step, these molecules are broken into lighter ones at 500°C (Appel et al., 2003). Hydrous pyrolysis produces a valuable bio-oil, with low oxygen content (higher calorific value).

Combining all the aforementioned factors, it may be generally concluded that low temperature and low heating rates are necessary in order to maximize char yield. Conversely, a combination of moderate temperature, short gas residence time and high heating rate is essential if liquid (bio-oil) is the desired product.

Gasification

Gasification is a process that converts solid or liquid carbonaceous biomasses into useful and convenient combustible gases (e.g., H_2, CO, CO_2, and CH_4) which can be burned to release energy or used for the production of value-added chemicals. The process is carried out in the presence of partial oxygen (O_2) or suitable oxidants supply (e.g., steam or CO_2), at very high temperatures (1200°C), and sometimes at high pressure (15-50 bar). The presence of a gasifying medium (e.g., steam or oxygen) is required to rearrange biomass molecular structure in order to convert the solid feedstock into liquid and gaseous products (Basu, 2010).

A generic gasification process involves four main steps.

1) Pre-heating and drying (100-200°C). In this step, the biomass is dried to remove the excessive moisture. This process is really important since water evaporation requires a high amount of energy that is no more recoverable. Only biomasses with 10-20% of moisture can be fed into the gasifier to produce a fuel gas with high heating value (Basu, 2010).

2) Pyrolysis (~400°C). Pyrolysis can be considered as a step of gasification. During this phase, biomass feedstock are decomposed into tar and volatile hydrocarbon gases (both condensable and non-condensable) before the beginning of the main gasification reactions. This step does not require external agents.

3) Char gasification and 4) combustion (up to 1200°C). After pyrolysis, liquids, gases and char undergo different reactions. Liquid and gaseous products are subjected to rearrangement and secondary cracking to produce combustible gases (i.e., CO, H_2, CH_4, H_2O, CO_2) which will be recovered and stored for subsequent transformations/applications or immediately used for energy production. Conversely, the solid part (char) undergoes several gasification and combustion reactions resulting in combustible gases and unconverted carbon residues.

The combustion reactions involving volatile compounds and part of the char can be described according the following reactions (Klass, 1998; Knoef, 2005):

1) $C + O_2 \rightarrow CO_2 - 394$ kJ/mol

2) $2H_2 + O_2 \rightarrow 2H_2O - 242$ kJ/mol

(1) and (2) are oxidation reactions occurring in the presence of oxygen. Since these reactions are exothermic, enough heat is generated to dry the feedstock, to break up its chemical bonds and to maintain a high temperature (necessary to drive the following gasification reactions) (Zhang et al., 2010).

The last gasification step consists in the reduction of the combustion products (i.e., CO_2, H_2O and some remaining non-combusted pyrolysis products) into carbon monoxide, hydrogen and methane through the catalytic action of a red-hot charcoal bed. The reactions occurring in the last step are described below (Klass, 1998; Knoef, 2005; Higman and van der Burgt, 2008):

3) $C + CO_2 \rightleftarrows 2CO + 172$ kJ/mol (Boudouard reaction)

4) $C + H_2O_{steam} \rightleftarrows CO + H_2 + 131$ kJ/mol

5) $CO + H_2O \rightleftarrows CO_2 + H_2 - 41.2$ kJ mol

6) $C + 2H_2 \rightleftarrows CH_4 - 74.8$ kJ/mol

7) $2C + O_2 \rightarrow CO - 111$ kJ/mol

Reactions (3-6) take place in both directions depending on the specific temperature, pressure, and reactant concentrations in the system (Zhang et al., 2010). Reactions (4) and (5) are the main gasification reactions, called water–gas shift reactions. These have great importance due to their significant role in hydrogen generation. Reaction (6) is indicated as methanation. It proceeds slowly at low-temperatures and in the absence of any catalyst.

At the end of gasification, the resulting gas products contain moisture, hydrogen, carbon monoxide, carbon dioxide, methane, aliphatic hydrocarbons, benzene, and toluene, as well as small amounts of ammonia, hydrochloric acid, and hydrogen sulfide (Maschio et al., 1992; McKendry,

2002b; Basu, 2010). From this mixture, H_2 and CO must be separated to produce a pure and valuable syngas.

When air or oxygen is employed, gasification may seem similar to combustion, but actually it presents many advantages (Rezaiyan and Cheremisinoff, 2005). The only purpose of combustion is the production of heat obtained by using an excess of oxygen to break biomass chemical bonds in order to release their energy. Moreover, combustion generates carbon dioxide which is released in the atmosphere acting as a greenhouse gas, and solid residues that have to be treated as hazardous wastes (Rezaiyan and Cheremisinoff, 2005). Conversely, the objective of gasification is the production of valuable gases that can be stored for various applications. Since these gases are not released into the atmosphere, the overall process is considered environmental friendly. Moreover, gasification requires 65% less oxygen than combustion and produces gases with a high H/C ratio (high calorific value). In this way, the energy of the original biomass is not released merely as heat, but preserved in a gaseous form (syngas) which have a versatile usage. Synthetic gas applications range from: steam or heat generation, fuel gas for hydrogen production, substitute for natural gas production (e.g., methane), fuel cell feed, and synthesis of chemical compounds (e.g., methanol, ammonia) (Rezaiyan and Cheremisinoff, 2005).

Liquefaction

Direct liquefaction is a low-temperature (250-330°C) and high pressure (5-20 MPa) thermochemical process during which biomass is broken down into fragments of small molecules in water or other suitable solvents (Demirbas, 2000). These light fragments are unstable and reactive, thus they re-polymerize into oily compounds with various ranges of molecular weights (Demirbas, 2000; Zhong and Wei, 2004). Ligno-cellulosic materials are the most widely used for bio-oil production through liquefaction (Zhong and Wei, 2004). Since they are rich in hydroxyl groups, they can be converted into intermediates for the production of biopolymers (e.g., epoxy resins and polyurethane foams) (Maldas and Shirai, 1997; Liang et al., 2006).

Compared with pyrolysis, liquefaction technology is more challenging as it requires more complex and expensive reactors and fuel feeding systems (Demirbas, 2000). Liquefaction does not require feedstock pre-drying but it needs solvents to prevent the condensation of oily molecules into undesirable solid char products (Zhang et al., 2010). It also involves the use of catalysts to reduce the reaction temperature required, enhance reaction kinetics, and improve the yield of the desired liquid products (Maldas and Shirai, 1997).

By the three latter bio-energetic processes, any organic material, including plant and municipal wastes, could be totally converted into char, bio-oil and gas. Thus, the use of these 'green' techniques should be considered a viable alternative to waste landfill or combustion as it may facilitate their disposal converting them into clean energy.

2.3 Carbon terminology

Several solid products are created when carbon-rich biomass is heated to high temperatures. The differences between these materials are subtle but present and mainly related to their applications. The following list of terms is

intended to better define the various carbonaceous products (Lehmann and Joseph, 2009).

Char: a carbonaceous solid material resulting from the thermal decomposition of any organic material, of natural origin or synthetic. This category includes, for example, forest fires residues and particulate matter originating from the incomplete combustion of fossil hydrocarbons.

Biochar: the solid product of the thermal decomposition (pyrolysis or gasification) of biomass. It is used mainly as fuel for urban heating and cooking or as soil amendment in order to improve soil functions and to reduce emissions from biomass that would otherwise naturally degrade to greenhouse gases.

Charcoal: is produced from carbonaceous materials, heated at high temperatures (above 500°C) and for long periods of time (over 10 hours). Charcoal is characterized by high adsorption capacity thus it is not used as a soil amendment. Its major application is in remediation processes, such as water filtration and adsorption of gas, liquid and solid contaminants.

Black Carbon (BC): consists of different forms of refractory organic matter obtained by the incomplete combustion of fossil fuels, biofuel, and biomass. BC also includes carbonaceous residues from vegetation fires and both anthropogenic or natural soot. Given the wide diversity of combustion conditions to which BC may be subjected, this is represented by a continuum of different materials. For example, BC contributes to the 30% of the total carbon stored in soils (Schmidt and Noack, 2000), acting as a reservoir for nutrients and enhancing soil fertility. But in specific conditions, black carbon is considered the second major contributor to global climate change after carbon dioxide emissions (Ramanathan and Carmichael, 2008). Indeed, when suspended in the atmosphere, BC can strongly absorb the visible solar radiation generating heat which warms the air, with important implications for cloud formation and hydrological cycles. When it is deposited over snow

and sea ice, it can decrease the surface albedo leading to temperature increase and ice melting (Ramanathan and Carmichael, 2008).

2.4 Biochar and its applications

The next paragraphs will focus on biochar origins, characteristics, benefits and applications stressing the importance of the factors (i.e., feedstock nature and process conditions) influencing char chemical and physical properties.

The overall atmospheric and soils benefits determined by biochar use are resumed in Figure 4.

2.4.1 Biochar origins - *Terra Preta*

The application of biochar to soils is not a new idea. The first observations regarding the positive effects of carbon stored in soil come from ancient farm management practices carried out between 500 and 8000 years ago throughout the Brazilian Amazon. These practices produced a kind of soil known as '*Terra Preta de Indio'* or '*Amazonian Dark Earths'* (Glaser et al., 2002), characterized by high levels of fertility without any external input of fertilizers. This is an unusual condition in this area since the surrounding soils have low fertility as they are very acidic and highly weathered (Lehmann et al., 2006; Lehmann and Joseph, 2009). Conversely, *Terra Preta* soils have high levels of organic matter, carbon and nutrients such as nitrogen, phosphorus, potassium and calcium (Novotny et al., 2009). These positive characteristics have been attributed to the high char content. Since the char consists of partially combusted biomass, *Terra Preta* soils also present a characteristic dark color (Fig. 5) (Glaser et al., 2002).

These findings suggested that application of biochar to soils could enhance its agronomic potential, thereby resulting economically viable and profitable.

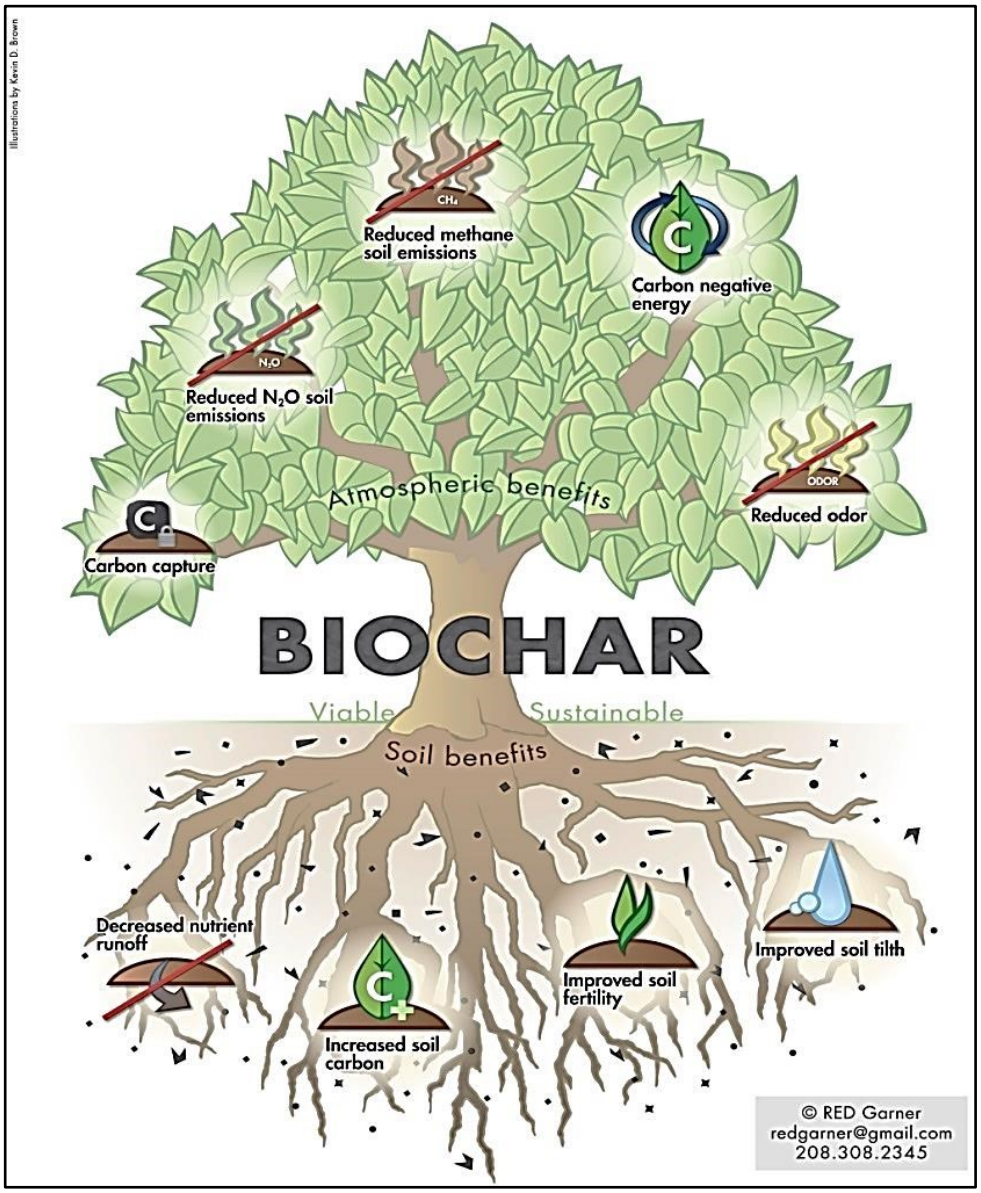

Figure 4 - Overall atmospheric and soil benefits determined by biochar use (reprinted by permission from RED Garner).

Figure 5 – Example of dark *Terra Petra* soils (on the left) compared to Ferralsol (on the right). (Reprinted from Naturwissenschaften, vol. 88, Glaser et al., The 'Terra Preta' phenomenon: A model for sustainable agriculture in the humid tropics, 37–41, Copyright 2001, with kind permission from Springer Science and Business Media).

2.4.2 Biochar atmospheric benefits

Generally, any form of organic matter integrated in soils will be quickly degraded thereby producing carbon dioxide (CO_2), well known as an harmful greenhouse gas. According to IPCC data (2013), global carbon emissions from land use and land use change account for 1.9±0.8Gt per year representing about 20% of the total anthropogenic CO_2 emissions.

A way to reduce greenhouse gas emissions can be the transformation of organic matter into a highly stable and less biodegradable form. Biochar has a high stability and high resistance to chemical, physical and biological decomposition (Schmidt and Noack, 2000; Novotny et al., 2009). This stability derives from its chemical composition consisting of polycyclic

aromatic rings conjugated to form highly crystalline structures (Mao et al., 2012). As a consequence, biochar results highly recalcitrant and able to persist in the environment longer than any other form of organic carbon (Lehmann, 2007). For this reason, biochar is considered as an important carbon sink, able to sequester large quantities of CO_2 when applied to soil (Fig. 4) (Lehmann, 2007).

The production of biochar can, therefore, be accounted as a C-neutral route. Indeed, the amount of carbon emitted during the process is equivalent to the quantity removed from the atmosphere to produce the starting biomass through photosynthesis (Fig. 6) (Mathews, 2008). Pyrolysis could even be considered as a C-negative process since its gaseous products are not released into the atmosphere but stored, refined and subsequently used for energy purposes. Further, the resulting biochar can be incorporated into soils thereby sequestering carbon in a stable and permanent sink (Fig. 6) (Mathews, 2008).

The prospects of carbon sequestration using biochar are quite promising. A rough calculation by Amonette et al. (2007) shows that approximately 1.2Gt of carbon (about 13% of the total annual anthropogenic CO_2 emissions) could be removed each year from the atmosphere using biochar.

In addition to the reduction of CO_2, several studies (Kraxner et al., 2003; Rondon et al., 2005; Yanai et al., 2007) have also shown a decrease in natural soil emissions of nitrogen oxides (N_xO_y) and methane (CH_4) (greenhouse gases having a much higher global warming potential than CO_2) after biochar application (Fig. 4). For example, Rondon et al. (2005) found that CH_4 emissions were completely suppressed and N_2O emissions were reduced by 80% when biochar was applied to soil. Zhang et al. (2010) found that biochar applied to rice paddy significantly increased rice yields and decreased N_2O emission, but it also increased total CH_4 emissions. Conversely, Liu et al. (2011) found a 50-90% reduction of CH_4 emissions from paddy soils amended with biochar, compared with those without biochar.

Resuming, biochar and bioenergy production could contribute to global climate change mitigation by replacing the use of fossil fuels and, at the same time, by sequestering carbon in stable reserves in the soil.

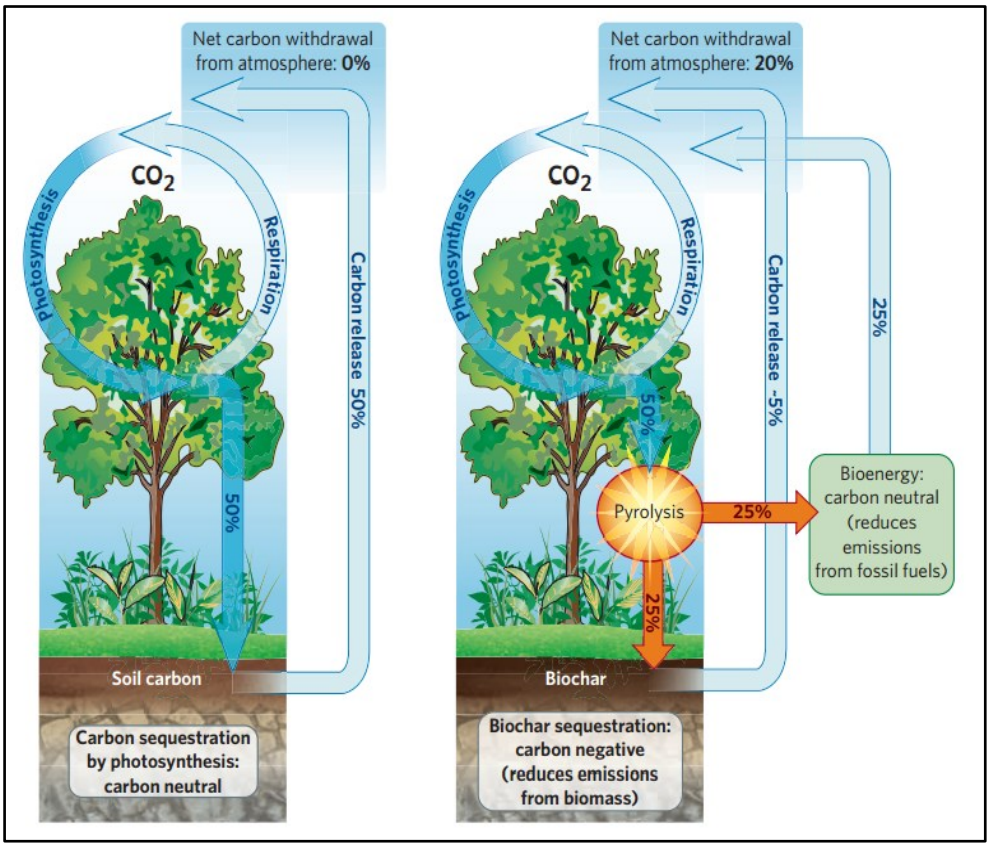

Figure 6 – Carbon neutral and carbon negative processes (Reprinted by permission from Macmillan Publishers Ltd: NATURE, vol. 447, Lehmann, J. A Handful of Carbon. Copyright 2007).

2.4.3 Biochar soils benefits

During pyrolysis, most of the mineral nutrients that are present in biomass are concentrated into the biochar fraction. Therefore, soil application of this carbonaceous material could be a convenient mean of recycling those nutrients to agricultural lands (Laird et al., 2011).

Several studies have shown significant agronomic benefits, such as increased crop production, in soils amended with biochar. The improvements in soil fertility were related to an increase in: soil nutrient retention (Glaser et al., 2002; Lehmann et al., 2003), soil water permeability and plant water availability (Asai et al., 2009; Herath et al., 2013), soil cation exchange capacity (Liang et al., 2006; Steiner et al., 2007), and the neutralization of phytotoxic compounds (Steiner et al., 2007). Furthermore, char affects soil microbial community and may have a positive impact on plant resistance to disease due to its suppressive effect on soil pathogens (Matsubara et al., 2002). All these effects are due to biochar elemental composition that can directly modify soil chemical properties, and provide a chemically active surface able to change nutrients dynamics, as well as to catalyze useful reactions. Moreover, biochar porous structure and high surface area (Fig. 7) contribute to modify soil physical characteristics with benefits for radical growth, and favor the absorption and retention of nutrients and water making them more available to plants.

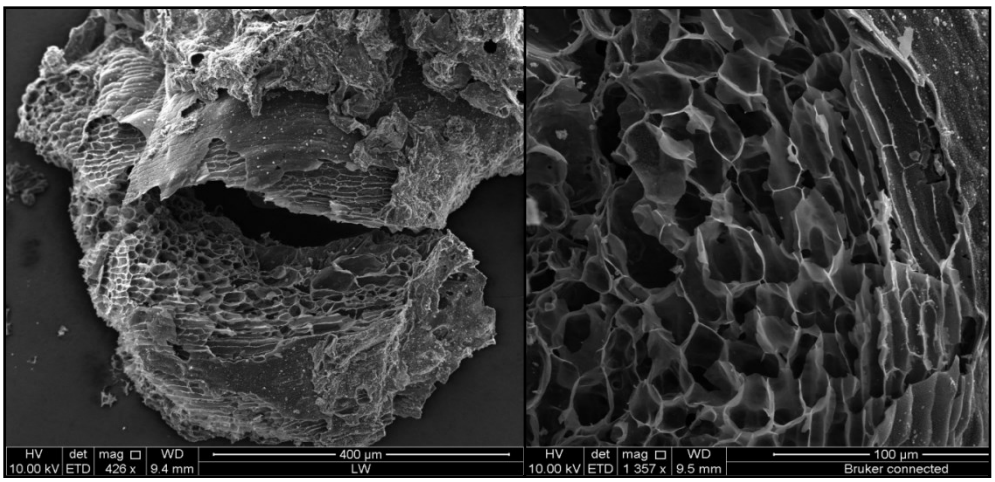

Figure 7 – High porosity of biochar from poultry manure, retrieved at 600°C for 2 h.

Effects on soil chemical characteristics

An important issue for a sustainable cultivation is to find the correct equilibrium between the supply of sufficient nutrients for a healthy plant growth (especially N and P), and the reduction of nutrient leaching. The loss of nutrients from agricultural soils has several negative effects: depletion of soil fertility, drop of crop yields, soil acidification, increase of the fertilizer costs for farmers, reduction in the quality of surface and ground waters by eutrophication (Laird et al., 2010a). The use of a soil amendment able to retain nutrients could help to solve this problem.

Several works (Glaser at al., 2002; Lehmann et al., 2003; Laird et al., 2010a) reported an increase in soils ability to retain plant available nutrients and a decrease in the leaching of nutrients and agricultural chemicals when char was used as soil amendment. For example, Laird et al. (2010a) found a significant decrease in total amounts of P, Mg, Si and N leaching using biochar, despite the simultaneous addition of swine manure. By contrast, total amounts of leached K and Ca increased. Beck et al. (2011) observed that the soils containing biochar had an increased retention of nitrate, total nitrogen, phosphate, total phosphorus, and total organic carbon compared to the control without biochar. These positive effects are mainly related to biochar high surface area, high surface charge density, negative surface charge (Liang et al., 2006), and to biochar capacity to stimulate soil microbial activity (Steiner et al., 2008a; 2008b).

In more details, due to its high porosity as well as the presence on its surface of both polar and non-polar functional groups, biochar can efficiently adsorb organic molecules and nutrients (Liang et al., 2006). After its soil inclusion, char surface undergoes oxidation leading to the formation of phenolic and carboxylic functional groups which represent negative pH-dependent charges (Cheng et al., 2008). This determines the increase of soil cation exchange capacity (CEC) and enhances the retention of alkaline and alkali earth metal

cations (i.e., Mg, Ca, Na and K) necessary for plant growth, in an exchangeable and thus plant-available form (Sombroek et al., 1993; Liang et al., 2006; Cheng et al., 2008; Laird et al., 2010b).

A further effect of biochar is the increase of soil pH, caused by its alkaline metals content (Glaser et al., 2002; Sohi et al., 2010). This characteristic is particularly valuable in acidic soils since the increase of pH leads to an increase in the solubility of important elements for plants, such as phosphorous, calcium and potassium (Laird et al., 2011). By contrast, it could be harmful on alkaline/calcareous soils since biochar application could determine an excessive increase of soil pH (Mozaffari et al., 2002).

Finally, char application to soils allows the development of microbial communities (i.e., mycorrhizal fungi) which are particularly important for nutrient cycling (Ishii and Kadoya, 1994; Lambers et al., 2008) thereby contributing to the mobilization of key elements for plants and crops.

The net chemical impact of amending soils with biochar can be resumed as: 1) increased nutrient use efficiency (more availability for plant), 2) reduction in the amount of fertilizer needed to grow a crop and 3) improved water quality reducing leaching and pollution.

Adsorption capacity

In addition to retain nutrient elements in a plant-available form, biochar also has an affinity for both inorganic and organic compounds, and may sorb toxic by-products from soils and wastewaters (Yu et al., 2006). Several studies have been conducted to investigate how charcoal can effectively retain polar compounds, e.g. polar organic pesticides (Sudhakar and Dikshit, 1999; Sheng et al., 2005; Lian et al., 2011), and hydrophobic molecules, such as polycyclic aromatic hydrocarbons (Kleineidam et al., 1999; Schmidt and Noack, 2000; Chen and Chen, 2009; Chen and Yuan, 2011), lignin and tannin (Mohan and Karthikeyan, 1997).

The adsorptive capacity of biochar depends both on its physical (i.e., its porous structure) and chemical (i.e., presence of specific surface functional groups) properties. Chun et al. (2004) showed that the high surface area and the presence of surface polar groups on wheat biochar were determinant in the uptake of neutral organic contaminants, such as benzene and nitrobenzene. Keech et al. (2005) related the ability of wood-biochar to adsorb large molecules, such as phenolic compounds, to the presence on its surface of a large number of macropores.

In addition to organic compounds, char can also effectively bind inorganic molecules. Various studies demonstrated biochar capacity to absorb nitrate (Mizuta et al., 2004), phosphate (Beaton et al., 1960) and metal ions (Beesley et al., 2010; Namgay et al., 2010; Uchimiya et al., 2010; Fellet et al., 2011; Karami et al., 2011). For example, Beesley and Marmiroli (2011) found that biochar from hardwoods rapidly uptaked and reduced cadmium (Cd) and zinc (Zn) mobility from a contaminated soil. Uchimiya et al. (2011) reported a decrease in soils copper (Cu) content, using broiler litter biochar as amendment. Mohan et al. (2011) used activated carbon (AC), oak bark and oak wood char for chromium (Cr) remediation from contaminated surface water. They obtained that oak chars removed the same amount of Cr(VI) than AC, despite their much lower surface area (1-3m^2g^{-1} vs 1000m^2g^{-1}). Therefore, the highest remediation potential of biochar depended on the presence of a large amount of specific surface functional groups that serve as adsorption sites for heavy metals. Indeed, a relatively high concentration of surface acidic groups can allow the formation of chelates with metal ions, and help the binding of positively charged ions (Laird et al., 2011).

In conclusion, biochar sorptive capacity can be effectively used to mitigate diffuse pollution from agriculture, and to immobilize potentially toxic organic and inorganic compounds, thereby reducing contamination from soils or wastewaters.

Effects on soil physical characteristics

Besides influencing soil chemical properties, char also affects soil physical structure.

Biochar is a low density material that reduces soil bulk density (Laird et al., 2010b), thereby increasing water infiltration, water holding capacity, root penetration, and soil aeration (Glaser et al., 2002; Beck et al., 2011). Numerous studies report positive effects of biochar application on soil physical properties. Glaser et al. (2002) observed that water retention in *Terra Preta* soils was 18% higher than in adjacent soils where the amount of charcoal was lower or absent. Asai et al. (2009) applied biochars derived from wood residues to rice cultivation. They found improvements on soil water permeability, water holding capacity and plant water availability. More recently, Herath et al. (2013) found that corn stover biochar application on two different soils improved significantly the aggregate stability and the porosity of both soils considered, ameliorating their hydraulic properties.

The enhancement of soil water retention properties depends on biochar mineral and organic content (Sohi et al., 2010) as well as its porous nature (predominantly μm sized pores) that reflects the cellular structures of the original feedstock.

Despite the possible positive effects, the application of char to different soils should be carefully investigated since it could also have detrimental effects. For example, Sohi et al. (2010) suggested that biochar effects on water retention will be particularly positive in sandy soils (due to their typical large porosity), neutral in medium-textured soils, and potentially detrimental in clay soils.

Effects on soil microorganisms

Soil amendment with biomass-derived black carbon (biochar) determines changes in soil microbial community and soil biogeochemistry (Pietikäinen et al., 2000; Warnock et al., 2007). Several studies documented the stimulation of indigenous arbuscular mycorrhizal fungi (AMF) by biochar (Ishii and Kadoya, 1994; Matsubara et al., 2002; Rillig et al., 2010), and this has been associated with enhanced plant growth (Rondon et al., 2007; Graber et al., 2010).

According to literature (Pietikäinen et al., 2000; Warnock et al., 2007; Lehmann et al., 2011), the main mechanisms that could explain how biochar influences the abundance and/or the activity of soil biota and plant roots are:

1. Increase of nutrients (i.e., N, P and metal ions) amount and availability, affecting both plants and microorganisms.

Biochar labile components have the potential to stimulate microbial activity (Steiner et al., 2008b). Moreover, an increase in soil nutrient retention and availability results in enhanced host plant performance and elevated tissue nutrient concentrations which allow higher colonization rates of the host plant roots by microorganism (Ishii and Kadoya, 1994).

2. Water retention.

It improves soil hydration and protects soil biota against desiccation.

3. Adsorption of inhibitory compounds.

Microbial abundance increases due to the sorption of compounds that would otherwise inhibit microbial growth (Lehmann et al., 2011). For example, Kasozi et al. (2010) found that high temperature corn stover biochar has a high adsorption capacity for catechol, which is toxic to microorganisms (Chen et al., 2009).

4. Biochar structure serves as a refuge from predators.

Most of the pores within biochar are large enough to accommodate soil microorganisms (including bacteria and fungi), excluding their larger

predators (Warnock et al., 2007). Thus, char pore structure offers a physical protection from soil predators and allows a better attachment to various microorganisms. The latter makes them less susceptible to leaching in soil and determines an increase in bacterial growth rates (Pietikäinen et al., 2000; Ezawa et al., 2002).

As reviewed by Lehmann et al. (2011), the effects of biochar on soil biota are highly variable and not always positive. Consequently, further evaluations are needed to better understand the impacts that the application of different kind of chars can produce on different soils.

Soil fertility and crop production

Biochar effects on soils physicochemical properties also influence soil fertility and crop production. Currently, many studies demonstrating significant agronomic benefits due to char application to soils have been conducted (Sohi et al., 2010; Yuan et al., 2011). Early researches from 1980s and 1990s showed marked favorable impacts of low charcoal additions (0.5 t ha^{-1}) on various crop species, but growth inhibition at larger rates (Glaser et al., 2001). Ishii and Kadoya (1994) applied char as a soil conditioner on citrus cultivation reporting an increase in the fresh weights of roots, shoots and the whole tree. Further works conducted on different crops and soil types demonstrated that adding charcoal to soil increased significantly seed germination, plant growth and crop yields (Glaser et al., 2002; Lehmann et al., 2003; Kimetu et al., 2008; Steiner et al., 2008c; Major et al., 2010).

Biochar amendments result promising especially in combination with fertilizers. For example, Yamato et al. (2006) found an enhancement of maize and peanut yields in Indonesian soils where bark charcoal was applied together with N. The same results were reported in Australian semi-arid soils by Chan et al. (2007).

However, some studies showed no significant effects of char applications on crop yield and some other adverse dose-dependent effects (Kishimoto and Sigiura, 1985; Mikan and Abrams, 1995; Blackwell et al., 2007; Rondon et al., 2007; Rillig et al., 2010). Indeed, some chars have unfavorable properties which cause long-term alterations in soil chemistry, and can inhibit permanently woody plants growth (Mikan and Abrams, 1995). Rondon et al. (2007) studied the effects of the addition of increasing amount of biochar on *Phaseolus vulgaris* cultivation. They found that biomass production and plant total N uptake decreased as biochar applications were increased. The same results were reported for rice grain cultivation where char was applied without additional N fertilization (Asai et al., 2009). Deenik et al. (2010) reported an enhanced soybean plant growth for soils amended with a low volatile matter (11%) biochar, but significantly lower plant growth for soils amended with a high volatile matter (35%) biochar.

These findings suggest that the extent of biochar effects on crop productivity is very variable due to the high variability of the potential biophysical interactions and processes that occur when it is applied to soil. A better knowledge of the relevant properties of a high variety of charred materials, and how these properties influence field responses, is essential to identify the best char to be applied to a particular kind of soil and for a specific crop.

2.5 Factors influencing biochar characteristics

2.5.1 Original feedstock

The starting biomass plays an important role in determining biochar properties. Both the chemical composition and the physical structure of the parental materials are precisely reflected on the final product (Fig. 8) (Zhao et al., 2013).

Char can be produced from organic biomass of different nature. At present, the feedstock used, at a commercial scale or in research facilities, include

wood chips and pellets (de Jong et al., 2003), tree bark (Mohan et al., 2011), crop residues including straw, nut shells and rice husks (Shinogi and Kanri, 2003), organic wastes as: bagasse from the sugarcane industry (Erlich et al., 2006), olive wastes (Yaman, 2004), broiler litter (Uchimiya et al., 2010), dairy manure and sewage sludge (Shinogi et al., 2003). Indeed, the use of agricultural or industrial discards for energy production results beneficial compared to their disposal as wastes.

Figure 8 – Starting biomasses (on the upper part) compared with their derivative biochar (on the lower part). Conifer residues (on the left) and chicken manure (on the right).

A literature review on natural and lab-produced biochars showed that the chemical composition of these products differed significantly, mainly due to parental biomass (Krull et al., 2009).

Feedstock of distinct nature have a different composition in terms of cellulose, hemicellulose, lignin and minerals (Mohan et al., 2006). These differences are reflected in a dissimilar behavior during pyrolysis (Basu,

2010). During the thermal treatment, the organic components are gradually degraded. Hemicellulose is the first which undergoes degradation, in the temperature range 200-260°C, followed by cellulose (240-350°C) and lignin (280-500°C). Due to their different thermal behavior, the proportion of these components in the starting biomass influences the degree of reactivity and determines the ratios of volatile carbon (bio-oil and gas) and stabilized carbon (char) in the pyrolysis products (Basu, 2010). For example, raw materials with low content of lignin, minerals and nitrogen (e.g., herbaceous biomass and agricultural byproducts) are used for bio-oil and fuel gas production. Conversely, the feedstock chosen to obtain a higher yield in terms of solid product are high in lignin content (e.g., forestry residues and walnut shells) and manures (Demirbas, 2004b; Laird et al., 2011).

After pyrolysis, the original structure of the feedstock, its carbon skeleton, porosity and mineral content are retained in the solid product (Figs. 8 and 9) (Laird et al., 2011; Zhao et al., 2013). Indeed, char elemental content reflects the element concentration in the starting feedstock (Lima and Marshall, 2005). According to Antal and Grønli (2003) and Zhao et al. (2013), chars derived from wood materials have low ash content (often less than 3%) and high C content. Conversely, chars derived from herbaceous biomass (i.e., switchgrass, digester fiber, peanut hulls), biosolids and manures have lower carbon content, but greater N, P, K and S contents than woody feedstock (Novak et al., 2009; Granatstein et al., 2009). Biochars produced from biosolids and manures are typically high in ash content. For example, chicken-litter chars can have a mineral content larger than 45 percent (Lima and Marshall, 2005; Cimò et al., submitted).

Besides the elemental content, also the vascular structure of the original plant material is retained in the pyrolysis solid product. For example, wood material is made of fibers (i.e., vessels, fibers and parenchyma in angiosperms and tracheid in gymnosperms) which walls have channels

carrying gas and moisture (Keech et al., 2005). The size of these channels determines char pore size (Fig. 9) (Warnock et al., 2007). For this reason, chars derived from wood biomasses often have higher surface area than grass ones (Kloss et al., 2012), and plant species having many large diameter cells in their stem tissues can lead to biochars containing larger amounts of macropores (Lehmann and Joseph, 2009).

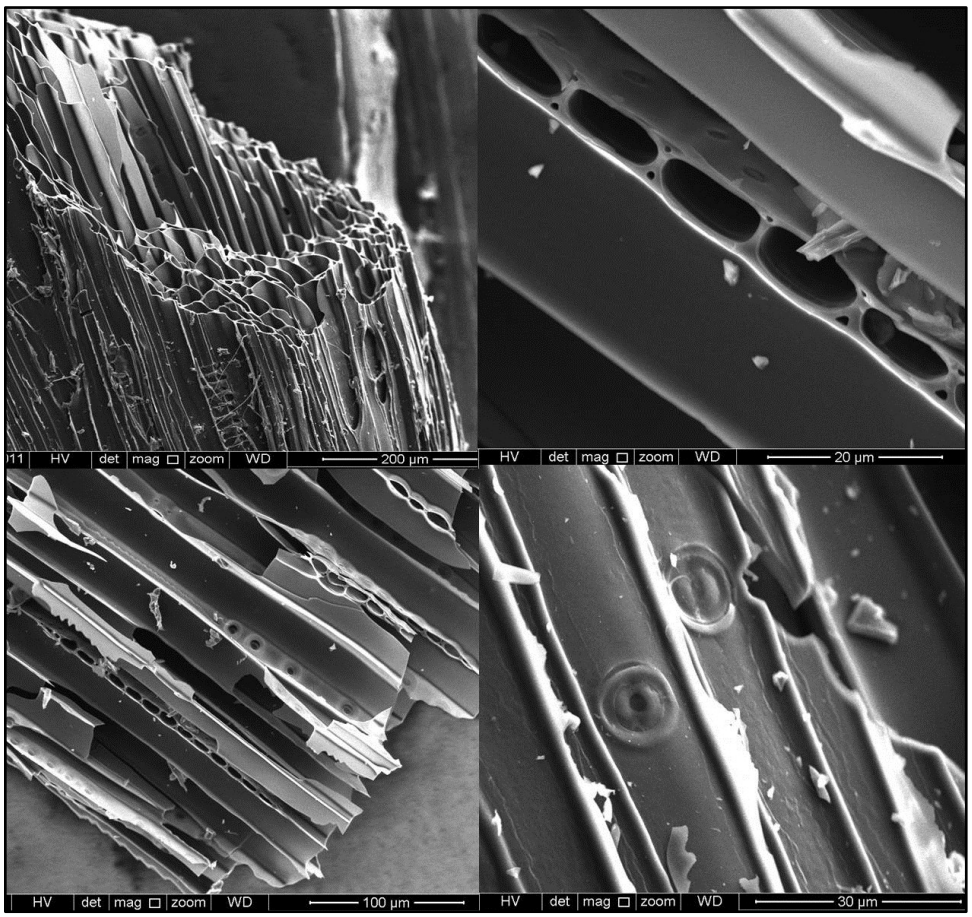

Figure 9 – Vascular structures of the original plant material (fir) reflected in its pyrolysis product (500°C, 30 min).

As aforementioned, char physical structure (e.g., surface area and pore size distribution) is typically related to its capacity to retain water, nutrient and

pollutants from the surrounding environment. This property, in turn, influences its effect when applied to soil.

To maximize its benefits, it is crucial to understand biochar physicochemical variations originating from the parent material. Optimizing biochar for a specific agronomical or environmental application requires a careful selection of a determined feedstock in order to produce a char with the desired characteristics.

2.5.2 Process temperature

Pyrolysis process greatly affects biochar characteristics and properties and, consequently, its potential value in terms of agronomic performance or carbon sequestration. Both the process and its parameters (mainly the final temperature reached and the residence time) are particularly important in determining the nature of the final product.

Two important parameters influenced by process temperature (PT) are pyrolysis yield and char elemental content. As PT increases, the yield in terms of solid product decreases (Lehmann, 2007; Zhao et al., 2013), whereas the proportion of inorganic mineral substance increases (Al-Wabel et al., 2013). During pyrolysis, the starting material loses organic matter in the form of hydrogen, oxygen and nitrogen compounds, thereby resulting rich in inorganic materials (Shinogi and Kanri, 2003; Demirbas, 2004b; Laird et al., 2011). For example, in char produced from chicken manure, the ash content increases from 40% to 60%, as temperature rises from 300°C to 600°C (Cimò et al., submitted). Parallel to ash content, pH rises with PT (Lehmann, 2007; Al-Wabel et al., 2013; Zhao et al., 2013).

Several studies (Antal and Grønli, 2003; Lehmann and Joseph, 2009) also reported a consistent increase in char carbon content with increasing temperature. Biochars produced at low PT (<350°C) have C content variable from 15 to 60%. Between 400 and 500°C, the C content rises in the range 60-

80% and above 500°C, it reaches values higher than 80%. But this statement is valid mostly for wood-derived char. Indeed, carbon materials produced from animal products (e.g., manure) showed the opposite trend (Alèn et al., 1996; Gaskin et al., 2008), probably due to their higher ash content. According to Gaskin et al. (2008), char carbon concentration decreases with increasing mineral content of the feedstock.

Furthermore, as reported in literature (Antal and Grønli, 2003; Lehmann and Joseph, 2009; De Pasquale et al., 2012), as PT is raised up, the amount of alkyl carbons contained in biochars decreases while that of the aromatic moieties increases (Fig. 10). Briefly, in the range 250–450°C, charcoal aromaticity increases with PT. Once PT reaches 500°C and above this temperature, char results mainly composed by highly recalcitrant forms of organic matter, i.e. poly-condensed aromatic carbon (Fig. 10). As a consequence, chars produced at high temperatures (>500°C) are more stable, and resist to microbial and abiotic degradation much longer than low-temperature (300°C) ones (Uchimiya et al., 2011).

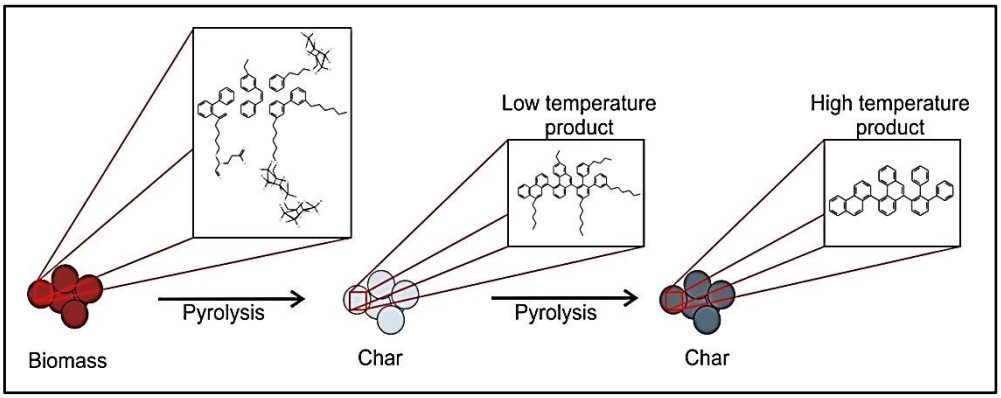

Figure 10 – Changes in biochar chemical structure and aromaticity due to pyrolysis temperature.

As PT increases, the loss of volatile compounds from the feedstock matrix determines a decrease in the surface functional groups able to generate

surface charge and provide ion exchange sites (Guo and Rockstraw, 2007). Chun et al. (2004) reported a reduction in total acidity with PT, in chars produced from wheat residues. Indeed, the chars produced at low temperatures (300-400°C) had a more polar and organic nature (higher total number of functional groups) than the ones produced above 500°C. Further studies (Glaser et al., 2002; Song and Guo, 2012; Al-Wabel et al., 2013) found a decrease in C=O and C-H functional groups on char from different biomasses, as PT rose from 300 to 700°C. This loss of polar functional surface groups as PT increases, determines the reduction of biochar retention ability. For example, Uchimiya et al. (2010; 2011) found a reduction in char heavy metal retention capacity with increasing charring temperature.

Many researchers emphasize the strong influence of process temperature also on char physical structure, such as total surface area (SA) and pore size distribution (Raveendran and Ganesh, 1998; Li et al., 2008; Lehmann and Joseph, 2009; Uchimiya et al., 2010). PT influences the amount of volatile organic compounds (VOC) released from the starting feedstock (Daud et al., 2001) resulting in porosity development. As PT increases, more VOC are released, thereby forming pores.

The findings about pore development during pyrolysis are contrasting. Several authors (Haga et al., 1991; Daud et al., 2001; Feng and Bhatia, 2003; Uchimiya et al., 2010; Bunt et al., 2012; Song and Guo, 2012) reported a progressive pore growth (increase in both pore volume and average pore size) with increasing temperatures (up to 700°C) due to the release of volatile compounds. Conversely, Chan et al. (1999), Sharma et al. (2001; 2004) and Lu et al. (2013) found an increase in chars SA when PT was raised from 300°C to 500°C, followed by its decrease above 500°C. This decrement was attributed to char structural ordering and micropore coalescence. Khalil (1999) reported very low SAs for charcoals produced from a wide variety of biomasses, pyrolyzed at temperatures around 500°C. Ronsse et al. (2013)

explained these phenomena with a restructuration taking place in biochar due to the presence of ash melting at high temperatures. Thus, in addition to PT, char SA depends on other factors, such as the starting feedstock and its ash content.

Summarizing, biochar physicochemical properties are mainly affected by feedstock characteristics and pyrolysis temperature. In particular, certain properties (e.g., biochar yield, pH, recalcitrance and volatile matter) are predominantly controlled by production temperature, whereas others (e.g., biochar carbon content, CEC, mineral concentrations and ash content) are mainly influenced by feedstock nature. By an appropriate combination of feedstock and production temperature, it would be possible to affect biochar properties in order to produce a 'designed' biochar for specific environmental or agricultural applications. For example, biochars having high porosity may be used as sorbents, those with high recalcitrance can be applied in carbon fixation, those rich in available nutrients and minerals (or with high water holding capacity) could be better used as amendments to improve soil quality.

2.6 The Italian legislation on fertilizers

In Italy, the legislative Decree No.75 (29 April 2010) "Riordino e revisione della disciplina in materia di fertilizzanti"(Gazzetta Ufficiale n. 121 del 26 maggio 2010 - Supplemento ordinario) defines the characteristics, classification and trade of fertilizers.

In order to be used and/or commercialized, fertilizers must meet the obligations under the directives of the Italian law and must be included in a national register. For the inclusion of new products in the lists of allowed fertilizers, they must meet several requirements. For example, they must be carefully characterized in terms of physical, chemical and toxicological

properties using official standard methods, their production process and its operating parameters must be traceable and standardized, and the production company must be registered in the 'manufacturers of fertilizers' register. In addition, fertilizer effects on the environment and living organisms must be known in order not to present risks, whether immediate or delayed, for one or more environmental sections.

Since each biochar produced from a different starting biomass and under different production processes has unique features and characteristics, it is not possible to generically include all the biochars in the list of soil improvers. Indeed, according to the Italian law, every single type of biochar should be characterized, described, tested and approved for use.

To solve this problem at a worldwide level, the International Biochar Initiative (IBI) organization is promoting a Biochar Certification Program, whose primary goal is to create a standardized and recognized system to certify biochar. To be certified, the materials must comply the IBI Biochar Standards to ensure that chars intended for soil application meet minimal physicochemical requirements and pass tests designed to identify the presence of certain potential toxicants. The final purpose of the program is to provide biochar manufacturers (or producers) the opportunity to certify their products in order to allow their use or sale as fertilizer, at the same time ensuring their safety.

References

Al-Wabel MI, Al-Omran A, El-Naggar AH, Nadeem M, Usman ARA (2013) Pyrolysis temperature induced changes in characteristics and chemical composition of biochar produced from conocarpus wastes. Bioresource Technol 131:374–379

Alèn R, Kuoppala E, Oesch P (1996) Formation of the main degradation compound groups from wood and its components during pyrolysis. J Anal Appl Pyrol 36:137-148

Amonette JE, Lehmann JC, Joseph S (2007) Terrestrial carbon sequestration with biochar: A preliminary assessment of its global potential. In: AGU Fall Meeting Abstracts: 6 pp

Antal MJ, Grønli M (2003) The Art, Science, and Technology of Charcoal Production. Ind Eng Chem Res 42(8):1619-1640

Appel BS, Adams TN, Roberts MJ, Lange WF, Freiss JH, Einfeldt CT, Carnesi MC (2003) Process for conversion of organic, waste, or low-value materials into useful products. Patent N. US8003833 B2

Asai H, Samson BK, Stephan HM, Songyikhangsuthor K, Homma K, Kiyono Y, Inoue Y, Shiraiwa T, Horie T (2009) Biochar amendment techniques for upland rice production in Northern Laos 1. Soil physical properties, leaf SPAD and grain yield. Field Crop Res 111:81–84

Basu P (2010) Biomass gasification and pyrolysis : practical design and theory. Elsevier. 365 pp

Beaton JD, Peterson HB, Bauer N (1960) Some aspects of phosphate adsorption by charcoal. Soil Sci Soc Am Proc 24:340–346

Beck DA, Johnson GR, Spolek GA (2011) Amending greenroof soil with biochar to affect runoff water quantity and quality. Environ Pollut 159(8-9):2111-2118

Beesley L, Moreno-Jimenez E, Gomez-Eyles JL (2010) Effects of biochar and green waste compost amendments on mobility, bioavailability and toxicity of inorganic and organic contaminants in a multi-element polluted soil. Environ Pollut 158:2282–2287

Beesley L, Marmiroli M (2011) The immobilization and retention of soluble arsenic, cadmium and zinc by biochar. Environ Pollut 159:474-480

Blackwell P, Shea S, Storer P, Solaiman Z, Kerkmans M, Stanley I (2007) Improving wheat production with deep banded oil mallee charcoal in Western Australia. In: The First Asia-Pacific Biochar Conference, Terrigal, Australia

Bridgewater AV, Meier D, Radlein D (1999) An overview of fast pyrolysis of biomass. Org Geochem 30:1479–1493

Bridgewater AV (2001) Thermal conversion of biomass and waste: the status. Birmingham (UK): Bio-Energy Research Group, Aston University

Brown R (2009) Biochar Production Technology. In: Lehmann J, Joseph S (eds) Biochar for Environmental Management: Science and Technology. Earthscan, London

Bunt JR, Waanders FB, Nel A, Dreyer L, van Rensburg PWA (2012) An understanding of the porosity of residual coal/char/ash samples from an air-blown packed bed reactor operating on inertinite-rich lump coal. J Anal Appl Pyrol 95:241–246

Chan ML, Jones JM, Pourkashanian M, Williams A (1999) The oxidative reactivity of coal chars in relation to their structure. Fuel 78(13):1539–1552

Chan KY, Van Zwieten L, Meszaros I, Downie A, Joseph S (2007) Agronomic values of greenwaste biochar as a soil amendment. Aus J Soil Res 45:629–634

Chen B, Chen Z (2009) Sorption of naphthalene and 1-naphthol by biochars of orange peels with different pyrolytic temperatures. Chemosphere 76:127–133

Chen B, Yuan M (2011) Enhanced sorption of polycyclic aromatic hydrocarbons by soil amended with biochar. J Soil Sediment 11:62–71

Chen H, Yao J, Wang F, Choi MMF, Bramanti E, Zaray G (2009) Study on the toxic effects of diphenol compounds on soil microbial activity by a combination of methods. J Hazard Mater 167: 846-851

Cheng CH, Lehmann J, Engelhard MH (2008) Natural oxidation of black carbon in soils: changes in molecular form and surface charge along a climosequence. Geochim Cosmochim Ac 72:1598–1610

Chun Y, Sheng G, Chiou CT, Xing B (2004) Compositions and Sorptive Properties of Crop Residue-Derived Chars. Environ Sci Technol 38:4649-4655

Cimò G, Kucerik J, Berns AE, Schaumann GE, Alonzo G, Conte P (submitted 2013) Effect of heating time and temperature on the chemical characteristics of biochar from poultry manure. J Agric Food Chem

Czernik S, Bridgewater AV (2004) Overview of applications of biomass fast pyrolysis oil. Energ Fuel 18:590–598

Czimczik CI, Preston CM, Schmidt MWI, Werner RA, Schulze ED (2002) Effect of charring on mass, organic carbon, and stable carbon isotope composition of wood. Org Geochem 33:1207–1223

Dagnall S (1995) UK strategy for centralized anaerobic digestion. Bioresource Technol 52(3):275-280

Daud WMAW, Ali WSW, Sulaiman MZ (2001) Effect of carbonization temperature on the yield and porosity of char produced from palm shell. J Chem Technol Biotechnol 76:1281-1285

de Jong W, Pirone A, Wòjtowicz MA (2003) Pyrolysis of *Miscanthus giganteus* and wood pellets: TG-FTIR analysis and reaction kinetics. Fuel 82:1139-1147

De Pasquale C, Marsala V, Berns AE, Valagussa M, Pozzi A, Alonzo G, Conte P (2012) Fast field cycling NMR relaxometry characterization of biochars obtained from an industrial thermochemical process. J Soil Sediment 12(8):1211-1221

Deenik JL, McClellan T, Uehara G, Antal MJ, Campbell S (2010) Charcoal volatile matter content influences plant growth and soil nitrogen transformations. Soil Sci Soc Am J 74(4):1259-1270

Demirbas A (2000) Mechanisms of liquefaction and pyrolysis reactions of biomass. Energ Convers Manage 41:633–646

Demirbas A (2004a) Combustion characteristics of different biomass fuels. Prog Energ Combust 30:219–230

Demirbas A (2004b) Effects of temperature and particle size on bio-char yield from pyrolysis of agricultural residues. J Anal Appl Pyrol 72(2):243-248

Demirbas A (2009) Biorefineries: Current activities and future developments. Energ Convers Manage 50:2782–2801

Demirbas A, Balat M (2007) Biomass pyrolysis for liquid fuels and chemicals: a review. J Sci Ind Res 66:797-804

Erlich C, Björnbom E, Bolado D, Giner M, Fransson TH (2006) Pyrolysis and gasification of pellets from sugar cane bagasse and wood. Fuel 85(10-11):1535-1540

Ezawa T, Yamamoto K, Yoshida S (2002) Enhancement of the effectiveness of indigenous arbuscular mycorrhizal fungi by inorganic soil amendments. Soil Sci Plant Nutr 48:897–900

Farrell AE, Plevin RJ, Turner BT, Jones AD, O'Hare M, Kammen DM (2006) Ethanol Can Contribute to Energy and Environmental Goals. Science 311:506-508

Fellet G, Marchiol L, Delle Vedove G, Peressotti A (2011) Application of biochar on mine tailings: effects and perspectives for land reclamation. Chemosphere 83:1262-1297

Feng B, Bhatia SK (2003) Variation of the pore structure of coal chars during gasification. Carbon 41:507–523

Fushimi C, Araki K, Yamaguchi Y, Tsutsumi A (2003) Effect of Heating Rate on Steam Gasification of Biomass. 2. Thermogravimetric-Mass Spectrometric (TG-MS) Analysis of Gas Evolution. Ind Eng Chem Res 42:3929-3936

Gaskin JW, Steiner C, Harris K, Das KC, Bibens B (2008) Effect of low-temperature pyrolysis conditions on biochar for agricultural use. T Asabe 51:2061–2069

Glaser B, Haumaier L, Guggenberger G, Zech W (2001) The 'Terra Preta' phenomenon: A model for sustainable agriculture in the humid tropics. Naturwissenschaften 88:37–41

Glaser B, Lehmann J, Zech W (2002) Ameliorating physical and chemical properties of highly weathered soils in the tropics with charcoal- a review. Biol Fert Soils 35:219-230

Graber ER, Harel YM, Kolton M, Cytryn E, Silber A, David DR, Tsechansky L, Borenshtein M, Elad Y (2010) Biochar impact on development and productivity of pepper and tomato grown in fertigated soilless media. Plant and Soil 337:481-496

Granastein D, Kruger CE, Collins H, Galinato S, Garcia-Perez M, Yoder J (2009) Use of biochar from the pyrolysis of waste organic material as a soil amendment. Final project report. Center for Sustaining Agriculture and Natural Resources, Washington State University, Wenatchee, WA. 168 pp

Gundale MJ, DeLuca TH (2006) Temperature and source material influence ecological attributes of Ponderosa pine and Douglas-fir charcoal. For Ecol Manag 231:86–93

Guo Y, Rockstraw DA (2007) Physicochemical properties of carbons prepared from pecan shell by phosphoric acid activation. Bioresource Technol 98:1513–1521

Haga T, Nishiyama Y, Agarwal PK, Agnew JB (1991) Surface structural changes of coal upon heat treatment at 200-900.degree.C. Energ Fuels 5(2):312–316

Herath HMSK, Camps-Arbestain M, Hedley M (2013) Effect of biochar on soil physical properties in two contrasting soils: an Alfisol and an Andisol. Geoderma (209–210):188–197

Higman C, van der Burgt M (2008) Gasification, 2nd ed. Gulf Professional Publishing. Elsevier.

Ishii T, Kadoya K (1994) Effects of charcoal as a soil conditioner on citrus growth and vesicular-arbuscular mycorrhizal development. J Am Soc Hortic Sci 63:529–535

Intergovernmental Panel on Climate Change (IPCC) Final report. Climate change 2013: The Physical Science Basis. Contribution of Working Groups I, II and III to the fifth assessment report of the intergovernmental panel on climate change. Geneva, Switzerland

Jenkins BM, Baxter LL, Miles Jr TR, Miles TR (1998) Combustion properties of biomass. Fuel Process Technol 54:17–46

Karami N, Clemente R, Moreno-Jiménez E, Lepp NW, Beesley L (2011) Efficiency of green waste compost and biochar soil amendments for reducing lead and copper mobility and uptake to ryegrass. J Hazard Mater 191:41–48

Karaosmanoglu F, Tetik E (1999) Charcoal from the pyrolysis of rapeseed plant straw-stalk. Energ Source 21:503–510

Kasozi GN, Zimmerman AR, Nkedi-Kizza P, Gao B (2010) Catechol and humic acid sorption onto a range of laboratory-produced black carbons (biochars). Environ Sci Technol 44:6189-6195

Keech O, Carcaillet C, Nilsson MC (2005) Adsorption of allelopathic compounds by wood-derived charcoal: the role of wood porosity. Plant and Soil 272:291–300

Khalil LB (1999) Porosity characteristics of chars derived from different lignocellulosic materials. Adsorpt Sci Technol 17:729−739

Kimetu JM, Lehmann J, Ngoze SO, Mugendi DN, Kinyangi JM, Riha S, Verchot L, Recha JW, Pell AN (2008) Reversibility of soil productivity decline with organic matter of differing quality along a degradation gradient. Ecosystems 11:726–739

Kishimoto S, Sugiura G (1985) Charcoal as a soil conditioner. Int Achieve Future 5:12–23

Klass DL (1998) Biomass for Renewable Energy, Fuels, and Chemicals. Academic Press, 650 pp.

Kleineidam S, Rugner H, Ligous B, Grathwohl P (1999) Organic matter facies and equilibrium sorption of phenanthrene. Environ Sci Tech 33:1637–1644

Kloss S, Zehetner F, Dellantonio A, Hamid R, Ottner F, Liedtke V, Schwanninger M, Gerzabek MH, Soja G (2012) Characterization of slow pyrolysis biochars: effects of feedstocks and pyrolysis temperature on biochar properties. J Environ Qual 41:990–1000

Knoef HAM (2005) Handbook Biomass Gasification. Biomass Technology Group Publisher, Enschede, The Netherlands

Kraxner F, Nilsson S, Obersteiner M (2003) Negative emissions from bioenergy use, carbon capture and sequestration (BECS): the case of biomass production by sustainable forest management from seminatural temperate forests. Biomass Bioenerg 24(4):285–296

Krull ES, Baldock JA, Skjemstad JO, Smernik RJ (2009) Characteristics of biochar: Organo-chemical properties. In: Lehmann J, Joseph S (eds) Biochar for Environmental Management, Science and Technology. Earthscan, London

Laird AD (2008) The charcoal vision: A win-win-win scenario for simultaneously producing bioenergy, permanently sequestering carbon, while improving soil and water quality. Agron J 100: 178-181

Laird D, Fleming P, Wang B, Horton R, Karlen D (2010a) Biochar impact on nutrient leaching from a Midwestern agricultural soil. Geoderma 158:436–442

Laird D, Fleming P, Davis DD, Horton R, Wang B, Karlen DL (2010) Impact of biochar amendments on the quality of a typical Midwestern agricultural soil. Geoderma 158:443–449

Laird DA, Rogovska N, Garcia-Perez M, Collins HP, Streubel JD, Smith M (2011) Pyrolysis and Biochar-Opportunities for Distributed Production and Soil Quality Enhancement. In: Braun R, Karlen DL, Johnson D (eds) Sustainable Alternative Fuel Feedstock Opportunities, Challenges and Roadmaps for Six U.S. Regions. Proceedings of the Sustainable Feedstock for Advanced Biofuel Workshop. SWCS publisher.

Lambers H, Raven JA, Shaver GR, Smith SE (2008) Plant nutrient-acquisition strategies change with soil age. Trends Ecol Evol 23:95–103

Lehmann J (2007) Bio-energy in the black. Front Ecol Environ 5(7):381–387

Lehmann J, Czimczik C, Laird D, Sohi S (2009) Stability of biochar in the soil. In: Lehmann J, Joseph S (eds). Biochar for environmental management: science and technology. Earthscan, London.

Lehmann J, da Silva Jr JP, Steiner C, Nehls T, Zech W, Glaser B (2003) Nutrient availability and leaching in an archaeological Anthrosol and a Ferralsol of the Central Amazon basin: fertilizer, manure and charcoal amendments. Plant and Soil 249:343–357

Lehmann J, Joseph S (2009) Biochar for environmental management: science and technology. London: Earthscan. 416 pp

Lehmann J, Rillig MC, Thies J, Masiello CA, Hockadayd WC, Crowley D (2011) Biochar effects on soil biota. A review. Soil Biol Biochem 43:1812-1836

Li W, Yang K, Peng J, Zhang L, Guo S, Xia H (2008) Effects of carbonization temperatures on characteristics of porosity in coconut shell chars and activated carbons derived from carbonized coconut shell chars. Ind Crop Prod 28:190–198

Lian F, Huang F, Chen W, Xing B, Zhu L (2011) Sorption of apolar and polar organic contaminants by waste tire rubber and its chars in single- and bi-solute systems. Environ Pollut 159:850-857

Liang L, Mao Z, Li Y, Wan C, Wang T, Zhang L (2006) Liquefaction of crop residues for polyol production. Bioresource 1:248–256

Liang B, Lehmann J, Solomon D, Kinyangi J, Grossman J, O'Neill B, Skjemstad JO, Thies J, Luizao FJ, Petersen J, Neves EG (2006) Black Carbon increases cation exchange capacity in soils. Soil Sci Soc Am J 70:1719-1730

Lima IM, Marshall WE (2005) Granular activated carbons from broiler manure: physical, chemical and adsorptive properties. Bioresource Technol 96:699–706

Liu Y, Yang M, Wu Y, Wang H, Chen Y, Wu W (2011) Reducing CH_4 and CO_2 emissions from waterlogged paddy soil with biochar. J Soil Sediment DOI 10.1007/s11368-011-0376-x

Loppinet-Serani A, Aymonier C, Cansell F (2008) Current and foreseeable applications of supercritical water for energy and the environment. ChemSusChem 1:486–503

Lu H, Zhang W, Wang S, Zhuan L, Yang Y, Qiu R (2013) Characterization of sewage sludge-derived biochars from different feedstocks and pyrolysis temperatures. J Anal Appl Pyrol 102:137–143

Major J, Rondon M, Molina D, Riha SJ, Lehmann J (2010) Maize yield and nutrition during 4 years after biochar application to a Colombian savanna oxisol. Plant and Soil 333(1-2):117-128

Maldas D, Shirai N (1997) Liquefaction of biomass in the presence of phenol and H_2O using alkalis and salts as the catalyst. Biomass Bioenerg 12:273–279

Mao JD, Johnson RL, Lehmann J, Olk DC, Neves EG, Thompson ML, Schmidt-Rohr K (2012) Abundant and Stable Char Residues in Soils: Implications for Soil Fertility and Carbon Sequestration. Environ Sci Technol 46:9571−9576

Marquevich M, Czernik S, Chornet E, Montané D (1999) Hydrogen from biomass: steam reforming of model compounds of fast-pyrolysis oil. Energ Fuel 13:1160–1166

Maschio G, Koufopanos C, Lucchesi A (1992) Pyrolysis, a promising route for biomass utilization. Bioresour Technol 42:219–231

Mathews JA (2008) Carbon-negative biofuels. Energy Policy 36:940–945

Matsubara YI, Hasegawa N, Fukui H (2002) Incidence of *Fusarium* root rot in asparagus seedlings infected with arbuscular mycorrhizal fungus as affected by several soil amendments. J Jpn Soc Hortic Sci 71:370–374

McKendry P (2002a) Energy production from biomass (part 1): overview of biomass. Bioresour Technol 83:37–46

McKendry P (2002b) Energy production from biomass (part 3): gasification technologies. Bioresour Technol 83:55–63

Mikan CJ, Abrams MD (1995) Altered forest composition and soil properties of historic charcoal hearths in southeastern Pennsylvania. Can J Forest Res 25:687–696

Mizuta K, Matsumoto T, Hatate Y, Nishihara K, Nakanishi T (2004) Removal of nitrate-nitrogen from drinking water using bamboo powder charcoal. Bioresource Technol 95:255–257

Mohan SV, Karthideyan J (1997) Removal of lignin and tannin color from aqueous solution by adsorption onto activated charcoal. Environ Pollut 97:183–187

Mohan D, Pittman CU, Steele PH (2006) Pyrolysis of wood/biomass for bio-oil: a critical review. Energ Fuel 20:848-889

Mohan D, Rajput S, Singh VK, Steele PH, Pittman Jr CU (2011) Modeling and Evaluation of Chromium Remediation from Water using Low Cost Bio-Char, a Green Adsorbent. J Hazard Mater 188(1-3):319-333

Mok WS-L, Antal Jr MJ, Szabo P, Varhegyi G, Zelei B (1992) Formation of charcoal from biomass in a sealed reactor. Ind Eng Chem Res 31:1116–1162

Mozaffari M, Russelle MP, Rosen CJ, Nater EA (2002) Nutrient Supply and Neutralizing Value of Alfalfa Stem Gasification. Ash. Soil Sci Soc Am J 66:171–178

Namgay T, Singh B, Singh BP (2010) Influence of biochar application to soil on the availability of As, Cd, Cu, Pb, and Zn to maize (*Zea mays* L.). Aust J Soil Res 48:638-647

National Non-Food Crops Centre. "NNFCC Renewable Fuels and Energy Factsheet: Anaerobic Digestion", http://www.nnfcc.co.uk/publications/nnfcc-renewable-fuels-and-energy-factsheet-anaerobic-digestion. Retrieved on 2013-11-06

Ni M, Leung DYC, Leung MKH, Sumathy K (2006) An overview of hydrogen production from biomass. Fuel Process Technol 87:461–472

Novak JM, Busscher WJ, Laird DL, Ahmedna M, Watts DW, Niandou MAS (2009) Impact of Biochar Amendment on Fertility of a Southeastern Coastal Plain Soil. Soil Science 174(2):105-112

Novotny EH, Hayes MHB, Madari BE, Bonagamba TJ, deAzevedo ER, de Souza AA, Song GX, Nogueira CM, Mangrich AS (2009) Lessons from the Terra Preta de Indios of the Amazon region for the utilization of charcoal for soil amendment. J Brazil Chem Soc 20:1003–1010

Ogawa M, Okimori Y, Takahashi F (2006) Carbon sequestration by carbonization of biomass and forestation: three case studies. Mitig Adapt Strat Gl 11:429-444

Pietikäinen J, Kiikkilä O, Fritze H (2000) Charcoal as a habitat for microbes and its effects on the microbial community of the underlying humus. Oikos 89:231-242

Piskorz J, Scott DS, Radlien D (1988) Composition of oils obtained by fast pyrolysis of different woods (Chapter 16). In: Soltes J, Milne TA (Eds.), Pyrolysis Oils from Biomass: Producing, Analyzing and Upgrading. American Chemical Society, 167–178

Pohlmeier A, Haber-Pohlmeier S, Stapf S (2009) A fast field cycling nuclear magnetic resonance relaxometry study of natural soils. Vadose Zone J 8**:**735-742

Probstein RF, Hicks RE (2006) Synthetic Fuels. Dover Publications, 63 pp.

Pütün AE (2002) Biomass to bio-oil via fast pyrolysis of cotton straw and stalk. Energ Source 24: 275-285

Ramanathan V, Carmichael G (2008) Global and regional climate changes due to black carbon. Nature Geosci 1(4):221-227

Raveendran K, Ganesh A (1998) Adsorption characteristics and pore-development of biomass-pyrolysis char. Fuel 77(7):769-781

Rezaiyan J, Cheremisinoff NP (2005) Gasification technologies – a primer for engineers and scientists. CRC Press Taylor & Francis Groups, Boca Raton (FL)

Rillig MC, Wagner M, Salem M, Antunes PM, George C, Ramke HG, Titirici MM, Antonietti M (2010) Material derived from hydrothermal carbonization: Effects on plant growth and arbuscular mycorrhiza. Appl Soil Ecol 45(3):238-242

Rocha JD, Brown SD, Love GD, Snape CE (1997) Hydropyrolysis: a versatile technique for solid fuel liquefaction, sulphur speciation and biomarker release. J Anal Appl Pyrol (40–41):91–103

Rondon M, Ramirez J, Lehmann J (2005) Charcoal additions reduce net emissions of greenhouse gases to the atmosphere. In Proceedings of the 3rd USDA Symposium on Greenhouse Gases and Carbon Sequestration; March 21–24, Baltimore, MD. 208 pp

Rondon MA, Lehmann J, Ramirez J, Hurtado M (2007) Biological nitrogen fixation by common beans (*Phaseolus vulgaris* L.) increases with bio-char additions. Biol Fert Soils 43:699-708

Ronsse F, van Hecke S, Dickinson D, Prins W (2013) Production and characterization of slow pyrolysis biochar: influence of feedstock type and pyrolysis conditions. GCB Bioenergy 5:104–115

Schmidt MWI, Noack AG (2000) Black carbon in soils and sediments: Analysis, distribution, implications, and current challenges. Global Biogeochem Cy 14(3):777-793

Sharma RK, Wooten JB, Baliga VL, Hajaligol MR (2001) Characterization of chars from biomass-derived materials: pectin chars. Fuel 80(12):1825-1836

Sharma RK, Wooten JB, Baliga VL, Lin X, Chan WG, Hajaligol MR (2004) Characterization of chars from pyrolysis of lignin. Fuel 83(11–12):1469-1482

Sheng G, Yang Y, Huang M, Yang K (2005) Influence of pH on pesticide sorption by soil containing wheat residue-derived char. Environ Pollut 134:457–463

Shinogi Y, Kanri Y (2003) Pyrolysis of plant, animal and human waste: physical and chemical characterization of the pyrolytic products. Bioresource Technol 90(3):241-247

Singh BP, Panigrahi MR, Ray HS (2000) Review of biomass as a source of energy for India. Energ Source 22:649–658

Sohi SP, Krull E, Lopez-Capel E, Bol R (2010) A review of biochar and its use and function in soil. Adv Agron 105:47-82

Shinogi Y, Yoshida H, Koizumi T, Yamaoka M, Saito T (2003) Basic characteristics of low-temperature carbon products from waste sludge. Adv Environ Res 7:661–665

Sombroek WG, Nachtergaele FO, Hebel A (1993) Amounts, dynamics and sequestering of carbon in tropical and subtropical soils. Ambio 22:417–426.

Song W, Guo M (2012) Quality variations of poultry litter biochar generated at different pyrolysis temperatures. J Anal Appl Pyrol 94:138–145

Steiner C, Teixeira WG, Lehmann J, Nehls T, Vasconcelos de Macêdo JL, Blum WEH, Zech W (2007) Long term effects of manure, charcoal and mineral fertilization on crop production and fertility on a highly weathered Central Amazonian upland soil. Plant Soil. DOI 10.1007/s11104-007-9193-9

Steiner C, de Arruda MR, Teixeira WG, Zech W (2008a) Soil respiration curves as soil fertility indicators in perennial central Amazonian plantations treated with charcoal, and mineral or organic fertilizers. Trop Sci 47:218–230

Steiner C, Das KC, Garcia M, Förster B, Zech W (2008b) Charcoal and smoke extract stimulate the soil microbial community in a highly weathered xanthic ferralsol. Pedobiologia 51(5-6):359-366

Steiner C, Glaser B, Teixeira WG, Lehmann J, Blum WEH, Zech W (2008c) Nitrogen retention and plant uptake on a highly weathered central Amazonian ferralsol amended with compost and charcoal. J Plant Nutr Soil Sci 171:893–899

Sudhakar Y, Dikshit AK (1999) Kinetics of endosulfan sorption onto wood charcoal. J Environ Sci Health B 34: 587–615

Trautmann N, Olynciw E (2000) Compost Microorganisms. Cornell Composting – Science & Engineering. Web reference.

Uchimiya M, Lima IM, Klasson KT, Chang S, Wartelle LH, Rodgers JE (2010) Immobilization of Heavy Metal Ions (Cu^{II}, Cd^{II}, Ni^{II}, and Pb^{II}) by Broiler Litter-Derived Biochars in Water and Soil. J Agr Food Chem 58:5538–5544

Uchimiya M, Wartelle LH, Klasson KT, Fortier CA, Lima IM (2011) Influence of pyrolysis temperature on biochar property and function as a heavy metal sorbent in soil, J Agr Food Chem 59:2501–2510

Uzun BB, Pütün AE, Pütün E (2007) Composition of products obtained via fast pyrolysis of olive-oil residue: effect of pyrolysis temperature. J Anal Appl Pyrol 9:147–153

Vassilev SV, Baxter D, Andersen LK, Vassileva CG (2010) An overview of the chemical composition of biomass. Fuel 89(5):913–933

Warnock DD, Lehmann J, Kuyper TW, Rilling MC (2007) Mycorrhizal responses to biochar in soil – concepts and mechanisms. Plant Soil 309:9-20

Williams RB, Jenkins BM, Nguyen D (2003) Solid waste conversion: a review and database of current and emerging technologies – final report. California Integrated Waste Management Board

Yaman S (2004) Pyrolysis of biomass to produce fuels and chemical feedstocks. Energ Convers Manage 45:651-671

Yamato M, Okimori Y, Wibowo IF, Anshori S, Ogawa M (2006) Effects of the application of charred bark of *Acacia mangium* on the yield of maize, cowpea and peanut, and soil chemical properties in South Sumatra, Indonesia. Soil Sci Plant Nutr 52:489–495

Yanai Y, Toyota K, Okazaki M (2007) Effects of charcoal addition on N_2O emissions from soil resulting from rewetting air-dried soil in short-term incubation experiments. Soil Sci Plant Nutr 53:181–188

Yang YN, Sheng GY, Huang MS (2006) Bioavailability of diuron in soil containing wheat-straw derived char. Sci Total Environ 354:170-178

Yanik J, Kornmayer C, Saglam M, Yüksel M (2007) Fast pyrolysis of agricultural wastes: characterization of pyrolysis products. Fuel Process Technol 88:942–947

Yu XY, Ying GG, Kookana RS (2006) Sorption and desorption behaviors of diuron in soils amended with charcoal. J Agric Food Chem 54:8545–8550

Yu XY, Ying GG, Kookana RS (2009) Reduced plant uptake of pesticides with biochar additions to soil. Chemosphere 76:665-671

Yuan JH, Xu RK, Wang N, Li JY (2011) Amendment of Acid Soils with Crop Residues and Biochars. Pedosphere 21(3):302–308

Yue Z, Teater C, Liu Y, MacLellan J, Liao W (2010) A sustainable pathway of cellulosic ethanol production integrating anaerobic digestion with biorefining. Biotechnol Bioeng 105:1031–1039

Zhang P, Sheng GY, Feng YC, Miller DM (2005) Role of wheat-residue-derived char in the biodegradation of benzonitrile in soil: nutritional stimulation versus adsorptive inhibition. Environ Sci Technol 39:5442-5448

Zhang A, Cui L, Pan G, Li L, Hussain Q, Zhang X, Zheng J, Crowley D (2010) Effect of biochar amendment on yield and methane and nitrous oxide emissions from a rice paddy from Tai Lake plain, China. Agr Ecosyst Environ139:469–475

Zhang L, Xu C, Champagne P (2010) Overview of recent advances in thermo-chemical conversion of biomass. Energ Convers Manage 51:969–982

Zhao L, Cao X, Mašek O, Zimmerman A (2013) Heterogeneity of biochar properties as a function of feedstock sources and production temperatures. J Hazard Mater 256-257:1-9

Zhong C, Wei X (2004) A comparative experimental study on the liquefaction of wood. Energy 29:1731–1741

CHAPTER 3 : EFFECT OF HEATING TIME AND TEMPERATURE ON THE CHEMICAL CHARACTERISTICS OF BIOCHAR FROM POULTRY MANURE

3.1 Introduction

Chicken or poultry manure (PM) consists of digested and transformed materials containing the original litter material, feathers, and spilled feed that accumulate on the floors of the buildings where the animals are grown (Roach et al., 2009).

PM can be considered as a valuable source of readily available plant nutrients, such as N, P, K and other micronutrients (Huang et al., 2011). For this reason, PM is traditionally used by farmers as an effective organic fertilizer (Chan et al., 2008). Many studies in both temperate and tropical regions reported that large increases in soil organic matter content and fertility can be achieved by adding chicken manures and wastes to soils (Khaleel et al., 1981; Lal and Kang, 1982; Metzger and Yaron, 1987; Davies and Payne, 1988; Sanchez et al., 1989; Haynes and Naidu, 1998). In particular, the use of poultry manure also contributes to raise soil pH with favourable effects on acidic soils (Perkins et al., 1964).

Notwithstanding the advantages of PM for increasing soil fertility, there are food safety and environmental concerns about its application on agricultural sites in its unmodified form (Wilkinson et al., 2003; Chan et al., 2007). Indeed, the misuse of chicken manure as fertilizer may result in serious environmental problems (Gay et al., 2003), e.g. human and animal health risks, odours, and leaching of nitrates and other pollutants into groundwater (Fan et al., 2000). For this reason, conversion of chicken manure to char has been proposed as an attractive methodology to reduce PM volume and weight, and its stink (Shinogi and Kanri, 2003; Popov et al., 2004).

Char is a fine-grained and highly porous carbonaceous material, arising from the pyrolitic decomposition of natural or synthetic organic materials (De Pasquale et al., 2012). Due to its high carbon content and its high resistance to biological and chemical decomposition, many authors consider char applied to soils as a useful carbon sink for the atmospheric CO_2 sequestration, thereby contributing to the mitigation of the global climate changes (Schmidt and Noack, 2000; Gaunt and Lehmann, 2008; Matthews, 2008; Lehmann et al., 2009).

Application of char to soils is nowadays controversial and still matter of debates. In fact, on the one hand, significant agronomic benefits due to char application to soils have been reported (Sohi et al., 2010; Uchimiya et al., 2010; Yuan et al., 2011). On the other hand, further studies reported insignificant effects of biochar on crop yields, but also some adverse dose-dependent peculiarities (Kishimoto and Sigiura, 1985; Mikan and Abrams, 1995; Rondon et al., 2007; Rillig et al., 2010). The variability of char effects on soil properties may be due to the large variety of potential biophysical interactions and processes that occur when it is applied to soils (De Pasquale et al., 2012; Conte et al., 2013).

Char characteristics depend on the properties of the biomasses and the techniques applied for its production (Krull et al., 2009; Sohi et al., 2010; De Pasquale et al., 2012). Indeed, from the chemical point of view, all the charred materials are recognized as poly-condensed aromatic systems where the degree of poly-condensation may differ according to the technique used for their production (Lehmann and Joseph, 2009). As an example, low-temperature-produced charred systems still contain plant-growth stimulating organic compounds. A low sorption capacity for cations has been observed for high-temperature chars, which can be improved by using even higher production temperatures (Gundale and DeLuca, 2006). In addition, the poly-aromatic macro-molecular structure of charred biomasses is responsible for

their chemical and microbial recalcitrance, which is also the cause of their long mean residence time in soils (Knicker, 2011).

The physical characteristics of the charred material also depend on the nature of the biomasses subjected to the thermal stress (Wiedner et al., 2013; Zhao et al., 2013). Indeed, plant species with many large diameter cells in the stem tissues can lead to biochars containing larger amounts of macropores (Lehmann and Joseph, 2009). Macropores in biochar applied to soils may enhance soil draining properties and the capacity to retain larger molecules, such as phenolic compounds (Warnock et al., 2007).

Based on this, we can infer that understanding biochar chemical and physical properties is crucial in order to address its agronomical and environmental uses and allow meaningful pre-application quality assessments.

The aim of the present chapter is to report about the changes occurring in the structure of poultry manure biochar when it is obtained at different temperatures and heating times. For this reason, cross polarization magic angle spinning (CPMAS) ^{13}C NMR spectroscopy and thermogravimetric analysis (TGA) were used. Results will show that production temperature is more important than heating time in determining the chemical characteristics of PM biochar. Our findings appear to confirm recent data obtained on different animal and vegetal biomasses (Wolf et al., 2013; Zhao et al., 2013).

3.2 Materials and Methods

3.2.1 Sample preparation

Poultry manure (PM) was collected from a Sicilian chicken farm, Conca d'Uovo, Misilmeri, Palermo, Italy (38°3'4'' N, 13°25'32'' E). After sampling, the material was air-dried to a maximum moisture content of 20%. The manure was then charred in 300 mL Pyrex flasks at atmospheric pressure by applying three temperatures: 350°C, 450°C, and 600°C. At the beginning, residual air was still present in the system. Once reaction started, oxygen was

consumed and pyrolysis proceeded under anoxic conditions. The effectiveness of the pyrolysis was confirmed by the NMR analyses described below. For each temperature, heating times of 30 min, 60 min, 90 min, and 120 min were employed. PM chars were allowed to cool down to room temperature after pyrolysis. They were then finely ground in a ceramic mortar and dried again at 105°C overnight. The dried materials were stored in a desiccator until analyses.

3.2.2 Chemical analyses of PM chars

Elemental contents (C, H, N) for all the samples were achieved by using a Vario MicroCUBE Elemental Analyser (Elementar, Hanau, Germany). All the results are reported in Table 4. C, H and N values were not corrected for the ash and moisture contents.

Samples	Heating time (min)	C (%)	H (%)	N (%)	C/H
Poultry manure (PM)		30±2	4±1	2.6±0.3	7±2
PM char at 350°C	**30**	32±2	2.6±0.3	2.1±0.1	12±2
	60	34±1	2.63±0.03	2.4±0.3	13.0±0.3
	90	30±2	2.4±0.2	2.1±0.2	12±2
	120	31±2	1.9±0.2	2.3±0.3	16±3
PM char at 450°C	**30**	27±2	1.3±0.2	1.62±0.08	21±4
	60	30±1	1.4±0.1	1.75±0.06	21±2
	90	29±1	1.5±0.1	1.88±0.02	19±2
	120	24±1	0.9±0.2	1.5±0.2	27±7
PM char at 600°C	**30**	26±7	0.6±0.2	1.2±0.4	42±25
	60	24±2	0.50±0.01	1.08±0.04	48±5
	90	24±1	0.64±0.09	1.23±0.02	37±7
	120	25±3	0.62±0.06	1.24±0.09	40±8

Table 4 - Elemental content of poultry manure (PM) and PM chars obtained at 350, 450 and 600°C for heating times of 30, 60, 90 and 120 min. The values were not corrected for the ash content.

3.2.3 Cross polarization magic angle spinning (CPMAS) ^{13}C NMR spectroscopy

A 7.05 T Varian UNITY INOVA™ (Varian Inc., Palo Alto, CA, USA), equipped with a Apex HX wide bore probe operating at a ^{13}C frequency of 75.4 MHz, was used to acquire the ^{13}C NMR spectra. The samples were packed in 6 mm zirconium rotors with Teflon® bottom and top spacers and Vespel® drive tips. The temperature was kept constant at 25.0±0.1°C. Magic angle spinning was carried out at 8000±1 Hz. A ^{1}H RF field strength of 50.3 kHZ and a ramp of 16 kHz to account for inhomogeneity of the Hartmann-Hahn condition were applied (Berns and Conte, 2010). VNMRJ software (Version 1.1 RevisionD, Varian Inc., Palo Alto, CA, USA) was used to acquire all the free induction decays (FID). Spectra elaboration was conducted by Mestre-C software (Version 4.9.9.9, Mestrelab Research, Santiago de Compostela, Spain). All the FIDs were transformed by applying first a 2 k zero filling and then an exponential filter function with a line broadening (LB) of 50 Hz. Fully automatic baseline correction using a Bernstein algorithm was applied for baseline corrections.

3.2.4 Thermogravimetric analysis (TGA)

Thermogravimetric analysis was carried out using a Netzsch Simultaneous Thermal Analyzer STA 449 F3 Jupiter (Netzsch-Gerätebau GmbH, Selb, Germany). Alumina crucibles were used as sample holder. Prior to analyses, grounded PM chars were equilibrated in a chamber with controlled humidity (relative humidity of 40%). For the thermoanalytical experiments, the following conditions were applied: heating rate of 10°C·min^{-1} from 30 to 1000°C, under dynamic air atmosphere, flow rate 50 ml·min^{-1}, sample mass about 10 mg (weighted with an accuracy of ±0.001 mg). The measurements were repeated three times for each sample. Data were analyzed using the Netzsch Star software (NETZSCH Proteus software). The TG curves were

derivated (DTG) in order to improve their resolution with respect to the number of degradation steps and their onsets. The first derivative of the TG trace represents the mass loss rate (expressed as $\%\cdot min^{-1}$) as a function of the temperature. DTG curves are represented as a series of peaks, instead of an "integrate" stepwise curve (TG), in which the areas under the peaks are proportional to the total mass change of the sample (Wendlandt, 1986). In this way, even subtle mass-changes, not evident in the TG curves, can be highlighted by a DTG peak (Wendlandt, 1986).

3.3 Results and Discussion

3.3.1 CPMAS ^{13}C NMR investigations

Figure 11 shows the CPMAS ^{13}C NMR spectra of the poultry manure (PM) and Figure 12 its char derivatives produced at 350, 450 and 600°C for charring times of 30, 60, 90 and 120 min.

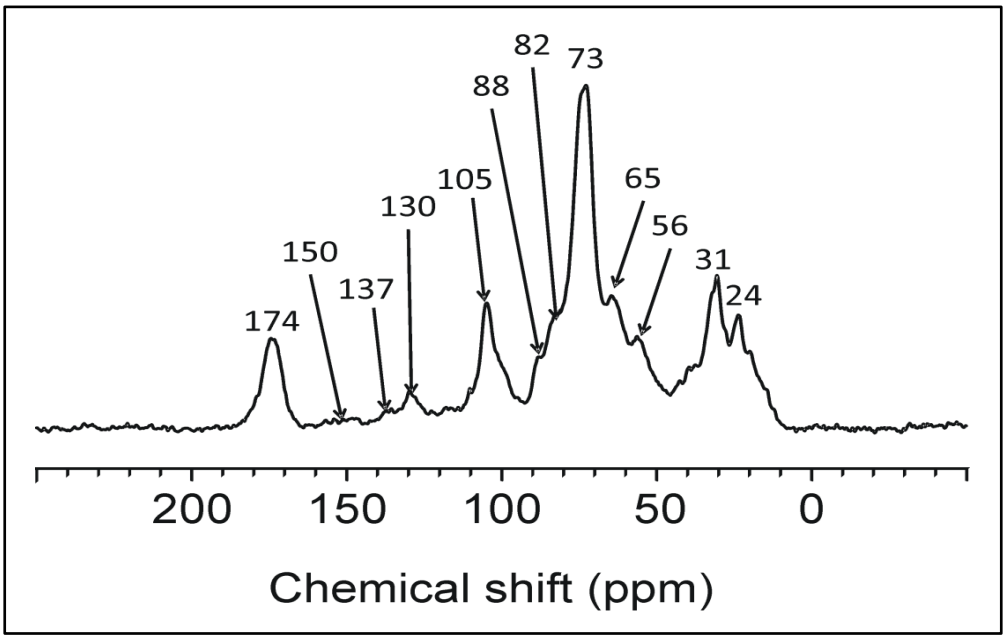

Figure 11 - CPMAS ^{13}C NMR spectrum of the poultry manure.

The PM spectrum (Fig. 11) reveals a signal pattern which is due to the typical plant material provided as food to chickens. In fact, signals in the region 0-50 ppm are traditionally attributed to alkyl systems. Here, a predominance of methylene (-CH_2-) chains (peaks at 24 and 31 ppm) due to lipids, cutin-like structures and other aliphatic bio-molecules can be observed (Gómez et al., 2007; Conte et al., 2010). The region comprised in the interval 50-60 ppm is assigned to both nitrogenated and oxygenated alkyl systems. However, only a signal at 56 ppm is visible. The latter is usually attributed to methoxyl groups in lignin-like structures (Gómez et al., 2007; Conte et al., 2010). The NMR signal pattern between 60 and 110 ppm is assigned to carbohydrates. Here, cellulose carbons resonate at 65 ppm (C-6), 73 ppm (C-2, C-3, C-5), 82 ppm (C-4 in amorphous cellulose, hemicellulose and cellulose oligomers) and 88 ppm (C-4 of cellulose on fibril surfaces) (Conte et al., 2010). The anomeric carbon in cellulose appears at 105 ppm (Gómez et al., 2007; Conte et al., 2010). The aromatic carbon spectral region is represented by the interval 110-160 ppm. The PM spectrum in Figure 11 reveals aromatic signals at 130, 137 and 150 ppm. Due to the aforementioned signal at 56 ppm, aromatic signals are most likely assigned to lignin-like systems (Wilson, 1987; Conte et al., 2010). In particular, the signal at 130 ppm is generated by *p*-hydroxyphenol derivatives, whereas those at 137 and 150, by syringil-like systems (Conte et al., 2010). The last signal at 174 ppm is assigned to carboxyl groups.

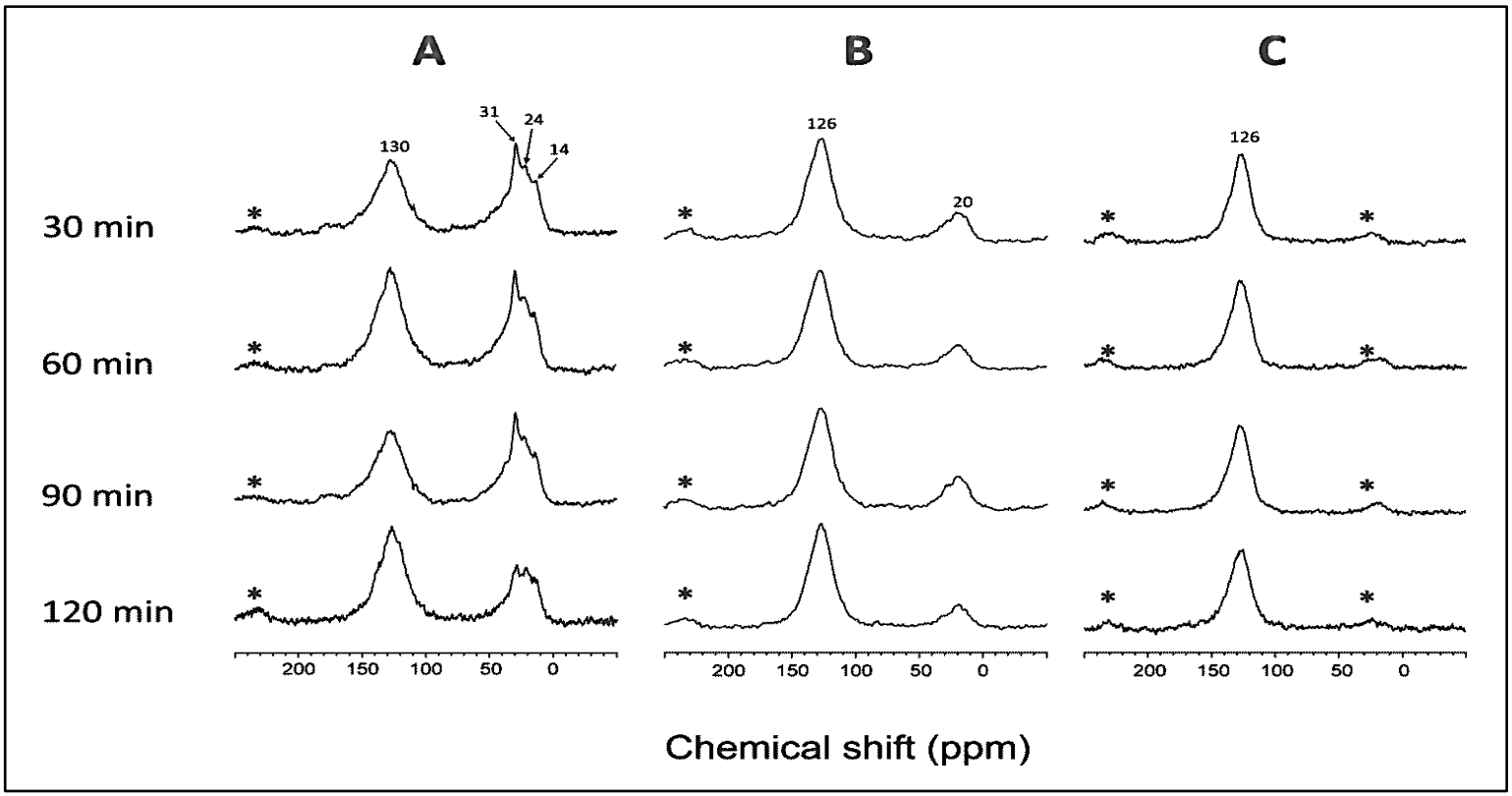

Figure 12 - CPMAS ^{13}C NMR spectra of the poultry manure chars produced at 350°C (A), 450°C (B) and 600°C (C) for the heating times of 30, 60, 90 and 120 minutes. The position of spinning sidebands (SSBs) is marked with an asterisk (*). Note that the high-field SSB is overlapped by the alkyl resonances in the chemical shift interval 0-50 ppm.

After pyrolysis at 350°C, the chemical composition of poultry manure drastically changed (Fig. 12A). In fact, regardless of the muffle residence time, only two sets of broad bands are observed in the alkyl (0-45 ppm) and aromatic (110-160 ppm) regions. In particular, three main signals can be recognized in the alkyl interval of the spectra, whereas the aromatic carbons produce only one broad signal centered at 130 ppm (Fig. 12A). The three main alkyl signals are placed at 14, 24 and 31 ppm. Whereas the latter two can be attributed to methylene chains as reported above, the former signal (14 ppm) is generated by methyl groups terminating alkyl chains. The presence of large amounts of alkyl carbons in the 350°C charred PM (Fig. 12A) shows that the temperature of 350°C is not sufficient to completely pyrolize the poultry manure. In particular, aliphatic chains and carbohydrates are converted partly to polycyclic aromatic systems and partly to shorter alkyl moieties. These can either be immobilized to bridge aromatic moieties or be methyl-containing linear substituents on aromatic rings (Lehmann and Joseph, 2009; De Pasquale et al., 2012).

At the longest residence time (120 min), the signal at 31 ppm, which stems from $–CH_2–$ groups inside aliphatic chains, is noticeably reduced compared to the signals at 24 and 14 ppm. This indicates that the aliphatic content decreases with longer residence times, and also the chain length is reduced.

As reported in literature (e.g. Lehmann and Joseph, 2009), the amount of alkyl carbons decreases while that of the aromatic moieties increases, as charring temperature is raised up. This is confirmed by the spectra of the poultry manure charred at 450 and 600°C (Figs. 12B and 12C, respectively). The pyrolysis at 450°C at all muffle residence times produces charred materials containing mainly aromatic carbons (broad band at 126 ppm in the spectra of Fig. 12B). A strong reduction of the alkyl signal intensity is observed as compared to the spectra in Figure 12A. The comparison between

the spectra in Figure 12A and 12B shows also a loss of resolution of the alkyl band in the spectrum of the biochar retrieved at 450°C. This finding can be explained by the reduction of the number of methyl-rich linear substituents and the formation of methyl-free alkyl bridges between aromatic rings.

The alkyl signal completely disappears after pyrolysis at 600°C (Fig. 12C), thereby supporting previous results showing that aromatic carbons are the main components in char systems when they are produced with temperatures above 500°C (Zhao et al., 2013).

It is worth noting that the NMR spectra of the chars obtained at each temperature were similar to each other regardless of the applied charring time (i.e. comparison of the spectra in Figure 12 from top to bottom along columns A, B and C). However, a shift of 4 ppm of the aromatic carbon chemical shift value can be observed when the spectra in Figure 12 are compared at the same charring time for the different temperatures. Indeed, the aromatic carbons resonate at 130 ppm in the spectrum of the poultry manure charred at 350°C, whereas they appear at 126 ppm in the spectra of the PM chars obtained at 450 and 600°C. According to McBeath and Smernik (2009), the higher the heating temperature applied for PM charring, the lower is the chemical shift value for the resonance of the aromatic carbons. This is due to the enhancement of the aromatic polycondensation degree as charring temperature is raised up.

The elemental content reported in Table 4 further confirms the results from CPMAS ^{13}C NMR experiments. On the one hand, no changes are observed in the elemental compositions of the chars retrieved at the different heating times when pyrolysis is done at the three temperatures of 350, 450 and 600°C. This indicates that heating temperature is more important than heating time in affecting the chemical nature of PM chars, thereby confirming recent results by Wolf et al. (2013) and Zhao et al. (2013) on different char materials. On the other hand, the C/H ratio increases with increasing charring

temperature (Tab. 4). The larger the C/H ratio, the higher the polycondensation degree of organic systems. This supports the conclusion that higher charring temperatures favor the formation of polycondensed aromatic rings (McBeath and Smernik, 2009).

3.3.2 Thermogravimetric analysis

Figure 13 reports the thermogravimetic (TG) records (full lines) of the poultry manure and its char products together with the first derivative curve (DTG, dashed lines). The latter curve reflects the rate of the thermo-oxidative degradation (Kucerik et al., 2004). The chemical similarity among chars as evidenced by CPMAS ^{13}C NMR spectroscopy (see above) is also reflected in the TG/DTG curves reported in Figure 13. For this reason, only the TG/DTG profiles of the chars obtained at the heating time of 120 min are reported in Figure 13.

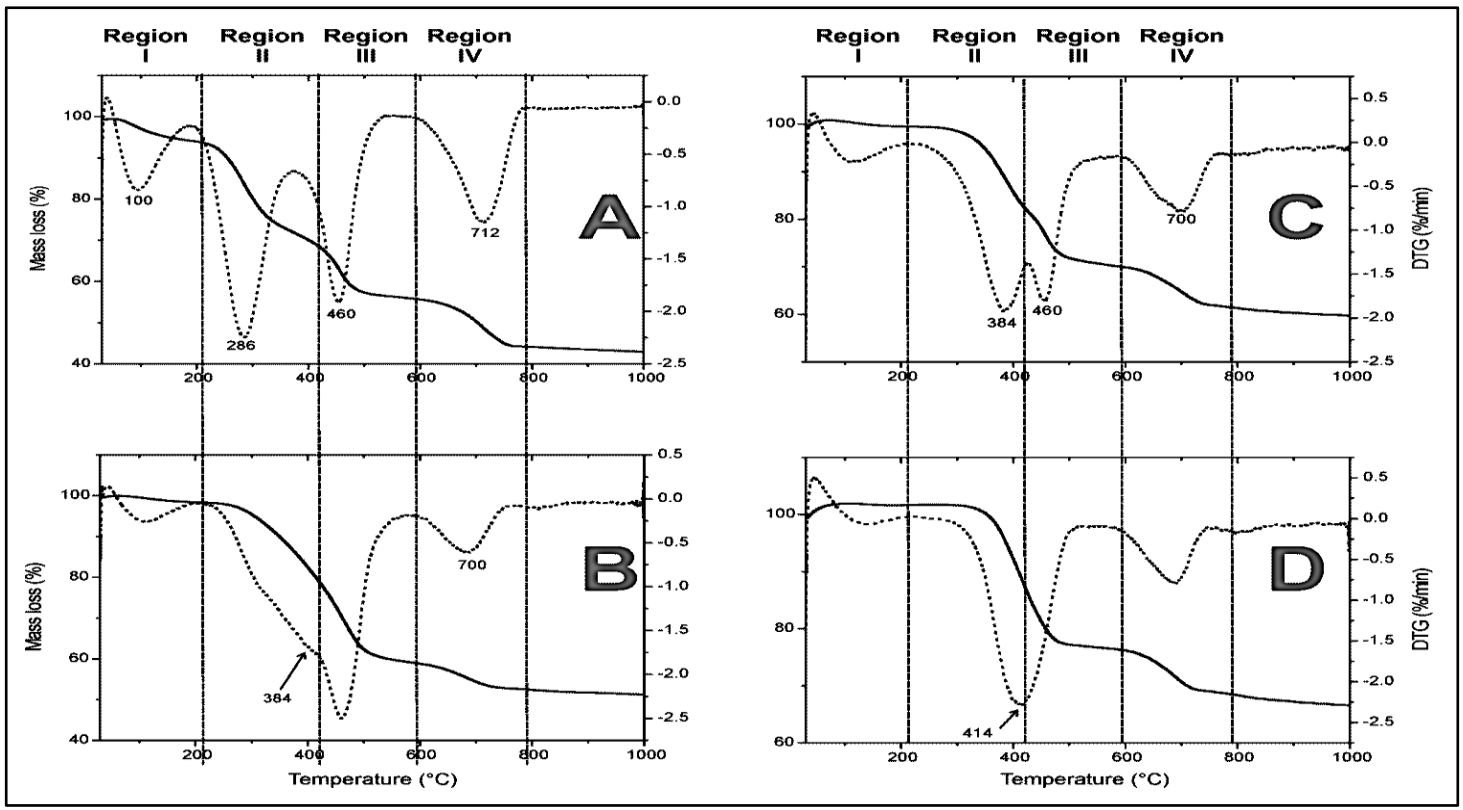

Figure 13 - Thermograms (TG, full lines) and first derivatives of the thermograms (DTG, dotted curves) for the poultry manure (A) and the PM chars obtained at 350°C (B), 450°C (C) and 600°C (D) for the heating time of 120 min.

Four different regions can be identified. Region I refers to water removal; region II describes the mass loss due to thermal transformation of carbohydrates and alkyl labile systems; region III is associated to the thermal transformation of aromatic moieties; region IV is due to transformation of the inorganic components of poultry manure chars.

TG investigations revealed that mass loss (ML) varied in the order: $ML_{600°C}<ML_{450°C}<ML_{350°C}\approx ML_{PM}$ (Fig. 13). This was expected because charring processes progressively reduce sample carbon, hydrogen and nitrogen contents as heating temperature is increased (Alèn et al., 1996; Gaskin et al., 2008). Table 4 supports the latter findings. Indeed, carbon amount varied from a mean value of ≈30% in the PM and PM chars obtained at 350°C, to an average of ≈28% in the 450°C PM chars and to an average of ≈25% in the chars retrieved at 600°C. Reduction of H and N contents followed the same trend. In fact, they were in the order $H_{PM}\approx H_{PM350°C}>H_{PM450°C}>H_{PM600°C}$ and $N_{PM}\approx N_{PM350°C}>N_{PM450°C}>N_{PM600°C}$, respectively.

Each TG/DTG curve has been operationally subdivided into four different mass loss steps at four specific temperature intervals (Fig. 13) (Dell´Abate et al., 2000; Kucerik et al., 2004). The first interval, comprised in the temperature range 40-210°C (region I in Fig. 13), is common for all the samples. It consists in a progressive mass loss having the maximum rate around 100°C. It refers to the loss of moisture adsorbed on poultry manure and chars during the equilibration stage (RH 40%) prior to analysis (Kucerik et al., 2004) (see Materials and Methods). Region II spans a temperature interval from 210 to 420°C whereas region III includes the interval 420-590°C (Fig. 13). Poultry manure evidenced the maximum rate of the progressive mass loss at around 286°C in region II. Conversely, the chars retrieved at 350°C and 450°C showed the maximum mass loss rate at around 384°C in the same region. Moreover, both poultry manure and PM chars produced at 350 and 450°C revealed a maximum ML rate at around 460°C in region III. Finally, the char sample retrieved at 600°C showed only one DTG peak at around 414°C placed in between regions II and III (Fig. 13D). The last thermal region IV, between 600 and 800°C (Fig. 13), with a DTG peak at around 700°C in all the samples, is attributed to the degradation of mineral

and biogenic salts (e.g., calcium and potassium carbonates), usually present in poultry manure (Dell´Abate et al., 2000; Liodakis et al., 2005).

Poultry manure has already been described as a complex mixture of alkyl moieties, sugars, aromatic systems and acidic functions (see discussion above on CPMAS ^{13}C NMR spectroscopy). The TG/DTG curves reported in Figure 13A confirm those findings. Indeed, region II in biomass thermograms is usually associated to the thermal-oxidative degradation of labile alkyl systems, carbohydrates, and fatty acids (Dell´Abate et al., 2000; Lopez-Capel et al., 2005). Conversely, region III is mainly assigned to mass loss of more recalcitrant aromatic moieties (Dell´Abate et al., 2000; Lopez-Capel et al., 2005) which come from original structures and, partially, from structures which developed during the degradation and recombination of aliphatic molecules (Kucerik et al., 2006). In particular, the highly oxygenated degree of the organic PM systems produces the mass loss at the temperature of 286°C in region II (Fig. 13A). Conversely, the larger chemical stability of aromatic systems is responsible for the thermal degradation at the temperature of 460°C as evidenced in region III (Fig. 13A).

As a result of pyrolysis at 350 and 450°C, poultry manure turns into a char mainly made by alkyl and aromatic domains. All the oxygenated functions are lost (see the CPMAS ^{13}C NMR spectroscopy discussion above). Alkyl systems are thermally more stable than the oxygen-rich moieties. For this reason, region II in Figure 13B and 13C reveals a mass loss at a temperature of 384°C, around 100°C higher than that observed in Figure 13A.

According to literature data (Kucerik et al., 2004; Lopez-Capel et al., 2005; Melligan et al., 2012), linkages of recalcitrant aromatic moieties disrupt between 430 and 600°C. This arises in region III, at 460°C, in poultry manure (Fig. 13A), and the chars retrieved at 350°C (Fig. 13B) and 450°C (Fig. 13C). Conversely, the aromatic systems of the chars obtained at 600°C

degraded at 414°C (Fig. 13D), a temperature 46°C lower than that observed in Figures 13A to 13C, and placed on the border of regions II and III.

In order to explain the thermo-oxidative instability of the aromatic domains of the 600°C PM chars as compared to the thermo-oxidative stability of the same domains in PM and PM chars at 350 and 450°C, differences in the conformational arrangements of the different molecular domains have been considered (Conte and Berns, 2008). Indeed, it is conceivable that the non-aromatic domains in poultry manure and its 350 and 450°C chars are mainly displaced on the surface of highly condensed or strongly associated poly-aromatic systems (Conte and Berns, 2008). Due to this, the surficial non-aromatic components are degraded first during the TG investigation. The stable products obtained by this first degradation step (Kucerik et al., 2006; Valkova et al., 2007) protect the inner aromatic constituents towards the thermo-oxidative degradation, thereby decelerating the effective heat flow and preventing the char particles from penetration of reactive atmosphere (Šesták, 2004). Conversely, the poly-aromatic domain in the 600°C PM chars is degraded at a lower temperature (414°C in Fig. 13D) than the other chars, due to the absence of the protective effect of the non-aromatic components.

3.4 Conclusions

The present chapter reports CPMAS ^{13}C NMR characterization and thermal investigation of poultry manure and its char derivatives obtained at 350, 450 and 600°C for charring times of 30, 60, 90 and 120 minutes. All the results revealed that char chemical nature is affected more by production temperature than by production time. Indeed, PM char composition at each temperature remained more or less unchanged as heating time was gradually switched from 30 to 120 min. In particular, PM chars obtained at 350 and 450°C contained both aromatic and alkyl domains whereas only aromatic systems were present after charring at 600°C. Unexpectedly, the aromatic

domains in the latter char revealed a lower thermal stability as compared to the former two. In fact, whereas aromatics in 350 and 450°C PM chars degraded at 460°C, those in the 600°C PM char were destroyed at 414°C. This result was explained by hypothesizing that the alkyl domains in chars produced at 350 and 450°C were mainly displaced on the surface of a rigid aromatic core. For this reason, the thermal destruction of the original aromatic core was retrieved only after the complete degradation of the products developed from the original alkyl systems. Alkyl removal by poultry manure charring at 600°C left unprotected the aromatic domain, thereby allowing the thermal degradation of the aromatic systems at a lower temperature than that measured for PM chars produced at the two lowest temperatures (350 and 450°C).

Due to the relevance which conformation has on the sorption properties of chars (e.g., kinetics and thermodynamics of char sorption or residence time of adsorbed species), the understanding of the role of alkyl and aromatic domains in these interactions is of great importance.

References

Alèn R, Kuoppala E, Oesch P (1996) Formation of the main degradation compound groups from wood and its components during pyrolysis. J Anal Appl Pyrolysis 36:137-148

Berns AE, Conte P (2010) Effect of RF Field Inhomogeneity and Sample Restriction on Spectral Resolution of CP/MAS-^{13}C NMR Spectra of Natural Organic Matter. Open Magn Reson J 3:75-83

Chan KY, Van Zwieten L, Meszaros I, Downie A, Joseph S (2007) Assessing the agronomic values of contrasting char materials on Australian hardsetting soil. In: Proceedings of the Conference of the International Agrichar Initiative, 30 April–2 May 2007, Terrigal, NSW, Australia

Chan KY, Van Zwieten L, Meszaros I, Downie A, Joseph S (2008) Using poultry litter biochars as soil amendments. Aust J Soil Res 46:437-444

Conte P, Berns AE (2008) Dynamics of Cross Polarization in Solid State Nuclear Magnetic Resonance Experiments of Amorphous and Heterogeneous Natural Organic Substances. Anal Sci 24(9):1183-1188

Conte P, De Pasquale C, Novotny EH, Caponetto G, Laudicina VA, Ciofalo M, Panno M, Palazzolo E, Badalucco L, Alonzo G (2010) CPMAS ^{13}C NMR characterization of leaves and litters from the reafforestated area of Mustigarufi in Sicily (Italy). Open Magn Reson J 3:89-95

Conte P, Marsala V, De Pasquale C, Bubici S, Valagussa M, Pozzi A, Alonzo G (2013) Nature of water-biochar interface interactions. GCB Bioenergy 5: 116-121

Dell'Abate MT, Benedetti A, Sequi P (2000) Thermal methods of organic matter maturation monitoring during a composting process. J Therm Anal Calorim 61(2):389–396

De Pasquale C, Marsala V, Berns AE, Valagussa M, Pozzi A, Alonzo G, Conte P (2012) Fast field cycling NMR relaxometry characterization of biochars obtained from an industrial thermochemical process. J Soil Sediment 2:1211–1221

Davies DB, Payne D (1988) Management of soil physical properties. In: Wild A (ed) Russell's Soil Conditions and Plant Growth, 11th edn. Longman, Harlow, Essex

Fan ZJ, Ai YW, Li JM, Li GW (2000) Discussion of controlling N loss from volatilization in animal manure. J Sichuan Normal Univ (in Chinese) 23(5):548–550

Gay SW, Schmidt DR, Clanton CJ, Janni KA, Jacobson LD, Weisberg S (2003) Odor, total reduced sulfur and ammonia emissions from animal housing facilities and manure storage units in Minnesota. Appl Eng Agric 19(3):347–360

Gaskin JW, Steiner C, Harris K, Das KC, Bibens B (2008) Effect of low-temperature pyrolysis conditions on biochar for agricultural use. T ASAE 51:2061–2069

Gaunt JL, Lehmann J (2008) Energy balance and emissions associated with biochar sequestration and pyrolysis bioenergy production. Environ Sci Technol 42:4152-4158

Gómez X, Diaz MC, Cooper M, Blanco D, Morán A, Snape CE (2007) Study of biological stabilization processes of cattle and poultry manure by thermogravimetric analysis and ^{13}C NMR. Chemosphere 68:1889-1897

Gundale MJ, De Luca TH (2006) Temperature and source material influence ecological attributes of ponderosa pine and Douglas-fir charcoal. For Ecol Manag 231:86–93

Haynes RJ, Naidu R (1998) Influence of lime, fertilizer and manure applications on soil organic matter content and soil physical conditions: a review. Nutr Cycl Agroecosys 51(2):123-137

Huang G, Wang X, Han L (2011) Rapid estimation of nutrients in chicken manure during plant-field composting using physicochemical properties. Bioresource Technol 102:1455–1461

Khaleel R, Reddy KP, Overcash MR (1981) Changes in soil physical properties due to waste applications: a review. J Environ Quality 10:133–141

Knicker H (2011) Pyrogenic organic matter in soil: its origin and occurrence, its chemistry and survival in soil environments. Quat Int 243(2):251–263

Krull ES, Baldock JA, Skjemstad JO, Smernik RJ (2009) Characteristics of biochar: Organo-chemical properties. In: Lehmann J, Joseph S (eds) Biochar for Environmental Management, Science and Technology. Earthscan, London

Kucerik J, Kovar J, Pekar M (2004) Thermoanalytical investigations of lignite humic acid fractions. J Therm Anal Calorim 76:55–65

Kucerik J, Kamenarova D, Valkova D, Pekar M, Kislinger J (2006) The role of various compounds in humic acids stability studied by TG and DTA. J Therm Anal Calorim 84(3):715-720

Kishimoto S, Sugiura G (1985) Charcoal as a soil conditioner. Int Achieve Future 5:12–23

Lal R, Kang BT (1982) Management of organic matter in soils of the tropics and subtropics. XII Cong Int Soc Soil Sci. New Delhi, India:152–178

Lehmann J, Czimczik C, Laird D, Sohi S (2009) Stability of biochar in the soil. In: Lehmann J, Joseph S (eds). Biochar for environmental management: science and technology. Earthscan, London

Lehmann J, Joseph S (2009) Biochar for environmental management: an introduction. In: Lehmann J, Joseph S (eds) Biochar for environmental management: science and technology. Earthscan, London, 1–13

Liodakis S, Katsigiannis G, Kakali G (2005) Ash properties of some dominant Greek forest species. Thermochim Acta 437:158-167

Lopez-Capel E, Sohi SP, Gaunt JL, Manning DAC (2005) Use of Thermogravimetry–Differential Scanning Calorimetry to characterize modelable soil organic matter fractions. Soil Sci Soc Am J 69:136–140

Matthews JA (2008) Carbon negative biofuels. Energ Policy 36:940-945

McBeath AV, Smernik RJ (2009) Variation in the degree of aromatic condensation of chars. Org Geochem 40:1161–1168

Melligan F, Dussan K, Auccaise R, Novotny EH, Leahy JJ, Hayes MHB, Kwapinski W (2012) Characterization of the products from pyrolysis of residues after acid hydrolysis of *Miscanthus*. Bioresource Technol 108:258-263

Metzger L, Yaron B (1987) Influence of sludge organic matter on soil physical properties. Adv Soil Sci 7:141–163

Mikan CJ, Abrams MD (1995) Altered forest composition and soil properties of historic charcoal hearths in southeastern Pennsylvania. Can J Forest Res 25:687–696

Perkins HF, Parker MB, Walker ML (1964) Chicken manure - its production, composition, and use as a fertilizer. Georgia Agr Exp St Bull

Popov V, Itoh H, Brebbia CA, Kungoles A (2004) Waste management and the environment II. WIT Press, Boston

Rillig MC, Wagner M, Salem M, Antunes PM, George C, Ramke HG, Titirici MM, Antonietti M (2010) Material derived from hydrothermal carbonization: Effects on plant growth and arbuscular mycorrhiza. Appl Soil Ecol 45(3):238-242

Roach S, Isenhart L, McKenna L, Cunningham M (2009) Filthy Feed - The Risky and Unregulated Practice of Feeding Poultry Litter to Cattle. FACT, Food Animal Concerns Trust

Rondon MA, Lehmann J, Ramirez J, Hurtado M (2007) Biological nitrogen fixation by common beans (*Phaseolus vulgaris* L.) increases with bio-char additions. Biol Fert Soils 43:699-708

Sanchez PA, Palm CA, Szott LT, Cuevas E, Lal R (1989) Organic input management in tropical agroecosystems. In: Coleman DC, Oades JM, Uehara G (eds) Dynamics of Soil Organic Matter in Tropical Ecosystems. University of Hawaii Press, Honolulu

Schmidt MWI, Noack AG (2000) Black carbon in soils and sediments: Analysis, distribution, implications, and current challenges. Global Biogeochem Cy 14(3):777-793

Šesták J (2004) Heat, thermal analysis and society. Nucleus HK Press, Hradec Kralove, Czech Republic

Shinogi Y, Kanri Y (2003) Pyrolysis of plant, animal and human waste: physical and chemical characterization of the pyrolytic products. Bioresource Technol 90(3):241-247

Sohi SP, Krull E, Lopez-Capel E, Bol R (2010) A review of biochar and its use and function in soil. Adv Agron 105:47-82

Uchimiya M, Lima IM, Klasson KT, Chang S, Wartelle LH, Rodgers JE (2010) Immobilization of Heavy Metal Ions (Cu^{II}, Cd^{II}, Ni^{II}, and Pb^{II}) by Broiler Litter-Derived Biochars in Water and Soil. J Agr Food Chem 58:5538–5544

Valkova D, Kislinger J, Pekar M, Kucerik J (2007) The kinetics of thermo-oxidative humic acids degradation studied by isoconversional methods. J Therm Anal Calorim 89(3):957-964

Warnock DD, Lehmann J, Kuyper TW, Rilling MC (2007) Mycorrhizal responses to biochar in soil—concepts and mechanisms. Plant Soil 300:9–20

Wendlandt WWM (1986) Thermal Analysis. Wiley, New York

Wiedner K, Rumpel C, Steiner C, Pozzi A, Maas R, Glaser B (2013) Chemical evaluation of chars produced by thermochemical conversion (gasification, pyrolysis and hydrothermal carbonization) of agro-industrial biomass on a commercial scale. Biomass and Bioenergy. DOI: 10.1016/j.biombioe.2013.08.026 (article in press)

Wilkinson KG, Harapas D, Tee E, Tomkins RB, Premier R (2003) Strategies for the Safe Use of Poultry Litter in Food Crop Production. Horticulture Australia Ltd, Sidney

Wilson MA (1987) N.M.R. techniques and applications in geochemistry and soil chemistry. Pergamon Press London 1sted.

Wolf M, Lehndorff E, Wiesemberg GLB, Stockhausen M, Schwark L, Amelung W (2013) Towards reconstruction of past fire regimes from geochemical analysis of charcoal. Org Geochem 55: 11-21

Yuan JH, Xu RK, Wang N, Li JY (2011) Amendment of Acid Soils with Crop Residues and Biochars. Pedosphere 21(3):302–308

Zhao L, Cao X, Mašek O, Zimmerman A (2013) Heterogeneity of biochar properties as a function of feedstock sources and production temperatures. J Hazard Mater 256-257:1-9

CHAPTER 4 : EFFECT OF PYROLYSIS CONDITIONS ON THE SURFACE PROPERTIES OF CHARS FROM POULTRY MANURE

4.1 Introduction

Climate change due to the excessive release of greenhouse gases (GHG) in the atmosphere have become one of the most important challenges the modern world is facing (Lehmann et al., 2006). In recent decades, international efforts have been directed toward the search for alternative and renewable energy sources in order to reduce the use of fossil fuels, considered the main responsible for global warming (Zhang et al., 2010). In this perspective, bioenergy seems a possible and viable strategy to complement and partly replace fossil fuels.

Bioenergy is a renewable and clean energy source derived from several biomasses (Zhang et al., 2010). Different kinds of waste biomasses (such as food residuals, agricultural crops, animal and municipal solid wastes) have the potential to be converted into energy and bio-products, which can be applied for power generation, transportation, as well as the production of biomaterials. The modern industrial systems for the production of bioenergy include thermochemical processes such as pyrolysis and gasification (Bridgewater, 2001). These practices involves the heating of various types of biomass (feedstock), under controlled conditions, to produce synthesis gas (or syngas) and oil (or bio-oils), commonly used as fuel or for the synthesis of chemical compounds (e.g., methanol and ammonia) (Rezaiyan and Cheremisinoff, 2005; Basu, 2010).

The third combustible produced by pyrolysis is a carbon-rich solid residue referred to as biochar, char or charcoal. This material is a highly porous fine grained substance, really similar in appearance to the coal produced by natural burning. Instead of being considered as an industrial waste, this solid

residue should be valorised as are the gaseous and liquid products. Indeed, thanks to its porous structure and high surface area, the pyrolitic char may have several applications. Used as amendment, biochar demonstrated to improve soil physicochemical characteristics (i.e., increase in water and nutrient retention, cation exchange capacity, pH, soil aeration), soil fertility and crop production (Liang et al., 2006; Polmehier et al., 2009; Sohi et al., 2010; Yuan et al., 2011; Herath et al., 2013). Furthermore, char porous structures is compatible with adsorption purposes (Bernardo et al., 2012). Several works (Sheng et al., 2005; Beesley et al., 2010; Uchimiya et al., 2010; Chen and Yuan, 2011; Karami et al., 2011; Lian et al., 2011) proved char capacity to remove both inorganic (e.g., nitrate, phosphate and metal ions) and organic compounds (e.g., pesticides and polycyclic aromatic hydrocarbons) from soils and wastewaters. Thus, biochar can be valorized as pollutants adsorbent or even as precursors for manufacturing activated carbons (Dias et al., 2007; Cao and Harris, 2010).

Char adsorptive capacity is closely related to its specific surface area and pore structure (Noll et al., 1992; Keech et al., 2005). In turn, these characteristics are influenced by the structure of the original feedstock (Warnock et al., 2007; Kloss et al., 2012), and the process conditions (mainly charring temperature and residence time). In particular, many researchers emphasize the strong influence of pyrolysis temperature on char physical structure (Raveendran and Ganesh, 1998; Li et al., 2008; Lehmann and Joseph, 2009; Uchimiya et al., 2010). Indeed, charring temperature affects the amount of volatiles released from the material and its final porous structure (Daud et al., 2001), resulting in large variations in biochar sorptive potential (Keiluweit et al., 2010). Thus, the knowledge of the char pore structure and how it changes as a function of pyrolysis temperature is of fundamental importance because of its marked influence on char adsorption behaviour (Chen et al., 2008).

The aim of the present study was to investigate about the changes occurring in the physical structure of biochar produced from poultry manure when it is obtained at different pyrolysis temperatures and heating times and how these structural changes can influence its agronomic or remediation potential.

Poultry manure (PM) was chosen as feedstock for biochar preparation since its misuse as organic fertilizer can produce serious environmental problems (Gay et al., 2003). This biomass is generally considered a valuable source for readily available plant nutrients (Huang et al., 2011) but its application to agricultural sites in its unmodified form may result in human and animal health risks, odors, and leaching of nitrates and other pollutants into groundwater (Fan et al., 2000). For these reasons, conversion of chicken manure to char has been proposed as an attractive methodology to reduce PM volume and weight, and its stink (Shinogi and Kanri, 2003; Popov et al., 2004).

Some studies have already examined PM biochar characteristics (Uchimiya et al., 2010). Further studies must be performed to evaluate the changes occurring in PM physical characteristics during pyrolysis process.

Poultry manure char surface morphology and its structural transformations were investigated by scanning electron microscopy (SEM) while fast field cycling (FFC) NMR relaxometry was used to retrieve informations on char pore size distribution and the nature of the interactions between water and char porous surface. In particular, it was possible to evaluate how different pyrolysis conditions affected water distribution in poultry manure biochar samples.

4.2 Materials and Methods

4.2.1 Biomass and biochars preparation

Biochar was produced using poultry manure (PM) as feedstock material. PM consists of digested and transformed materials also containing the original litter material, feathers, and spilled feed that accumulate on the floors of the buildings where the animals are grown (Roach et al., 2009).

PM was collected from a Sicilian chicken farm, Conca d'Uovo, Misilmeri, Palermo, Italy (38°3'4'' N, 13°25'32'' E). After sampling, the material was air dried to a maximum moisture content of 20.0%. Poultry litter samples were charred in 300 mL Pyrex flasks at atmospheric pressure by applying three temperatures: 350°C, 450°C, and 600°C. At the beginning, residual air was still present in the system. Once reaction started, oxygen was consumed and pyrolysis proceeded under anoxic conditions. For each temperature, samples were pyrolyzed at the following residence times: 30 and 120 min. Biochars were allowed to cool to room temperature, finely ground in a ceramic mortar and dried again in the oven, at 105°C, overnight. The dried materials obtained were then stored in a desiccator for subsequent use.

4.2.2 Surface area measurements

Specific Surface Areas (SAs) of the PM biochar samples were determined by gas adsorption using the Micromeritics Flowsorb 2309 apparatus (Dunstable, UK). Adsorption of N_2 was performed at -196°C. Before SA measurements, each sample was degassed at 300°C for 30 min. Samples SAs were determined by the dynamic Brunauer–Emmett–Teller (BET) method. All the measurements were done in triplicate. The surface BET areas of the examined chars are reported in Table 5. The analysis was not performed on PM original biomass since the pre-treatment at 300°C could be considered as a pyrolysis itself and the results would not have been real and reliable.

4.2.3 Sessile drop contact angle

To test the wettability of char surfaces, the contact angle (CA) was measured by computer analysis of digital pictures of droplets. This measurement requests to prepare flat surface samples of the investigated solids. A thin layer of each char sample was fixed to one side of a glass microscope slide using double sided adhesive tape (Bachmann et al., 2000). Five to six drops of distilled water (10µl) were placed on the surface. It was assumed that it needs five seconds to set the next drop (Diehl and Schaumann, 2007), so pictures were made in steps of five seconds respectively after setting of the last drop. In this way it is possible to get pictures of replicated droplets of the same age of 25 to 30 seconds by evaluation of only the first droplet on first picture, second droplet on second picture and so on. The digital camera (Canon A300) was controlled by Remote Capture DC programme. The pictures can be magnified and trimmed with the Zoom Browser EX and the contact angle between solid and liquid can be measured by SCA-20. The sessile drop contact angle (Θ_{sess}) was calculated from the tangent to the three-phase soil/water/air contact point associated with the ellipse that best fitted the drop shape (Diehl and Schaumann, 2007). Evaluation of replicates and transformation of measured contact angles request calculation in Excel. Zisman- and also OWRK-plot were made for all tested biochars. No temperature correction for the surface tension of the liquids has been done as temperature was close to 20°C (22°C room temperature) and there is not known how the correction factor is distributed on polar and dispersive component.

Contact angle (CA) values for all PM biochars examined resulted in the range 120°±3, showing no statistically significant differences between the samples. Generally, the solid surface is considered hydrophilic if the water contact angle is smaller than 90° (Förch et al., 2009). Conversely, if the water contact angle is larger than 90°, the solid surface is considered hydrophobic. Highly

hydrophobic surfaces made of low surface energy materials may have water contact angles as high as ~120° (Förch et al., 2009). Thus, biochar samples can be considered solids that present greatly hydrophobic surfaces.

4.2.4 Scanning Electron Microscopy (SEM)

Morphological structures of char were investigated by scanning electron microscopy (SEM, FEI Quanta 250, Hillsboro, OR, U.S.A.) fitted with the ETD detector, at 10kV, dwell 30μs. SEM photomicrographs were obtained for char particles dispersed evenly on conductive carbon tape, mounted on an aluminium sample stub. SEM describes char surface morphology by visual magnification of the surface, up to 100.000 times, under which details of char surface, such as pores, can be acquired. In this study, the micrographs were obtained at magnifications of 250X, 1000X, 1500X, 2000X and 2500X.

4.2.5 ^{1}H-NMR (Proton Nuclear Magnetic Resonance) Relaxometry

For NMR measurements, samples were prepared by addition of known amounts of water to weighed quantities of oven-dried ground biochar followed by gentle stirring. In details, 2g dry mass of the samples were filled in glass vessels, 4mL of demineralised deionized water were added, and the mixture was carefully mixed. After wetting of all surfaces, i.e. the peat surfaces turned dark and no dry areas were observed (Jaeger et al., 2010), the vessels were sealed with a plastic lid. The NMR experiment was performed after 24 hours to assure the complete wetting of the samples.

All ^{1}H NMR measurements were performed at a magnetic field strength of 0.176 T, i.e. at a proton Larmor frequency of 7.5 MHz (Minispec 7.5, Bruker, Germany). The temperature during the measurements was kept constant (25°C). The transversal relaxation time (T_2) distributions of water in biochar samples were determined using a CPMG (Carr–Purcell–Meiboom–Gill) pulse sequence (Meiboom and Gill, 1958). The following conditions were

employed: Number of Scans 32, Recycle Delay 12s, 71dB, τ Echo time 0.1ms, Echoes 25000 to 48000, Pulse attendance 14, Bandwidth broad 1MHz. The FIDs were acquired with the Bruker Minispec software and elaborated with OriginPro 7.5 SR6 (Version 7.5885, OriginLab Corporation, Northampton, MA, USA).

Data elaboration

The relaxation time distributions consist of a number of time constants with associated amplitudes representing an exponential decay curve, the FID (Free Induction Decay) signal. These distributions could be described by a third or fourth order process using exponential functions. Fittings with up to four exponential functions were tested to describe how the T_2 values and/or the relatives amplitude A(t) change depending on different pyrolysis temperatures and residence times. The best results (lower χ^2 and larger R^2) were determined using a four exponentials fitting:

$$y = y_0 + A_1^{(-x/t_1)} + A_2^{(-x/t_2)} + A_3^{(-x/t_3)} + A_4^{(-x/t_4)}$$

where t_i is the T_2 value corresponding to a different kind of interaction (weaker or stronger) between water and the surface of the porous medium investigated, and A_i is the amplitude of the T_2 components. In other words, the amplitude A_i is a measure of the amount of water relaxing with each relaxation time T_{2i}.

The choice of this equation was due to the large sample heterogeneity resulting in a multi-exponential behaviour of the decay/recovery curves (Morozova-Roche et al., 1999). If confined in porous media, relaxation is controlled by solid-fluid interactions at the surfaces of the pore space. Water molecules diffuse and eventually reach a pore wall surface where there is a finite probability that their spins are relaxed due to interactions with fixed spins, paramagnetic ions or paramagnetic crystal defects (Bayer et al., 2010). Due to the dependency of the relaxation times on the water binding and distribution, NMR relaxometry can be used to describe the water

environment. In detail, the biochar T_2 distributions were operationally divided into the following T_2 range: I: 20-50ms; II: 70-180ms; III: 250-700ms, IV: 1000-2200ms. To describe how the T_2 values change, they were plotted as a function of pyrolysis temperatures and residence times. Results are shown in Figure 15.

4.2.6 Fast field cycling (FFC) NMR Relaxometry

For FFC NMR relaxometry investigations, 1g of dried biochar was weighted in NMR tubes, and 3g of demineralised deionized water were added followed by gentle stirring according to the procedure reported in Dunn et al. (2002).

^{1}H nuclear magnetic resonance dispersion profiles (i.e. relaxation rates R_1 or T_1^{-1} vs. proton Larmor frequencies) were acquired on a Stelar Smartracer Fast-Field-Cycling Relaxometer (Stelar s.r.l., Mede, PV–Italy) at a constant temperature of 25°C.

The proton spins were polarized at a polarization field (B_{POL}) corresponding to a proton Larmor frequency (ω_L) of 8MHz for a period of polarization (T_{POL}) corresponding to about five times the T_1 estimated at this frequency. After each B_{POL} application, the magnetic field intensity (indicated as B_{RLX}) was systematically changed in the proton Larmor frequency ω_L comprised in the range 0.01-10.0MHz. The period τ, during which B_{RLX} was applied, has been varied on 16 logarithmic spaced time sets, each of them adjusted at every relaxation field in order to optimize the sampling of the decay/recovery curves.

Free induction decays (FID) were recorded following a single ^{1}H 90° pulse applied at an acquisition field (B_{ACQ}) corresponding to the proton Larmor frequency of 7.20MHz. A time domain of 100μs sampled with 512 points was applied. Field-switching time was 3ms, while spectrometer dead time was 15μs. For all the experiments, a recycle delay of 6s was used. A non-polarized FFC sequence was applied when the relaxation magnetic fields

were in the range of the proton Larmor frequencies comprised between 10.0 and 3.6MHz whereas a polarized FFC sequence was applied in the proton Larmor frequencies B_{RLX} range of 3.0-0.01MHz (Kimmich and Anoardo, 2004).

FFC NMR data elaboration

R_1 values were achieved by interpolating the ^1H magnetization decay/recovery curves at each B_{RLX} value (i.e. ^1H signal intensity versus τ) with the stretched exponential function (also known as Kohlrausch-Williams-Watts function) reported in equation [1] after exportation of the experimental data to OriginPro 7.5 SR6 (Version 7.5885, OriginLab Corporation, Northampton, MA, USA). This equation provided the best fitting with the largest coefficients of determination ($R^2 > 0.998$). The choice of this function was due to the large sample heterogeneity resulting in a multi-exponential behavior of the decay/recovery curves (Morozova-Roche et al., 1999). This approach has the advantage that it is able to handle a wide range of behaviors within a single model. For this reason, assumptions about the number of exponentials to be used in modeling NMRD data are not necessary.

$$I(\tau) = I_0 \exp\left[\left(-\tau/T_1\right)\right]^k \qquad [1]$$

In equation [1], $I(\tau)$ is the ^1H signal intensity at each fixed B_{RLX}, I_0 is the ^1H signal intensity at the thermal equilibrium, T_1 is the average proton spin lattice relaxation time and k is a heterogeneity parameter related to the stretching of the decay process. This function can be considered as a superposition of exponential contributions and thus describes the likely physical picture of some distribution in T_1.

The NMRD profiles reporting the calculated R_1 values (T_1^{-1}) vs Larmor angular frequency (ω_L) were then exported to OriginPro 7.5 SR6 and fitted with a Power Law function of the type (Murray et al., 2008):

$$R_1(\upsilon) = 1/T_1(\upsilon) = a*\upsilon^{-b} + c \qquad [2]$$

In equation [2], R_1 is the longitudinal relaxation rate, a is a measure of the strength of coupling of the proton spins to the solid lattice, b is the exponent or power, and the parameter c is a field-independent offset.

The nuclear magnetic resonance dispersion (NMRD) profiles (i.e. $R_1=T_1^{-1}$ values vs ω_L) for the water saturated PM and the relative biochars are shown in Figure 17. Table 7 reports the NMRD parameters obtained by fitting the NMRD profiles with the equation [2].

Relaxation data at the lowest proton Larmor frequency (10kHz) were also evaluated by UPEN algorithm (Alma Mater Studiorum – Università di Bologna, Italy) (Borgia et al., 1998; 2000) to obtain the T_1 distributions at this magnetic field and, therefore, information on pore distribution and water interaction. The resulting T_1 distributions were then exported to OriginPro 7.5 and fitted with a Gaussian function to obtain the deconvolution curves ($R^2 > 0.99$) (Fig. 16). Results are reported in Table 6.

4.3 Results and Discussion

4.3.1 Surface area measurements

Many researchers emphasize the strong influence of process temperature on the char chemical properties and its physical structure, e.g. total surface area and pore size distribution (Raveendran and Ganesh, 1998; Li et al., 2008; Lehmann and Joseph, 2009; Uchimiya et al., 2010). In particular, charring temperature can be related to the amount of energy required to break the chemical bonds of the raw material used as feedstock. In other words, a higher process temperature determines the allocation of a greater amount of energy able to degrade a larger number of chemical bonds. More bonds are broken, more volatile molecules are released giving rise to a porous material. Thus, process temperature influences the amount of volatiles released from the material (Daud et al, 2001) and, as a consequence, it affects char surface

area, especially the development of porosity. According to Raveendran and Ganesh (1998) and Yang et al. (2008), porosity progress is related to moisture evaporation, volatile release and the rate of their evolution. During pyrolysis, biochar loses organic molecules in the form of volatile compounds. This massive volatilization of organic species contributes to the development of biochar pore structure, i.e. causing the opening of original closed pores, the formation of new pores, and an increase in pore size of existing and newly formed pores (Bunt et al., 2012). According to Fu et al. (2012), the evolution of pores can be divided into two stages. During the first stage, the pore volume increases due to organic matter volatilization. Moreover, a large number of new pores are created and part of original blocked pores are opened. In the second stage, as organic matter volatilisation continues, new pores are still continuously created, existing pores are enlarged, and the coalescence of smaller pores to form larger pores results in larger pore volume. Following the model described from Simons (1979) and Sorensen et al. (2000), as pyrolysis proceeds and a larger amount of volatile matter is released, the larger pores will grow and incorporate the closed or smaller pores into an open pore structure. This mechanism is responsible for a relative depletion of the small pores and enhanced growth of the large pores, and leads to a reduction of the total surface area.

The findings about pore development on char surface during pyrolysis are contrasting. Several authors (Haga et al., 1991; Daud et al., 2001; Feng and Bhatia, 2003; Bunt et al., 2012; Song and Guo, 2012) reported a progressive pore growth (increase in both pore volume and average pore size) with increasing temperatures (up to 700°C) due to the release of volatile compounds. On the contrary, Chan et al. (1999), Sharma et al. (2001; 2004) and Lu et al. (2013) found an increase in the surface area of char produced at increasing charring temperatures in the range 300-500°C, followed by a decrease of the SA above 500°C produced by chars structural ordering and

micropore coalescence. Khalil (1999) reported very low surface areas for charcoals (from a wide variety of biomass feedstocks) pyrolyzed at temperatures near 550°C.

Poultry manure biochars present a similar behaviour. BET results (Tab. 5) show an increase in the surface area (SA) of biochar samples (30min residence time) from 9±0.5 to 17±0.8$m^2\ g^{-1}$ as temperature rises from 350 up to 450°C. Then, above 450°C, the SA decreases again to 12±1$m^2\ g^{-1}$.

The same trend is shown for the samples retrieved at 120°C.

Sample Name	**PM 35030**	**PM 350120**	**PM 45030**	**PM 450120**	**PM 60030**	**PM 600120**
SA (m^2g^{-1})	9 ± 0.5	11 ± 0.4	17 ± 0.8	17 ± 0.9	12 ± 1	13 ± 0.9

Table 5. BET surface area values of the examined PM biochars.

According to De Pasquale et al. (2012), SA values can be inversely related to pore sizes: as surface area increases, the pore size becomes smaller. BET data follow the models described above. During pyrolysis, the organic matter volatilization determines the creation of new small pores and the opening of original blocked pores leading to an increase of the char total surface area. As charring temperature rises (up to 600°C), volatilisation continues, the pores grow and enlarge, and some small pores combine to form bigger ones resulting in the reduction of the total surface area. Ronsse et al. (2013) explained this phenomena assuming a restructuration taking place in the biochar accompanied by the presence of ash melting at high temperatures. As a result, high temperature chars contain high amount of ash (i.e., poultry manure) and could have a low SA value due to the fusion of molten ash filling up pores on char surface.

Resuming, the biochar surface area values grow as follow: $PM_{35030}<PM_{350120}<PM_{60030}=PM_{600120}<PM_{45030}=PM_{450120}$.

Charring temperature affects biochar pore structure determining first an increase and then a decrease of the surface area. On the contrary, charring residence time has an influence in surface area development only at the lowest temperature examined (350°C).

Figure 14 shows the surface morphology and the pore development on PM biochar surface. From the SEM micrographs, it can be seen the opening of the pores and their increase in size as temperature rise (from top to bottom) but also as residence time is increased from 30 to 120 min (from left to right). The SA values observed for PM chars are higher than the ones reported by Song and Guo (2012) (around $4 m^2 g^{-1}$) but lower than the ones found by Uchimiya et al. (2010) (40-$95 m^2 g^{-1}$), even if in the same order of magnitude. These differences are probably due to different ways of biochar producing or sample processing. Even other authors (Sneath et al., 2013; Tatarková et al., 2013; Xu and Zhao, 2013) found low SAs for biochars produced from different feedstock. Indeed, to obtain biochar products with high SA is necessary an additional activation by chemical (Koutcheiko et al., 2007), physical (Azargohar and Dalai, 2006; Uchimiya et al., 2010) or mechanical (Peterson et al., 2012) means.

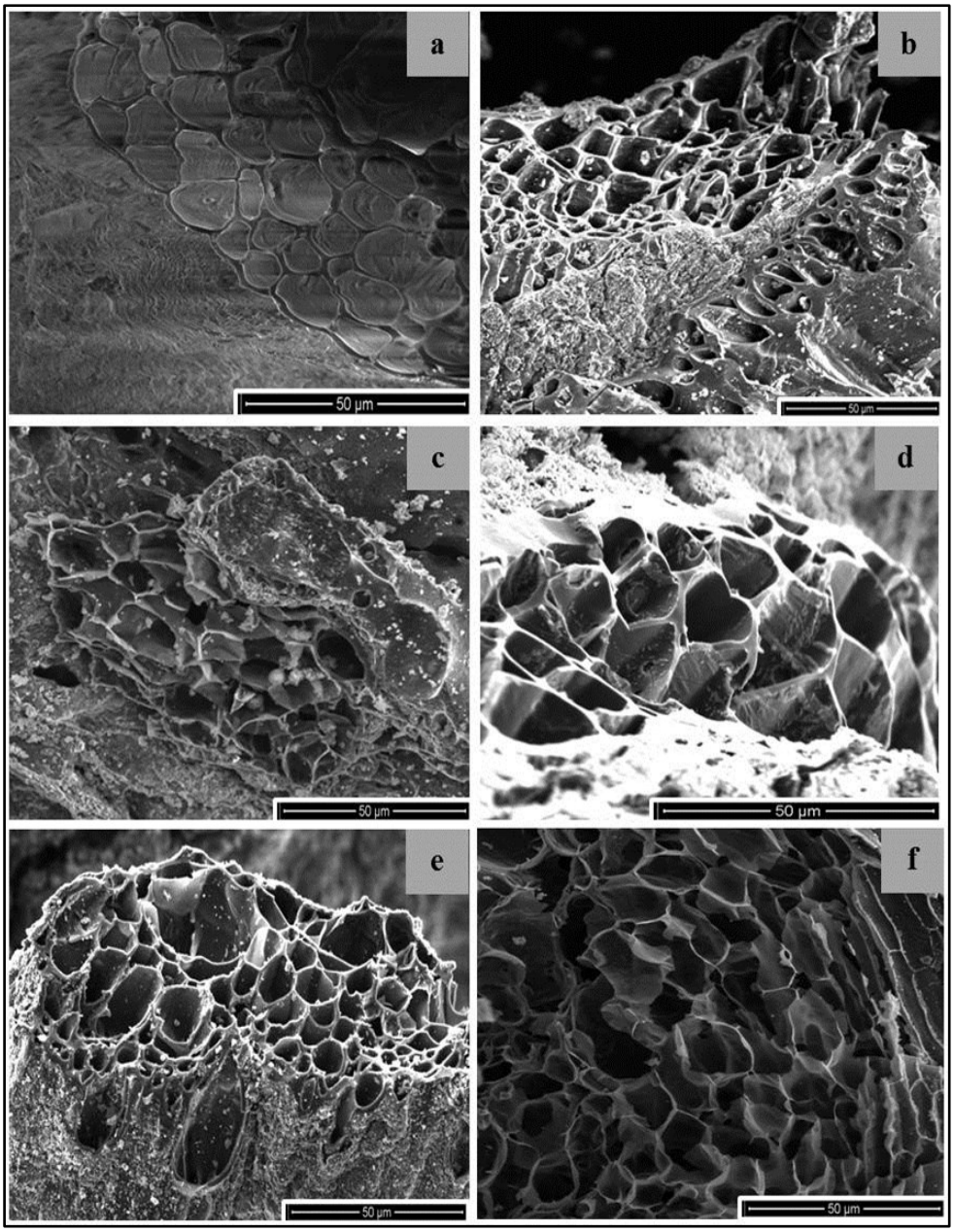

Figure 14 - SEM micrographs showing the surface morphology and the macro-pore development on a) PM_{35030}, b)PM_{350120}, c) PM_{45030}, d)PM_{450120}, e)PM_{60030}, f)PM_{600120} (scale bar=50 µm).

4.3.2 Nature of the interactions between water and biochar porous surface

As discussed in Material and Methods, T_2 distributions of water in PM chars are better described by a four exponentials fitting. As a consequence, the resulting T_2 values can be divided into four T_2 ranges. Every T_2 range corresponds to a different water state or rather water interacting with char with different strengths: from loosely bound water (large T_2) to tightly bound water (shorter T_2). Each range could also be related to water filling pores with different size (Bayer et al., 2010). The faster the motions are (e.g. water in large-sized pores), the lower is the dipolar interaction efficiency, thereby favouring longer T_2 values. Conversely, slower molecular dynamics (as for water constrained in small-sized pores) can be associated with shorter relaxation times due to stronger nuclear dipolar interactions (Bakhmutov, 2004).

In our study, the shortest T_2 values (<50ms) were associated to water molecules strongly interacting with biochar surface or diffusing in smallest-sized pores, whereas the water which is free or trapped in the largest-sized pores is represented by the highest values of T_2 (>1000ms). In detail, the PM biochar T_2 distributions were operationally divided into the following T_2 range: T_{2a}: 20-50ms; T_{2b}: 70-180ms; T_{2c}: 250-700ms, T_{2d}: 1000-2200ms. The shortest relaxation time (T_{2a}) was related to micropores or tightly surface bound water, T_{2b} to mesopores or medium-strength bound water, T_{2c} to macropores or loosely bound water and T_{2d} to macropores or free water.

Actually, the T_2 boundary conditions vary between different publications. Our limits are different from the ones fixed by Bayer et al. (2010) who differentiate three range of T_2:

- short relaxation times (T_2 : below 60 ms) → micropores
- medium relaxation times (T_2 : 60-300 ms) → mesopores
- longer relaxation times (T_2 : > 300 ms) → macropores

Conversely, our subdivision range is similar to the distinction made by Jaeger et al. (2010) since they discerned four T_2 ranges (I: 0.1-3ms, II: 3-30ms, III: 30-300ms, IV: >300ms).

Figure 15 shows the T_2 values of saturated PM chars plotted as a function of pyrolysis temperature. The results show an increase in all relaxation times with pyrolysis temperature. The same trend, albeit with minor differences, is found as charring time rises from 30 to 120 minutes.

The increase of T_2 with increasing pyrolysis temperatures is representative of an increase in the mobility of the involved water molecules (Wynne-Jones and Blanshard, 1986; Jaeger et al., 2010). It means that biochars produced at higher temperatures have weaker interactions with water than char obtained at lower temperatures.

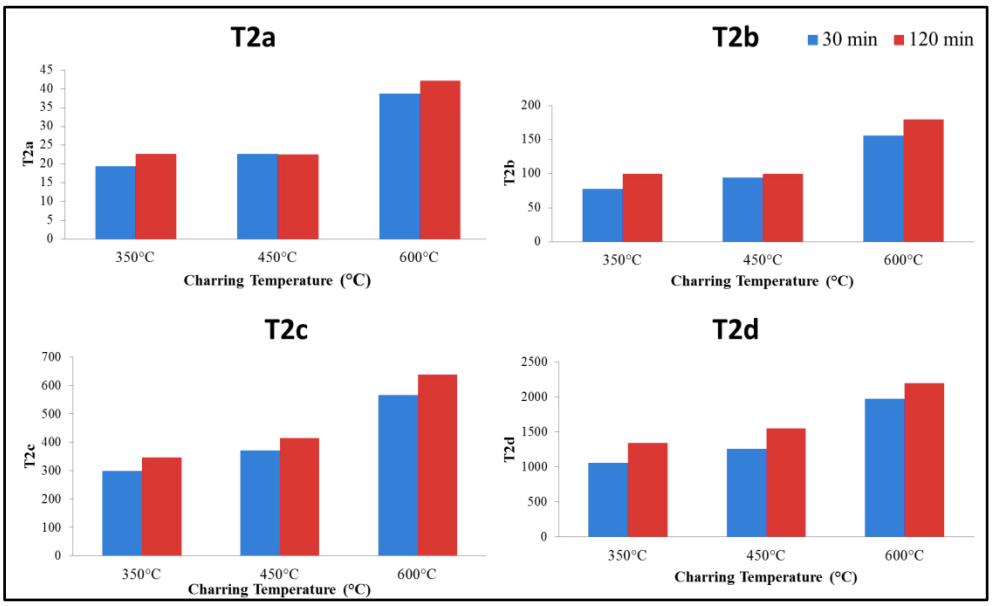

Figure 15 - Transversal relaxation time (T_2) values of saturated PM chars plotted as a function of pyrolysis temperature.

There are several possible explanation to this phenomena.

1) The shift of relaxation times towards higher values could indicate water movement into bigger pores or the presence of water into macropores. It

suggests that chars treated at higher temperatures contain larger dimension pores. This is partially confirmed by BET SA data, since PM_{600} has a lower SA than PM_{450}, previously explained by the increase in the pores size with charring temperature.

2) Another reason could be the reduction in the amount of char surface polar functional groups able to interact with water. Indeed, the interactions between solids and liquids are influenced by the density and the type of sites able to interact with water protons at the available surfaces of organic and mineral materials (Diehl et al., 2010). Thus, change in sample wettability could depend on the variable number of proton-accepting surface sites.

It is well know that as pyrolysis temperature rises, produced biochars exhibit a decrease of labile compounds (e.g., aliphatics), resulting composed of sole aromatic moieties (Antal and Grønli, 2003; Lehmann and Joseph, 2009; De Pasquale et al., 2012). For example, Song and Guo (2012) reported a reduction in acidic groups on poultry manure char surface (i.e., phenolic, lactone and carboxylic group) as temperature rises from 300°C to 600°C. Thus, with increasing charring temperature, biochar loses polar functional surface groups able to interact with water protons. Consequently, there could be a reduction of its affinity for water.

3) An additional explanation is that pore walls or char surfaces become increasingly hydrophobic (due to their reduced organic matter content) with increasing temperature or residence time. However, this last hypothesis was not confirmed by contact angle data, since CA results are comparable between char produced at different temperatures, showing no significant differences.

All results considered, the first explanation seems to be the most reliable and convincing. Indeed, in the previous chapter, chemical composition of PM char was found to be influenced by pyrolysis temperature regardless of the applied charring time. Conversely, in this study, proton trasversal relaxation

times were found to be significantly affected also by muffle residence time (T_2 increases after 120min treatment). Thus, these differences cannot be explained only by a different chemical composition of the samples but also by a different physical structure. Therefore, the loss of strong interaction between water and biochar surface with charring temperature most likely depends on an increase in the samples pores size.

4.3.3 Biochar pore distribution

Proton longitudinal relaxation times (T_1) in liquid systems within porous media are affected by the collisions between the liquid-state molecules and the walls of the porous boundaries (Callaghan and Coy, 1994). Space restrictions (e.g., water in small-sized pores) do not allow fast molecular motions determining short relaxation times. If water strongly interacts with the porous surface or with polar functional groups on the solid surface, the proton dipolar interaction efficiency is enhanced and consequently the T_1 value is short. Conversely, an increase in water mobility (i.e., presence of large pores) weakens the dipolar interaction producing the shift of T_1 values towards higher values (Callaghan and Coy, 1994; Pohlmeier et al., 2009). According to this, longitudinal relaxation times (T_1) distributions at a fixed proton Larmor frequency (i.e., 10kHz in the present study) can be used to extrapolate pore distribution of porous media.

Figure 16 reports the distributions of the longitudinal relaxation times (T_1), also referred to as relaxograms, at the proton Larmor frequency of 10kHz as obtained by applying the UPEN algorithm (see Materials and Methods).

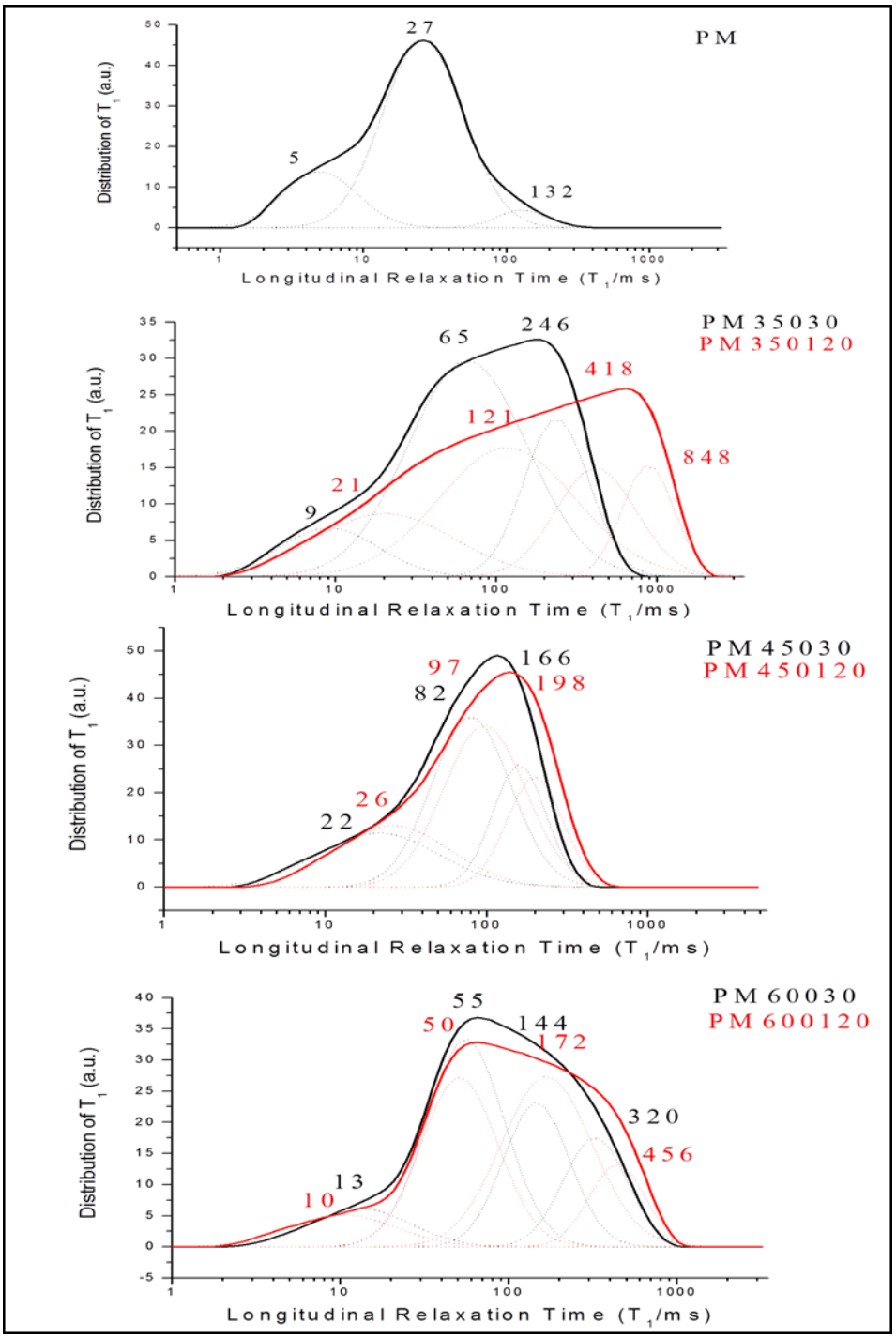

Figure 16 - Spin-lattice longitudinal relaxation time (T_1) distributions of the water saturated PM and the relative biochars obtained at the proton Larmor frequency of 10 kHz. The ordinate is the percent of the total extrapolated signal per Neper (factor of e) of relaxation time.

The relaxograms of PM and relative chars show a complex distribution due to the complexity and heterogeneity of biochar samples. The PM_{350} and PM_{600} samples produce a very broad and multimodal T_1 distribution which is referred to a high porosity heterogeneity (Pohlmeier et al., 2009). As shown in Figure 16, the PM_{35030} relaxogram develops in the range 2-800ms and displays three main T_1 peaks at 9, 65 and 246ms. The PM_{350120} sample has the widest T_1 distribution (covering the range 2-2200ms) and displays four main T_1 peak at 21, 121, 418 and 848ms respectively. The PM_{60030} and PM_{600120} relaxograms are wide and span the T_1 decades from 2 to 1000ms. The four components for PM_{600} are centered at 13, 55, 144 and 320ms for PM_{60030} and 10, 50, 172 and 456ms for PM_{600120}. On the contrary, PM and PM_{450} exhibit sharper bands in the range 1-600ms, centered at 5, 27 and 132ms for PM; 22, 82 and 166ms for $PM_{45030,}$ and 26, 97 and 198ms for PM_{450120}. Thus, these samples have a more homogenous pore size distribution. The relative peak areas, reported as % of the total area, are reported in Table 6.

PM		PM 35030		PM 350120		PM 45030		PM 450120		PM 60030		PM 600120	
T_1 Peak (ms)	Area (%)	T_1 Peak (ms)	Area (%)	T_1 Peak (ms)	Area (%)	T_1 Peak (ms)	Area (%)	T_1 Peak (ms)	Area (%)	T_1 Peak (ms)	Area (%)	T_1 Peak (ms)	Area (%)
5	20	9	12	21	21	22	25	26	26	13	10	10	9
27	75	65	63	121	43	82	51	97	50	55	44	50	36
132	4	246	25	418	21	166	25	198	23	144	26	172	42
/	/	/	/	848	14	/	/	/	/	320	19	456	13

Table 6 - Values of the parameters obtained from the deconvolution of the T_1 distributions (10kHz) of the water saturated biochars.

As said before, relaxation time values are associated to water mobility within the biochar porous surface. In the relaxograms, T_1 values appear continuously distributed representing the wide heterogeneity of the biochar porous system which contains different sized pores (micro, meso and macropores). The left

part of the graph (shorter T_1 values: 0-50ms) is produced by water restricted in small-sized pores while the right zone of the relaxogram (higher T_1 values: >300ms) is shaped by water moving into large pores (macropores). The intermediate T_1 values (50-300ms) are generated by medium-size pores.

Due to their broad T_1 distributions, the H_2O-char complex can be considered multifarious systems which present different kinds of water, from the slow moving bound water (short longitudinal relaxation time) to the fast-moving bulk water (long T_1). The different components in the relaxograms are produced by different kinds of water trapped in different dimensions pores. For example, PM has a sharp relaxogram centered at short T_1 values. This indicates that the starting biomass is mainly composed by micropores and contains small cavities and hydrophilic moieties able to interact with water. PM_{450} samples also produce a sharp relaxogram but centered at longer T_1 values, indicative of a higher presence of medium dimension pores. Medium-sized pores are also representative of PM_{35030} sample (T_1 peaks<250ms).

On the contrary, PM_{350120} and PM_{600} have very broad T_1 distributions, with peaks centered at the longest longitudinal relaxation time values. This indicates that these samples present a high porosity heterogeneity and a large amount of large-sized pores (Pohlmeier et al., 2009).

This finding is confirmed by SA data: even though PM_{350} and PM_{600} have a high porosity heterogeneity, they show the lowest values of SA. Therefore, PM_{350} and PM_{600} surfaces consist mainly of macropores. On the contrary, the higher SA in PM_{450} is associated to a higher porosity homogeneity and to the presence of medium dimension pores.

In summary, biochar porosity homogeneity grows with pyrolysis temperature from 350 to 450°C. Conversely, as temperature rises to 600°C, pore heterogeneity as well as the number of macropores increase.

Furthermore, the longitudinal relaxation times (T_1 peaks) of the protons belonging to each different water component become longer as charring

residence time rises from 30 to 120 min. This confirms T_2 findings and points out the presence of larger dimension pores in biochar samples produced at increasing residence times, and the influence of charring time in determining the physical structure of biochars from poultry manure.

4.3.4 Nuclear magnetic resonance dispersion (NMRD) profiles

The NMRD profiles (i.e. $R_1=T_1^{-1}$ values vs ω_L) for the water saturated PM and the relative chars are shown in Figure 17. From these graphs, it can be seen that the longitudinal relaxation rates vary in the order: $R_{1(PM)}>R_{1(PM35030)}>R_{1(PM350120)}$ (Fig. 17a), $R_{1(PM)}>R_{1(PM45030)}>R_{1(PM450120)}$ (Fig. 17b), and $R_{1(PM)}> R_{1(PM60030)}>R_{1(PM600120)}$ (Fig. 17c), in the whole range of the proton Larmor frequencies (0.01-10MHz) investigated in the present study.

These results confirm T_2 findings since the decrease in the relaxation rate (R_1) can be compared to the increase in relaxation times (T_2) with charring residence time. Indeed, as relaxation times (T_2), the longitudinal relaxation rates (R_1) measured for the water saturated samples can be related to the dipolar interactions between water and sample surface. According to the discussion above, the fastest R_1 is produced by a higher dipolar interaction efficiency or higher interaction between water and char surface. Consequently, the strength of interaction between water and analyzed samples varies in the order: $PM>PM_{30min}>PM_{120min}$ for each temperature considered.

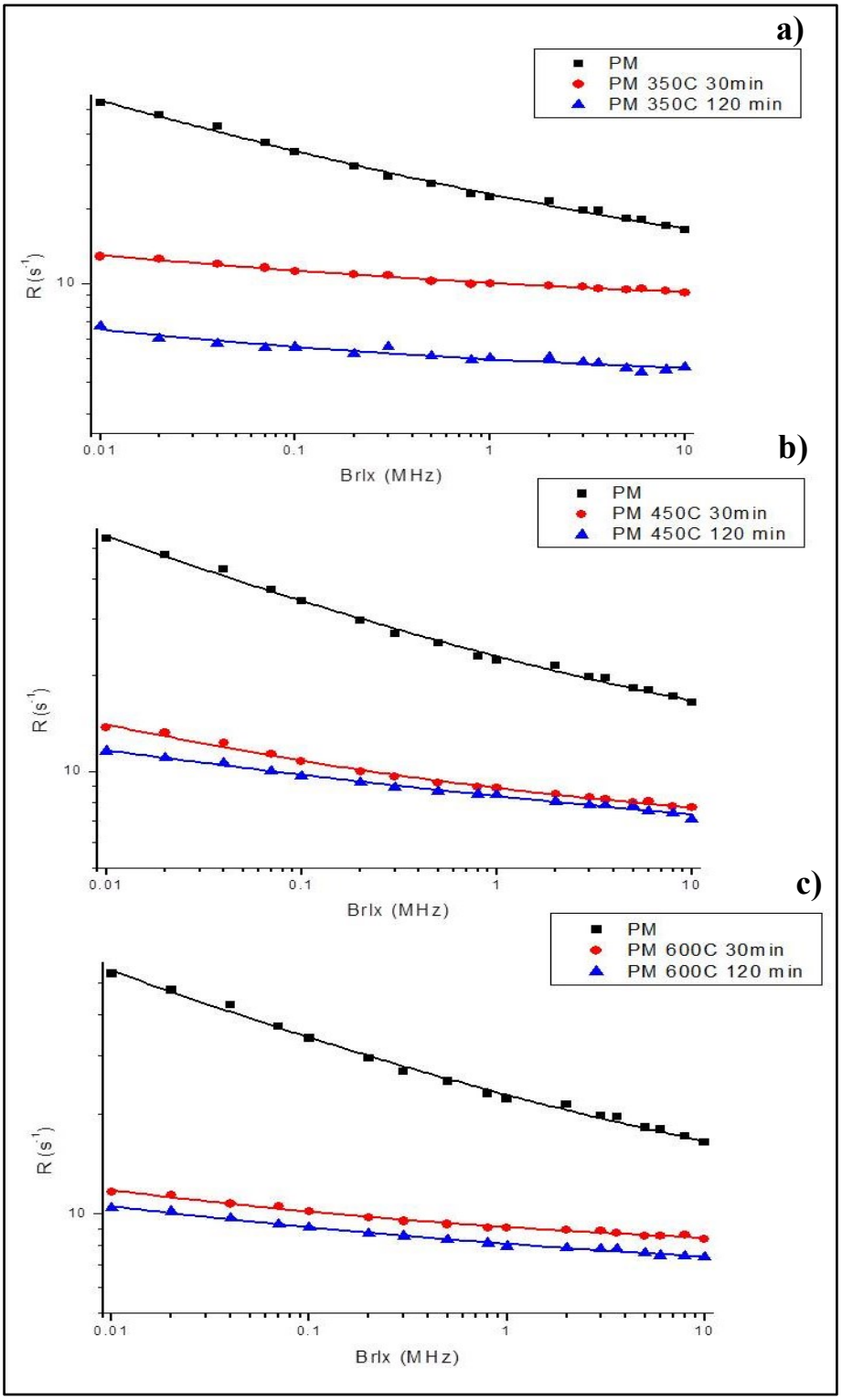

Figure 17 - NMRD profiles of the PM and its relative chars fitted with the Eq.2.

As the residence time increases, biochar ability to interact with water decreases. The NMRD profiles belonging to PM_{35030} and PM_{350120} have the major differences, while PM_{450} and PM_{600} profiles show only slight differences, although significant, among the two different charring times. This trend was also found for BET SA data and in T_1 relaxograms confirming that charring time has a major influence on char physical characteristics at the lowest temperature examined (350°C).

Resuming, water-char interaction depends on biochar physical properties as well as its chemical composition. At low charring temperatures (350°C), residence time is the parameter that mostly affects PM chars physical properties. Vice versa, above 450°C, charring time has a minor effect in char structuring, and pyrolysis temperature become the main factor in determining biochar qualitative composition and physical organization.

The qualitative evaluation of the NMRD profiles in Figure 17 is confirmed by their quantitative assessment through application of equations [2] (see Materials and Methods). Table 7 reports the values of three parameters of the power function (a, b and c) for the water saturated poultry manure sample and its relative chars. In particular, the parameter a is a measure of the strength of coupling of the proton spins to the solid lattice (Murray et al., 2008). When the a value is low, the char-water interaction strength is weaker. On the other hand, dipolar interactions become stronger as a value increases.

Table 7 shows that $a_{PM} > a_{PMbiochars}$, $a_{PM35030} > a_{PM350120}$, $a_{PM45030} = a_{PM450120}$, $a_{PM60030} = a_{PM600120}$ confirming above discussions.

Sample Name	PM	PM 35030	PM 350120	PM 45030	PM 450120	PM 60030	PM 600120
a	14±1.7	3±0.5	1±0.5	3±0.5	4±0.9	2±0.3	2±0.4
b	0.3±0.02	0.2±0.03	0.2±0.08	0.2±0.03	0.1±0.02	0.2±0.03	0.2±0.02
c	9±1.6	7±0.5	4±0.5	6±0.5	4±0.8	7±0.3	6±0.4

Table 7 - Values of the Power Law parameters of the examined samples.

4.4 Conclusions

The present chapter reports about the fast field cycling-NMR relaxometry investigation on the physical features of biochar samples produced at different pyrolysis conditions and how these characteristics affect biochar interaction with water. In the previous chapter, chemical analysis such as elemental and metal content, CPMAS ^{13}C NMR spectrometry and thermogravimetry (TGA) revealed that char chemical nature was affected more by production temperature than by production time. Indeed, PM char composition at each temperature examined remained more or less unchanged as heating time was switched from 30 to 120 min. Conversely, in the present study, differences in char physical properties were found to be produced both by pyrolysis temperature and residence time. In particular, charring time has a major effect at the lowest temperature used (350°C). Vice versa, above 450°C, the pyrolysis temperature has a major influence in char structuring. Furthermore, NMR results suggest a reduction of biochar affinity for water as pyrolysis temperature or charring time increases. This reduction could be explained by: 1) the loss of acidic functional groups on poultry manure char surface (e.g., phenolic, lactone and carboxylic group) able to interact with water protons, 2) the increase in char hydrophobicity (due to their reduced organic matter content) or 3) the increase in biochar pores size with charring temperature or muffle residence time. All the results considered, the last explanation resulted to be the most reliable and convincing since the loss of strong interaction between water and biochar surface most likely depends on an increase in the pores size.

The combination of ^{1}H-T_1 and T_2 NMR relaxometry provided more information on the nature of the surface of porous media with respect to the analytical techniques used previously. The combination of several techniques provided good basis for the comprehension of complex systems making it essential for the complete characterization of the char as a porous medium.

References

Antal MJ, Grønli M (2003) The Art, Science, and Technology of Charcoal Production. Ind Eng Chem Res 42(8):1619-1640

Azargohar R, Dalai AK (2006) Biochar as a precursor of activated carbon. In: Twenty-Seventh Symposium on Biotechnology for Fuels and Chemicals. Humana Press 762-773

Bachmann J, Ellies A, Hartge KH (2000) Development and application of a new sessile drop contact angle method to assess soil water repellency. J Hydrol (231–232):66-75

Bakhmutov VI (2004) Practical NMR relaxation for chemists. Wiley, Chichester

Bayer JV, Jaeger F, Schaumann GE (2010) Proton nuclear magnetic resonance (NMR) relaxometry in soil science applications. Open Magn Reson J 3:15-26

Basu P (2010) Biomass gasification and pyrolysis : practical design and theory. Elsevier. 365 pp

Beesley L, Moreno-Jimenez E, Gomez-Eyles JL (2010) Effects of biochar and green waste compost amendments on mobility, bioavailability and toxicity of inorganic and organic contaminants in a multi-element polluted soil. Environ Pollut 158:2282–2287

Bernardo M, Lapa N, Gonçalves M, Mendes B, Pinto F, Fonseca I, Lopes H (2012) Physico-chemical properties of chars obtained in the co-pyrolysis of waste mixtures. J Hazard Mater (219–220):196–202

Bridgewater AV (2001) Thermal conversion of biomass and waste: the status. Birmingham (UK): Bio-Energy Research Group, Aston University

Borgia GC, Brown RJS, Fantazzini P (1998) Uniform-Penalty Inversion of Multiexponential Decay Data. J Magn Reson 132:65-77

Borgia GC, Brown RJS, Fantazzini P (2000) Uniform-Penalty Inversion of Multiexponential Decay Data: II. Data Spacing, T_2 Data, Systematic Data Errors, and Diagnostics. J Magn Reson 147:273-285

Bunt JR, Waanders FB, Nel A, Dreyer L, van Rensburg PWA (2012) An understanding of the porosity of residual coal/char/ash samples from an air-blown packed bed reactor operating on inertinite-rich lump coal. J Anal Appl Pyrol 95:241–246

Callaghan PT, Coy A (1994) PGSE NMR and molecular translational motion in porous media. In: Tycho R (ed.) NMR probes and molecular dynamics. Kluwer Academic Publishers, Dordrecht NL, 489-523.

Cao X, Harris W (2010) Properties of dairy-manure-derived biochar pertinent to its potential use in remediation. Bioresource Technol 101:5222–5228

Chan ML, Jones JM, Pourkashanian M, Williams A (1999) The oxidative reactivity of coal chars in relation to their structure. Fuel 78(13):1539–1552

Chen B, Yuan M (2011) Enhanced sorption of polycyclic aromatic hydrocarbons by soil amended with biochar. J Soil Sediment 11:62–71

Chen B, Zhou D, Zhu L (2008) Transitional adsorption and partition of nonpolar and polar aromatic contaminants by biochars of pine needles with different pyrolytic temperatures. Environ Sci Technol 42(14):5137–5143

Daud WMAW, Ali WSW, Sulaiman MZ (2001) Effect of carbonization temperature on the yield and porosity of char produced from palm shell. J Chem Technol Biotechnol 76:1281-1285

Day D, Evans RJ, Lee JW, Reicosky D (2005) Economical CO_2, SO_x, and NO_x capture from fossil-fuel utilization with combined renewable hydrogen production and large-scale carbon sequestration. Energy 30:2558-2579

De Pasquale C, Marsala V, Berns AE, Valagussa M, Pozzi A, Alonzo G, Conte P (2012) Fast field cycling NMR relaxometry characterization of biochars obtained from an industrial thermochemical process. J Soil Sediment 12(8):1211-1221

Dias JM, Alvim-Ferraz MCM, Almeida MF, Rivera-Utrilla J, Sánchez-Polo M (2007) Waste materials for activated carbon preparation and its use in aqueous-phase treatment: a review. J Environ Manage 85:833–846

Diehl D, Schaumann GE (2007) The nature of wetting on urban soil samples: wetting kinetics and evaporation assessed from sessile drop shape. Hydrol Process 21:2255–2265

Diehl D, Bayer JV, Woche SK, Bryant R, Doerr SH, Schaumann GE (2010) Reaction of soil water repellency to artificially induced changes in soil pH. Geoderma 158:375–384

Dunn KJ, Bergman DJ, Latorraca GA (2002) Handbook of geographic exploration-seismic exploration: nuclear magnetic resonance petrophysical and logging applications. Elsevier, Oxford

Fan ZJ, Ai YW, Li JM, Li GW (2000) Discussion of controlling N loss from volatilization in animal manure. J Sichuan Normal Univ (in Chinese) 23(5):548–550

Feng B, Bhatia SK (2003) Variation of the pore structure of coal chars during gasification. Carbon 41:507–523

Förch R, Schönherr H, Jenkins ATA (Eds) (2009) Surface design: applications in bioscience and nanotechnology. John Wiley & Sons. 511 pp

Fu P, Hu S, Xiang J, Yi W, Bai X, Sun L, Su S (2012) Evolution of char structure during steam gasification of the chars produced from rapid pyrolysis of rice husk. Bioresource Technol 114:691-697

Gay SW, Schmidt DR, Clanton CJ, Janni KA, Jacobson LD, Weisberg S (2003) Odor, total reduced sulfur and ammonia emissions from animal housing facilities and manure storage units in Minnesota. Appl Eng Agric 19(3):347–360

Haga T, Nishiyama Y, Agarwal PK, Agnew JB (1991) Surface structural changes of coal upon heat treatment at 200-900.degree.C. Energ Fuels 5(2):312–316

Herath HMSK, Camps-Arbestain M, Hedley M (2013) Effect of biochar on soil physical properties in two contrasting soils: an Alfisol and an Andisol. Geoderma (209–210):188–197

Huang G, Wang X, Han L (2011) Rapid estimation of nutrients in chicken manure during plant-field composting using physicochemical properties. Bioresource Technol 102:1455–1461

Jaeger F, Shchegolikhina A, Van As H, Schaumann GE (2010) Proton NMR relaxometry as a useful tool to evaluate swelling processes in peat soils. Open Magn Reson J 3:27-45

Karami N, Clemente R, Moreno-Jiménez E, Lepp NW, Beesley L (2011) Efficiency of green waste compost and biochar soil amendments for reducing lead and copper mobility and uptake to ryegrass. J Hazard Mater 191:41–48

Keech O, Carcaillet C, Nilsson MC (2005) Adsorption of allelopathic compounds by wood-derived charcoal: the role of wood porosity. Plant Soil 272:291–300

Keiluweit M, Nico PS, Johnson MG, Kleber M (2010) Dynamic Molecular Structure of Plant Biomass-Derived Black Carbon (Biochar). Environ Sci Technol 44:1247–1253

Khalil LB (1999) Porosity characteristics of chars derived from different lignocellulosic materials. Adsorpt Sci Technol 17:729−739

Kimmich R, Anoardo E (2004) Field-cycling NMR relaxometry. Prog Nucl Magn Reson Spectrosc 44:257–320

Kloss S, Zehetner F, Dellantonio A, Hamid R, Ottner F, Liedtke V, Schwanninger M, Gerzabek MH, Soja G (2012) Characterization of slow pyrolysis biochars: effects of feedstocks and pyrolysis temperature on biochar properties. J Environ Qual 41:990–1000

Koutcheiko S, Monreal CM, Kodama H, McCracken T, Kotlyar L (2007) Preparation and characterization of activated carbon derived from the thermo-chemical conversion of chicken manure. Bioresource Technol 98(13):2459-2464

Lehmann J, Gaunt J, Rondon M (2006) Bio-char sequestration in terrestrial ecosystems – A review. Mitig Adapt Strat GL 11:403–427

Lehmann J, Joseph S (2009) Biochar for environmental management: science and technology. London: Earthscan. 416 pp

Li W, Yang K, Peng J, Zhang L, Guo S, Xia H (2008) Effects of carbonization temperatures on characteristics of porosity in coconut shell chars and activated carbons derived from carbonized coconut shell chars. Ind Crop Prod 28:190–198

Lian F, Huang F, Chen W, Xing B, Zhu L (2011) Sorption of apolar and polar organic contaminants by waste tire rubber and its chars in single- and bi-solute systems. Environ Pollut 159:850-857

Liang B, Lehmann J, Solomon D, Kinyangi J, Grossman J, O'Neill B, Skjemstad JO, Thies J, Luizao FJ, Petersen J, Neves EG (2006) Black Carbon increases cation exchange capacity in soils. Soil Sci Soc Am J 70:1719-1730

Lu H, Zhang W, Wang S, Zhuan L, Yang Y, Qiu R (2013) Characterization of sewage sludge-derived biochars from different feedstocks and pyrolysis temperatures. J Anal Appl Pyrol 102:137–143

Meiboom S, Gill D (1958) Modified spin-echo method for measuring nuclear relaxation times. Rev Sci Instrum 29(8):688-691

Morozova-Roche LA, Jones JA, Noppe W, Dobson CM (1999) Independent Nucleation and Heterogeneous Assembly of Structure during Folding of Equine Lysozyme. J Mol Biol 289:1055-1073

Murray E, Carty D, Innis PC, Wallace GG, Brougham DF (2008) Field-Cycling NMR Relaxometry Study of Dynamic Processes in Conducting Polyaniline. J Phys Chem 112:17688–17693

Noll KE, Gounaris V Hou WS (1992) Adsorption Technology for Air and Water Pollution Control. Lewis Publisher, Michigan

Peterson SC, Jackson MA, Kim S, Palmquist DE (2012) Increasing biochar surface area: Optimization of ball milling parameters. Powder Technol 228:115–120

Pohlmeier A, Haber-Pohlmeier S, Stapf S (2009) A fast field cycling nuclear magnetic resonance relaxometry study of natural soils. Vadose Zone J 8:735-742

Popov V, Itoh H, Brebbia CA, Kungoles A (2004) Waste management and the environment II. WIT Press, Boston

Raveendran K, Ganesh A (1998) Adsorption characteristics and pore-development of biomass-pyrolysis char. Fuel 77(7):769-781

Rezaiyan J, Cheremisinoff NP (2005) Gasification technologies – a primer for engineers and scientists. CRC Press Taylor & Francis Groups, Boca Raton (FL)

Roach S, Isenhart L, McKenna L, Cunningham M (2009) Filthy Feed - The Risky and Unregulated Practice of Feeding Poultry Litter to Cattle. FACT, Food Animal Concerns Trust

Ronsse F, van Hecke S, Dickinson D, Prins W (2013) Production and characterization of slow pyrolysis biochar: influence of feedstock type and pyrolysis conditions. GCB Bioenergy 5:104–115

Sharma RK, Wooten JB, Baliga VL, Hajaligol MR (2001) Characterization of chars from biomass-derived materials: pectin chars. Fuel 80(12):1825-1836

Sharma RK, Wooten JB, Baliga VL, Lin X, Chan WG, Hajaligol MR (2004) Characterization of chars from pyrolysis of lignin. Fuel 83(11–12):1469-1482

Sheng G, Yang Y, Huang M, Yang K (2005) Influence of pH on pesticide sorption by soil containing wheat residue-derived char. Environ Pollut 134:457–463

Shinogi Y, Kanri Y (2003) Pyrolysis of plant, animal and human waste: physical and chemical characterization of the pyrolytic products. Bioresource Technol 90(3):241-247

Simons GA (1979) The Structure of Coal Char: Part II.—Pore Combination. Comb Sci Technol 19(5-6):227-235

Sneath HE, Hutchings TR, de Leij FAAM (2013) Assessment of biochar and ironfiling amendments for the remediation of a metal, arsenic and phenanthrene co-contaminated spoil. Environ Pollut 178:361-366

Sohi SP, Krull E, Lopez-Capel E, Bol R (2010) A review of biochar and its use and function in soil. Adv Agron 105:47-82

Song W, Guo M (2012) Quality variations of poultry litter biochar generated at different pyrolysis temperatures. J Anal Appl Pyrol 94:138–145

Sørensen HS, Rosenberg P, Petersen HI, Sørensen LH (2000) Char porosity characterization by scanning electron microscopy and image analysis. Fuel 79:1379–1388

Tatarková V, Hiller E, Vaculík M (2013) Impact of wheat straw biochar addition to soil on the sorption, leaching, dissipation of the herbicide (4-chloro-2-methylphenoxy) acetic acid and the growth of sunflower (*Helianthus annuus* L.). Ecotox Environ Safe 92:215–221

Uchimiya M, Lima IM, Klasson KT, Chang S, Wartelle LH, Rodgers JE (2010) Immobilization of Heavy Metal Ions (Cu^{II}, Cd^{II}, Ni^{II}, and Pb^{II}) by Broiler Litter-Derived Biochars in Water and Soil. J Agr Food Chem 58:5538–5544

Warnock DD, Lehmann J, Kuyper TW, Rilling MC (2007) Mycorrhizal responses to biochar in soil – concepts and mechanisms. Plant Soil 309:9-20

Wynne-Jones S, Blanshard JMV (1986) Hydration studies of wheat starch, amylopectin, amylose gels and bread by proton magnetic resonance. Carbohyd Polym 6(4):289-306

Xu R-K, Zhao A-Z (2013) Effect of biochars on adsorption of Cu(II), Pb(II) and Cd(II) by three variable charge soils from southern China. Environ Sci Pollut Res DOI 10.1007/s11356-013-1769-8

Yang YB, Sharifi VN, Swithenbank J, Ma L, Darvell LI, Jones JM, Pourkashanian M, Williams A (2008) Combustion of a Single Particle of Biomass. Energ Fuel 22:306–316

Yuan JH, Xu RK, Wang N, Li JY (2011) Amendment of Acid Soils with Crop Residues and Biochars. Pedosphere 21(3):302–308

Zhang L, Xu C, Champagne P (2010) Overview of recent advances in thermo-chemical conversion of biomass. Energ Convers Manage 51:969–982

CHAPTER 5 : EVALUATION OF INORGANIC CONTAMINANT REMOVAL FROM AQUEOUS SOLUTIONS USING BIOCHAR FROM CHICKEN MANURE, CONIFER AND POPLAR WOOD AS ADSORBENT

5.1 Introduction

Over the last decades, agricultural and industrial activities development and increasing human pressure on the natural environment resulted in its significant deterioration, and led to serious alterations in the elements flow between lithosphere, hydrosphere, atmosphere and biosphere (Schmidt et al., 2004). Natural environment contamination, in particular that caused by heavy metals, is one of the major problems humanity is actually facing. Both water and land bodies receive every day contributes of exogenous heavy metals (e.g, Cu, Fe, Mn, Zn) from atmospheric depositions, agricultural sources (application of fertilizer and pesticides) (Gaur et al., 2005) and industrial effluents from a wide range of industries (e.g., mining, electroplating, tanneries, microelectronics, pharmaceutical, chemical, metallurgical) (Tchobanoglous and Burton, 1991; Volesky and Holan, 1995).

The presence of heavy metal ions in water poses a serious threat to human beings as well as ecosystems (Machida et al., 2006). Indeed, due to their lack of degradation, high persistence and accumulation capacity (Randall et al., 1974; Garg et al., 2007), heavy metals can easily reach high concentration levels. Over long term, this will result in severe adverse effects, i.e. soil fertility reduction, agricultural products quality deterioration, surface and ground water contamination (Taiz and Zeiger, 2002).

To remediate polluted sites and to reduce exposure risk to humans and ecosystems, an effective and affordable technological solution should be found. Several physicochemical and biological methods for inorganic contaminant removal from aqueous effluents have already been studied.

These include ion exchangers, chemical oxidation/reduction, chemical precipitation, phytoremediation, reverse osmosis, ultra filtration, electro dialysis, *etc.* (Salt et al., 1995; Gardea-Torresdey et al., 2002; Hartley and Lepp, 2008; Kumpiene et al., 2008). But conventional treatment technologies are not economical, and further generate a huge quantity of toxic chemical sludge (Sud et al., 2008).

According to literature (Franz et al., 2000; Machida et al., 2006; Cao et al., 2009; Uchimiya et al., 2011), carbonaceous materials could be used as major adsorbents for both organic and inorganic compounds thanks to the presence, on their surface, of specific adsorption sites, such as acidic functional groups (i.e., carboxylic and lactonic groups), basic nitrogen groups (e.g., pyridine) and phosphate. In particular, the adsorption of heavy metals by these materials can be efficiently achieved thanks to their porous structure as well as the presence of surface mineral and metal oxides (Machida et al., 2005; Uchimiya et al., 2010). For all these reasons, activated carbons have been lately applied for domestic and industrial waste water remediation. But the activation process and their use is not cost effective.

The use of biochar (biologically derived charcoal) could be a potential alternative to the existing conventional technologies for metal ions removal and/or recovery from aqueous solutions. Since char is generally obtained at lower temperature and without further activation processing, it requires less energy and cost to produce than activated carbon generation (Shinogi and Kanri, 2003; Lehmann, 2007). In addition, water remediation using carbonaceous materials is a passive treatment and it does not require specialized equipment or extensive labor as compared to other remediation methods.

Resuming, the use of biochar produced from biomaterials (e.g., agricultural wastes or industrial byproducts) has several advantages: low cost, high efficiency and minimization of chemical or biological sludge. Moreover,

turning abundant waste products (e.g., crop residues, animal manure) into materials that can absorb contaminants can have environmental implications for improving waste management and protecting the environment.

In recent years, several studies confirmed the potential of using biochar for heavy metals remediation of soils (Namgay et al., 2010; Uchimiya et al., 2010; 2011) and soil pore water (Beesley et al., 2010; Fellet et al., 2011; Karami et al., 2011). Biochar adsorption capacity resulted significantly affected by its physicochemical characteristics (e.g., surface area, pore distribution and surface functional groups content). These properties, in turn, vary widely depending on the biomass source, pyrolysis conditions, post- and pre-treatments (Krull et al., 2009; Sohi et al., 2010; Uchimiya et al., 2010; Lee et al., 2013) determining a high variability in char adsorptive potential. Therefore, the investigation on the sorption mechanisms of different kind of biochars is of paramount importance in order to address these materials to specific environmental applications.

The main objective of the present study was to determine the efficacy of three different kinds of biochars in removing inorganic contaminants from aqueous solutions.

A char produced by pyrolysis of chicken manure (CM) at 500°C and two char made by the gasification (1200°C) of conifer wood (CW) and poplar wood (PW) residues were first characterized by elemental analyses, BET surface area analyses, CPMAS ^{13}C NMR spectroscopy and Fast Field Cycling NMR Relaxometry. Then, their remediation application in the sorption of heavy metals (Cu, Ni and Pb) from aqueous solutions was also evaluated.

5.2 Materials and Methods

5.2.1 Biomass and biochars preparation

Biochars were obtained from three different feedstock: chicken manure, conifer wood chips and poplar wood chips.

Chicken manure (CM) samples were collected from a Sicilian chicken farm, Conca d'Uovo, Misilmeri, Palermo, Italy (38°3'4'' N, 13°25'32'' E). After sampling, the material was air-dried to a maximum moisture content of 20%.

Conifer wood chips (CW) were the result of mountain forestry management in North Italian Apennines (Valle Staffora, $44°45^{I}15^{II}$N, $9°13^{I}49^{II}$E). The tree species making the biomass feedstock were: Larch (*Larix decidua*), Scots pine (*Pinus sylvestris* L.), Black pine (*Pinus nigra* A.), Silver fir (*Abies alba* M.) and Spruce (*Picea excelsa* L.).

Poplar (*Populus spp.* L.) wood chips (PW) were obtained from dedicated short rotation forestry in the Po Valley (Gadesco Pieve Delmona, $45°10^{I}13^{II}$ N, $10°06^{I}01^{II}$ E). The age of the forest at the cutting down was five years.

Conifer and poplar biochar were provided by an Italian company: Advanced Gasification Technology (AGT). The chars were obtained from an industrial gasification process. During this process, carbonaceous feedstock are partially oxidized by heating at temperatures as high as 1200°C to obtain syngas. The reduction process generates a fine-grained charcoal dust, known as biochar, considered as a gasification waste product.

The manure was charred in 300 mL Pyrex flasks at atmospheric pressure, and at a constant temperature (500°C), for 120 minutes. At the beginning, residual air was still present in the system. Once reaction started, oxygen was consumed and pyrolysis proceeded under anoxic conditions. After pyrolysis, CM char was allowed to cool down to room temperature.

All the biochars were grinded to powder in a ceramic mortar and dried in the oven, at 105°C, overnight. The dried materials were then stored in a desiccator for subsequent use.

5.2.2 Biochars physicochemical analyses

PW and CW chars were already characterized by De Pasquale et al. (2012) (Tab. 8). To compare their characteristics to CM biochar, the same analyses were performed. Elemental content (C and N) was achieved by using a Vario MicroCUBE Elemental Analyser (Elementar, Hanau, Germany). C and N values were corrected for the ash content, obtained by loss on ignition at a burning temperature of 600°C in an electric muffle furnace (Tab. 8). Metals content (i.e., Na, K, Ca, Fe, Cu, Mn), pH and surface area measurements are also reported in Table 8. For further details concerning the methods used, refer to De Pasquale et al. (2012). P content, expressed as P_2O_5, was determined for all the chars using the method developed by Olsen et al. (1954).

5.2.3 CPMAS ^{13}C NMR Spectroscopy

A 7.05 T Varian UNITY INOVA™ (Varian Inc., Palo Alto, CA, USA), equipped with a Apex HX wide bore probe operating at a ^{13}C frequency of 75.4MHz, was used to acquire the ^{13}C NMR spectra. The samples were packed in 6 mm zirconium rotors with Teflon® bottom and top spacers and Vespel® drive tips. The temperature was kept constant at 25.0±0.1°C. Magic angle spinning was carried out at 8000± 1Hz. A ^{1}H RF field strength of 50.3kHZ and a ramp of 16kHz to account for inhomogeneity of the Hartmann-Hahn condition were applied. VNMRJ software (Version 1.1 RevisionD, Varian Inc., Palo Alto, CA, USA) was used to acquire all the free induction decays (FID). Spectra elaboration was conducted by Mestre-C software (Version 4.9.9.9, Mestrelab Research, Santiago de Compostela, Spain). All the FIDs were transformed by applying first a 2k zero filling and then an exponential filter function with a line broadening (LB) of 50Hz. Fully automatic baseline correction using a Bernstein algorithm was applied for

baseline corrections. CPMAS ^{13}C NMR spectra of the chicken manure, conifer and poplar wood biochars are showed in Figure 18.

5.2.4 FFC NMR Relaxometry and data elaboration

For fast field cycling (FFC) NMR relaxometry investigations, 1g of dried biochar was weighted in NMR tubes and 3g of demineralized deionized water were added followed by gentle stirring, according to the procedure reported in Dunn et al. (2002). The theory describing FFC NMR relaxometry can be found in Anoardo et al. (2001), Kimmich and Anoardo (2004) and Ferrante and Sykora (2005). The theory about the pulse sequence applied in the present study has been described in De Pasquale et al. (2012). ^{1}H nuclear magnetic resonance dispersion profiles (i.e. relaxation rates R_1 or T_1^{-1} vs. proton Larmor frequencies) were acquired on a Stelar Spinmaster FFC2000 Relaxometer (Stelar s.r.l.; Mede, PV, Italy) at a temperature of 25°C. For a detailed description of fast field cycling NMR relaxometry experiments and the successive data elaboration, the reader is referred to the methods described in Conte et al. (2013).

Relaxation data at the frequency of 10kHz were also evaluated by using the UPEN algorithm (Alma Mater Studiorum, Università di Bologna, Italy) (Borgia et al., 1998; 2000). The aim is to obtain T_1 distributions at this magnetic field and therefore information on pore distributions and water interactions. The choice of UPEN analyses at 10kHz was due to the larger NMR sensitivity at this frequency as compared to the other proton Larmor frequencies (Kimmich and Anoardo, 2004). The resulting T_1 distributions were then exported to Origin Pro 7.5 and fitted with a Gaussian function to obtain the deconvolution curves (R^2 >0.99) (Fig. 19). Results are reported in Table 9.

5.2.5 Metals adsorption studies

Distilled, deionized water (DDW) (resistivity of 18.2 MΩ·cm at 25°C) used throughout the experiments was produced by a Milli-Q Advantage A10 Ultrapure Water Purification System (Millipore Corporation, Massachusetts, USA). Stock solutions of Cu, Ni and Pb were prepared by dissolving $CuSO_4$, $NiSO_4$ or $Pb(NO_3)_2$ in DDW. Working standards were prepared by progressive dilution of stock solutions using DDW. Solution pH was adjusted to the desired value (pH=5) by adding HCl or NaOH 0.1M. The pH measurements were made using a pHmeter (Mettler-Toledo). Literature studies revealed that optimized value for biosorption of copper and lead is found around pH 5 (Chen et al., 2003; Sud et al., 2008) while nickel removal increases with solution pH until reaching a maximum at pH 8 (Lu and Liu, 2006).

Adsorption kinetics studies

Kinetics experiments were carried out in a series of stoppered vials. A weighed amount (0.5g) of adsorbent was introduced into the vial (30ml) with 5mL of 0.4M aqueous solutions of the metal for different contact times (0.5, 1, 2, 3, 4, 24, 48 hours). The samples were subjected to magnetic stirring (Stir=2) at room temperature (20°C±1) to attain the equilibrium.

Afterwards sample solutions were centrifuged at 3000 rpm for 10 minutes and then filtered by Whatman Filter Paper n.42. Filtered solution were diluted to final volume into a volumetric flask while solid phases were dried in the oven, at 105°C, overnight and then stored in a desiccator for further analysis. All the experiments were done in triplicate. Blank solutions were treated similarly (without adsorbent) and the recorded concentration by the end of each operation was taken as the initial one.

Adsorption kinetics models

Adsorption kinetics studies are important to understand sorption systems and mechanisms, i.e. chemical reactions rate and the factors affecting it. The measurement of sorption rate constants is important to evaluate the basic qualities of a good sorbent, such as its efficacy and/or the time required to remove the adsorbate compound (Abdullah et al., 2009; Uras, 2011).

Conventionally, metals absorption kinetics on porous materials are described by two mechanisms: pseudo-first-order or pseudo-second-order (Sharma and Forster, 1993; Ho and McKay, 2000; Ho et al., 2001). In order to analyze the sorption processes of different metals onto biochar as adsorbent, these two kinetic models were proposed. The pseudo-first-order equation can be written as:

$$\frac{dq_t}{dt} = k_1 (q_e - q_t)$$

where k_1 (min^{-1}) is the adsorption rate constant for pseudo-first-order model, q_e (mg g^{-1}) is the adsorption capacity at equilibrium, and q_t (mg g^{-1}) is the amount of adsorbate absorbed at time t (min).

The pseudo-second-order model can be presented in the following form:

$$\frac{dq_t}{dt} = k_2 (q_e - q_t)^2$$

where k_2 is the rate constant of pseudo-second-order model.

Adsorption experimental design

Batch adsorption experiments were carried out in a series of stoppered vials. A weighed amount (0.5g) of adsorbent was introduced into the vial (30ml) with 5ml aqueous solutions of copper, nickel or lead at various concentrations (25, 50, 75, 100, 200, 300, 400, 500, 600, 700 mM). Then, the samples were subjected to magnetic stirring at room temperature (20°C±1)

for a selected constant time (24h, coming from kinetic studies) to attain the equilibrium.

Samples solutions were centrifuged and filtered. The filtered solutions were diluted to final volume into a volumetric flask while solid phases were dried in the oven, at 105°C, overnight and then stored in a desiccator for further analysis. All sorption experiments were performed in triplicate.

The effects of contact time (0.5 to 48h), metal concentration (25–700mM) and different initial biomass (chicken manure, conifer and poplar residues) were investigated. Blank solutions were treated similarly (without adsorbent) and the recorded concentration by the end of each operation was taken as the initial one.

Sorption isotherm models

Batch adsorption studies were carried out to obtain metal equilibrium isotherms. Sorption isotherms represent the relationship between the amount of solute remaining in the solution at equilibrium and the amount adsorbed by a unit weight of solid sorbent (Park et al., 2006). Isotherm parameters express sorbent surface properties and affinity, at a fixed temperature and pH (Ho et al., 2011).

The most widely applied isotherms for data modeling are Langmuir and Freundlich, developed on thermodynamic equilibrium (Langmuir, 1918; Proctor and Toro-Vazquez, 1966). Other empirical adsorption models are Redlich–Peterson (1959) and Toth isotherms (Suen, 1996).

In this study, a theoretical model (Langmuir isotherm) and three empirical models (Freundlich, Redlich–Peterson and Toth isotherms) were utilized to describe the adsorption equilibrium of copper, nickel and lead on the three different biochars.

Langmuir function is the simplest theoretical model indicating a monolayer adsorption onto a surface with a finite number of identical sites. It is based on

the following basic assumptions: (i) molecules are adsorbed at a fixed number of well-defined localized sites, (ii) each site can hold only one molecule of adsorbate, (iii) all sites are energetically equivalent and (iv) there is no interaction between molecules adsorbed on neighboring sites.

The Langmuir sorption isotherm is described by the equation:

$$\frac{X}{m} = \frac{Q_m k_L C_e}{(1+k_L C_e)},$$

on linearization becomes:

$$\frac{C_e}{(\frac{X}{m})} = \frac{C_e}{Q_m} + \frac{1}{Q_m k_L}$$

where $\frac{X}{m}$ (or q_e) is the amount of absorbed substance at equilibrium as a function of absorbent mass (expressed in mg g^{-1}), and C_e represents the equilibrium concentration of the adsorbate in the liquid phase (mg ml^{-1}). Q_m and k_L are Langmuir constants, respectively related to sorption capacity and sorption energy, and calculated from the intercept and slope of the linear plot, with $\frac{C_e}{\frac{X}{m}}$ versus C_e (Yadav et al., 2011).

Freundlich isotherm is an empirical equation applicable to non-ideal sorption on heterogeneous surface, as well as multilayer sorption. The heterogeneity arises from the presence of different functional groups on adsorbent surface and from various adsorbent-adsorbate interactions (Hameed and El-Khaiary, 2008). It is described by the equation:

$$\frac{X}{m} = k_F C_e^{\frac{1}{n}}$$

and it can be written in the linear form as given below.

$$log\frac{X}{m} = log k_F + \frac{1}{n}\log C_e$$

k_F and n are Freundlich constants, respectively related to sorption capacity and intensity. These constants can be calculated from the slope and intercept of the linear plot, with $\log \frac{X}{m}$ versus $\log C_e$ (Pan et al., 2009).

Redlich-Peterson equation derives from a combination of Freundlich and Langmuir models. It approximates Freundlich model at high concentration, and Langmuir equation at low concentration. Redlich-Peterson equation is:

$$q_e = \frac{A\,Ce}{1 + BCe^p},$$

in the linear form:

$$\frac{Ce}{qe} = \frac{1}{A} + \frac{B}{A} C_e^p.$$

Even Toth model comes from an arrangement of the Freundlich and Langmuir models (Suen, 1996) and it is described by the equation:

$$q_e = \frac{A\ Ce}{(B + Ce^d)^{1/d}}.$$

Both in Redlich-Peterson and Toth equation, A, B and p/d are empirical parameters which should be determined from experimental data.

5.2.6 Atomic absorption spectroscopy (AAS)

After reaching equilibrium, the concentrations of residue metal ions in solution (not adsorbed by biochar) and the amount of cations adsorbed by biochar surface was determined using a Shimadzu AA-6300 with flame atomization (Milan, Italy). Prior to analysis, trace metal grade concentrated nitric and perchloric acids were used together with 30% hydrogen peroxide for the digestion of the biochar samples or filtered solutions. A CEM Mars 5 Microwave Accelerated Reaction System (Bergamo, Italy) was used for the digestion, following the procedure described in Tranchina et al. (2008). All reactants were purchased from Sigma (Milan, Italy).

5.2.7 Statistical analyses

Adsorption data were exported to Origin Pro 7.5 and fitted with the aforementioned kinetics or isotherm models. Regression correlation coefficient (R^2) and Chi-Square (χ^2) statistics were used to determine which equation provided the best data fitting.

5.3 Results and Discussion

5.3.1 Adsorbents characterization

Biochar chemical composition and physical structure are influenced by feedstock nature (Fushimi et al., 2003; Demirbas, 2004; Vassilev et al., 2010), the technique used for its production (Antal and Grønli, 2003; Erlich et al., 2006; Basu, 2010), as well as the process conditions (e.g. charring temperature and residence time) (Czimczik et al., 2002; Gundale and DeLuca, 2006; Brown, 2009).

A literature review on natural and lab-produced biochars showed that the chemical composition of charred products differed significantly (Krull et al., 2009), and feedstock was a primary factor governing this property. Indeed, biomasses of distinct nature have a different composition in terms of cellulose, hemi-cellulose and lignin, as reflected in their dissimilar behavior during pyrolysis (Basu, 2010). Actually, the proportions of these biopolymers determine the ratios of volatile carbon (in bio-oil and gas) and stabilized carbon (biochar) in the resulting pyrolysis products (Basu, 2010). According to Antal and Grønli (2003), char derived from wood materials have low ash content (often < 3%) and high C content. Conversely, biochars produced from biosolids and manures are typically high in ash content. For example, chicken-litter biochars can have ash content greater than 45% (Lima and Marshall, 2005).

The physicochemical characteristics of biochars produced from chicken manure, poplar wood and conifer wood residues are listed in Table 8.

Sample Name	pH (in H_2O)	Ash (g kg^{-1})	C (g kg^{-1})*	N (g kg^{-1})*	P_2O_5 (g kg^{-1})	Na (g kg^{-1})	K (g kg^{-1})	Ca (g kg^{-1})	Fe (g kg^{-1})	Cu (g kg^{-1})	Mn (g kg^{-1})	SA ($m^2 g^{-1}$)
Chicken Manure	10.4±0.1	610±15	670±20	34±1	14.2±0.6	9.4±0.6	74±2	214±8	2.2±0.2	0.10±0.01	0.5±0.03	14±1
Poplar wood	9.6±0.1	220±20	680±50	14±1	1.33±0.08	0.15±0.1	1.8±1	34±2	0.57±0.03	0.30±0.01	0.035±0.002	98±6
Conifer wood	10.3±0.1	80±7	760±70	3.9±0.2	0.31±0.05	0.18±0.2	0.87±0.04	9.8±0.5	1.8±0.1	0.25±0.02	0.032±0.001	66±5

*. obtained by accounting for the ash content

Table 8 - Biochars physicochemical characteristics.

Our findings support the previous statements since CM char has an ash content three times higher than PW char, even if their carbon content is not statistically different. Metals concentration is also greater in CM char (especially for Na, K, Ca and Mn), reflecting the highest level of ash in this sample. Conversely, CW char has the lowest ash percentage (8.0±0.7%) and the highest carbon content (76±7%). This result agrees with Gaskin et al. (2008) who found that biochars carbon concentrations decrease with increasing feedstock mineral content.

Regarding nitrogen and phosphate contents, both are higher in CM than in PW and CW chars (Tab. 8). In particular, they vary in the order: $N_{CM}>N_{PW}>N_{CW}$ and $P_{CM}>P_{PW}>P_{CW}$.

The occurrence on its surface of minerals, nitrogen and phosphate compounds could confer to biochar positive properties, e.g. enhancing its adsorption capacity. Indeed, N-groups can increase carbon surface polarity and its specific interactions with polar species via electrostatic forces or hydrogen bonding (Stöhr et al., 1991). According to literature (Montes-Moràn et al., 2004; Cho et al., 2005; Machida et al., 2006), mineral impurities (e.g., ash and metal oxides) and basic nitrogen groups (e.g., pyridine) can serve as adsorption sites for heavy metal cations on carbonaceous materials. Even phosphate has an important role in metal uptake. Indeed, it can induce the formation of insoluble Pb-phosphate precipitate (Cao and Harris, 2010). In addition, alkaline earth metal cations present on char surface, such as Na^{+} and Ca^{++}, could be replaced by heavy metals involving a cation exchange adsorption mechanism (Chen et al., 2007).

5.3.2 Biochar CPMAS ^{13}C NMR spectra

The CPMAS ^{13}C NMR spectra of the examined biochars are reported in Figure 18. The three spectra show only one broad signal spanning from 100 to 160ppm, and centered at 126ppm. According to McBeath and Smernik (2009) and Knicker (2011), the region between 110 and 160ppm is usually assigned to aromatic systems. In particular, the signal at 126ppm is produced by the diamagnetic currents produced by delocalized π-electrons in extended aromatic structures or graphite-like micro-crystallites (McBeath and Smernik, 2009; Krull et al., 2009; Knicker, 2011).

Biochars produced from chicken manure, conifer and poplar wood residues results composed mainly by aromatic moieties, even though they have been produced under different conditions.

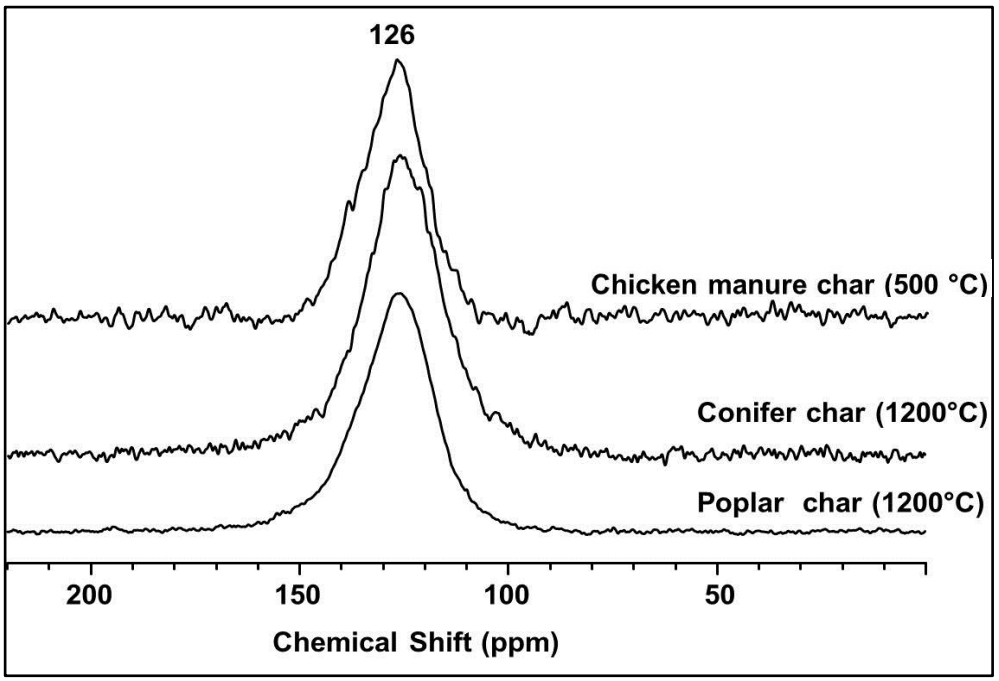

Figure 18 - CPMAS ^{13}C NMR spectra of chicken manure, conifer and poplar wood biochars.

According to literature (Freitas et al., 1999; Czimczik et al., 2002; Ascough et al., 2008; McBeath and Smernik, 2009), char aromaticity increases as pyrolysis temperature rises in the range 250–450°C. Once the pyrolysis temperature reaches 500°C, and above this temperature, most of the carbon is aromatic. Our data confirm this statement since the thermal treatment of chicken manure at the temperature of 500°C was sufficient to convert the original biomass in an aromatic char. Figure 18 shows that all the biochars examined are completely charred.

5.3.3 Biochars pore distributions

Proton longitudinal relaxation time (T_1) values reflect the strength of the interactions between protons (contained in the liquid system) and the molecules or the pores present on sample surface (Callaghan and Coy, 1994). When relaxation time is short, molecular motions are slow and the interaction between water and the sample surface is higher. In this case, water movement is affected by space restrictions, e.g. water can be enclosed into small-sized pores or it can bind surface functional groups. Conversely, an increase in water mobility (i.e. large pores or presence of bulk water) weakens the dipolar interaction between liquid system and porous media, producing the shift of T_1 towards higher values (Callaghan and Coy, 1994; Pohlmeier et al., 2009). According to this, T_1 distributions at a fixed proton Larmor frequency (i.e. 10kHz in the present study) can be used to extrapolate the pore distribution and the chemical interactions of water within biochar as a porous medium. Figure 19 reports biochars T_1 distributions (or relaxograms) at the proton Larmor frequency of 10kHz, and their deconvolution curves (see Materials and Methods). These distributions enlightened the presence of different kind of interactions between water and the three different char surfaces, attributable to a dissimilar pore size distribution.

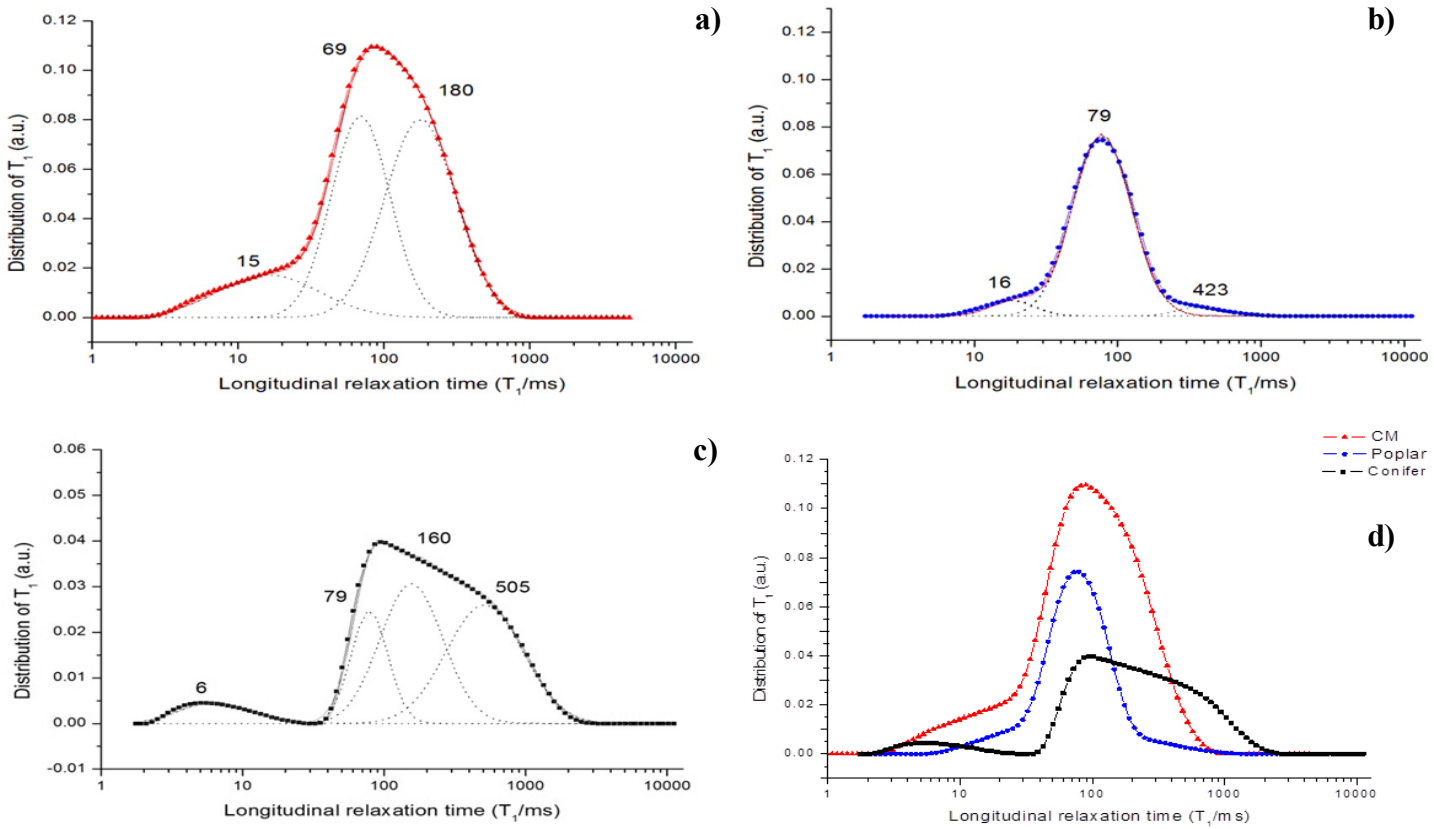

Figure 19 - Spin-lattice relaxation time (T_1) distributions (solid lines), obtained at the proton Larmor frequency of 10kHz, of the water saturated: a) chicken manure, b) poplar, and c) conifer biochars. The dot lines represents the different T_1 components (dot lines) obtained from deconvolution of the T_1 distributions. d) Comparison of all T_1 distributions.

Surface interactions of water into a porous media depend both on chemical and physical constraints. Water does not only enter pores, but also interacts with the organic and inorganic molecules present in the pore system. The left part of the graph (shorter T_1 values) is produced by water strongly interacting with biochar surface (e.g., restricted in small-sized pores) whereas the right zone of the relaxogram (higher T_1 values) is made by water moving into large pores (macropores). The intermediate T_1 values are generated by medium-sized pores.

Both CW and CM chars produce a very broad and multimodal T_1 distribution (Figs. 18a and 18c), referred to a high porosity heterogeneity (Pohlmeier et al., 2009). Conversely, PW char produces a sharp and symmetric relaxogram (Fig. 18b), indication of a homogenous pore size distribution (De Pasquale et al., 2012). Conifer and chicken manure biochar samples present a wider pore distribution compared to poplar chars.

In details, CW relaxogram is composed by four main peaks centered at 6, 79, 160 and 505ms (Fig. 18c). Whereas three peaks are observed in both CM and PW T_1 distribution, centered respectively at 15, 69 and 180ms (Fig. 18a) and 16, 79 and 423ms (Fig. 18b). The relative peak areas, reported as % of the total area, are reported in Table 9.

	Chicken manure		**Poplar wood**		**Conifer wood**	
	T_1 Peak (ms)	**Area (%)**	**T_1 Peak (ms)**	**Area (%)**	**T_1 Peak (ms)**	**Area (%)**
Micropore	15	14	16	6	6	7
Mesopore	69	39	79	91	79	17
	180	46	/	/	160	37
Macropore	/	/	423	3	505	39

Table 9 - Values of the parameters obtained from the deconvolution of the T_1 distributions (10kHz) of the water saturated biochars.

The maxima centered at the shortest T_1 value (6ms for CW, 15ms for CM and 16ms for PW) are produced by water highly bound, immobilized on char surface. These values can be associated to water trapped in very small-sized pores, but also to strong chemical interactions between water and polar functional groups on char surfaces. Table 9 shows that only a minor percentage of water in all the samples (7% for CW, 14% for CM and 6% for PW) belongs to this component.

The maxima centered at intermediate T_1 values (69 for CM, 79ms for both CW and PW) are related to water diffusing in medium-sized pores. This is the major water component in PW char (representing 91% of the total water in the sample) whereas it reduces to 39% in CM and only 17% in CW samples. The third peak (also related to medium sized pores) is the most represented in CM (46%), and it is also present in CW distribution (37%). Finally, the last peak is representative of CW sample (39%), indicating the presence of water weakly interacting with sample surface, e.g. confined in large-sized pores. This peak is also present on PW char relaxogram, but its area represents only 3% of the total.

Resuming, the results show that PW char surface has the strongest interaction with water due to the prevalence of small-sized pores whereas large pore sizes appear to be representative of CW char (Fig. 18d). CM biochar has intermediate characteristics since its surface contains pores of various dimensions.

The aforementioned findings are partially supported by BET measurements (Tab. 8). Indeed, SA values can be related to pore sizes in porous media (Schure et al., 1985; De Pasquale et al., 2012). In particular, the smaller the pore sizes, the larger is the surface area of the porous medium. Conversely, as the size of the pores increases, SA reduction is achieved.

PW sample is mainly composed by small-sized pores and consequently it has the highest SA (98±6 m^2g^{-1}). On the other hand, CM char has the lowest SA

($14\pm1 m^2g^{-1}$) therefore its surface should be composed mainly by large-sized pores (high T_1 values). Conversely, NMR data show that CM relaxogram covers the T_1 decades associated to small- and medium-sized pores or to high efficient interactions with the liquid system. As said before, surface interactions of water into a porous media do not depend only on physical constraints but also on chemical interactions. Therefore, it is conceivable to correlate the high efficiency of water binding CM char surface to chemical interactions rather than to its porous structure. Conversely, in PW and CW char, surface-water interactions are more dependent on physical restrictions.

5.3.4 Water-biochar surface interactions

Nuclear magnetic resonance dispersion (NMRD) profiles (i.e. $R_1=T_1^{-1}$ values vs ω_L) for water saturated biochars are shown in Figure 20. From these graphs, it can be seen that the longitudinal relaxation rates vary in the order: $R_{1(PW)}>R_{1(CM)}>R_{1(CW)}$ in the range 0.01-0.8MHz of the proton Larmor frequencies while in the range 0.8-40MHz, $R_{1(CM)}\geq R_{1(PW)}>R_{1(CW)}$.

Relaxation rate is the inverse of relaxation time and it represents an average value which describes the overall speed of relaxation. As longitudinal relaxation times (T_1), relaxation rates (R_1) measured in water saturated samples can be related to dipolar interactions between water and sample surface. According to the discussion in the previous chapter, the fastest R_1 is associated with a higher dipolar interaction efficiency or higher interaction between water and char surface. Consequently, in the range 0.01-0.8MHz, the strength of interaction between water and analyzed samples varies in the order: PW>CM>CW. Effectively, PW char has smaller-sized pores than CM and CW chars. As a consequence, water constrained in its pores undergoes faster relaxation rates. Conversely, CW sample has the highest pore size to which corresponds a loosely bound water (very low R_1 for all the proton Larmor frequencies examined).

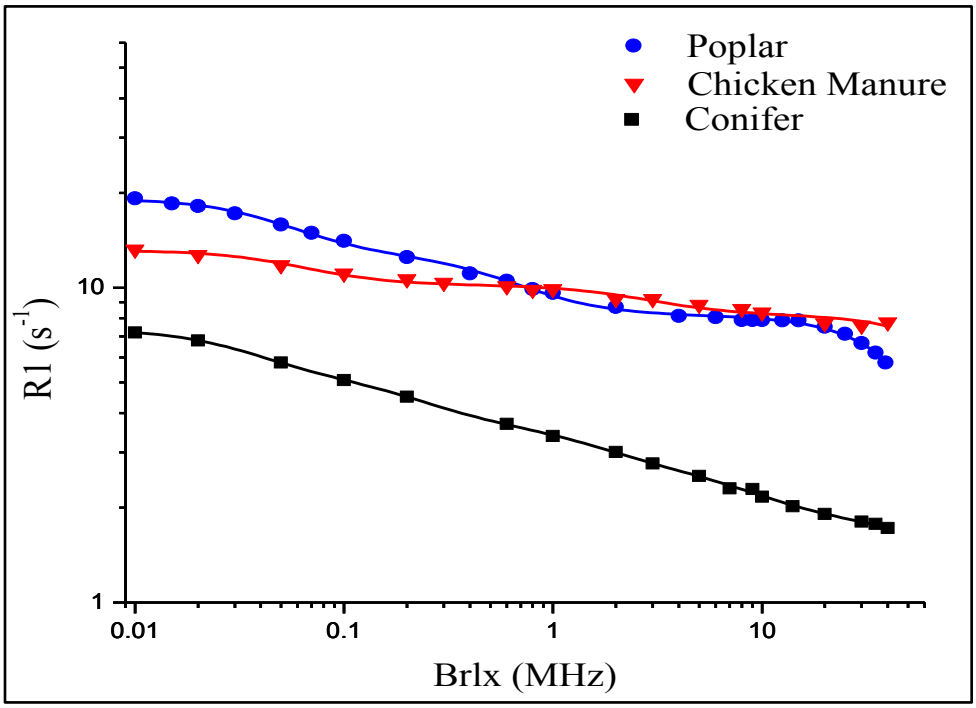

Figure 20 - NMRD profiles of the examined biochars fitted with the Halle equation.

CM char has an intermediate behavior. In the range 0.8-40MHz, its profile is comparable to PW one, thus water relaxes with the same rate in the two samples. Conversely, in the range 0.01-0.8MHz (associated to a slow motion regime), $R_{1(PW)}>R_{1(CM)}$ indicating that water relaxes faster and it is more strongly bound in PW char than in CM char. This can be explained by the presence of smaller size pore in PW char compared to CM sample.

5.3.5 Metals adsorption kinetics

Figure 21 shows the kinetics of copper, nickel and lead sorption onto conifer, poplar and chicken manure biochar surfaces. The equilibrium between metal in the solution and on char surface was reached after 24 hours, thus, the successive isotherm studies were performed in this timeframe.

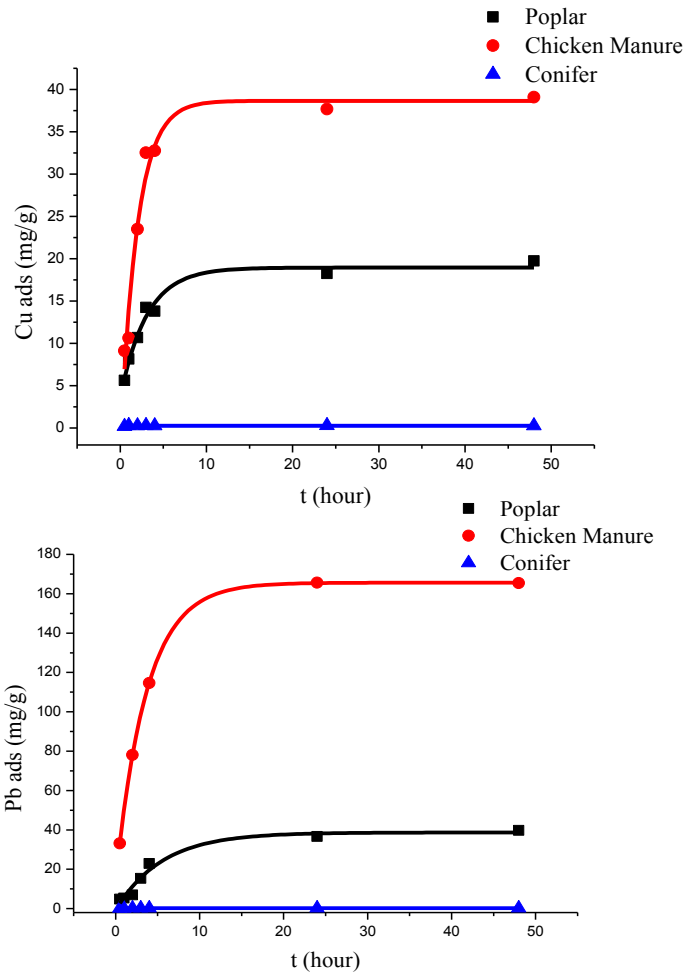

Figure 21- Kinetics of copper, nickel and lead sorption onto conifer, poplar and chicken manure biochar surfaces.

The shape of the curves representing metal uptake versus time (Fig. 21) suggests that a two-step mechanism occurs. The first portion of the curves indicates that most of the total amount of metals adsorbed was removed in the initial rapid uptake phase, after which equilibrium was slowly achieved. After 4 hours, the fractions of total amounts of nickel, copper and lead adsorbed were respectively 89, 70 and 58% on PW; 55, 84, 69% on CM and 69, 100, 100% on CW biochars.

The fast initial adsorption rate is due to the high metal concentration gradient at the beginning of adsorption, which represents a high driving force for metal transfer from the solution to adsorbent surface (Aksu and Tezer, 2005). Then, the number of available adsorbing sites on adsorbent surface decreases determining a reduction in the adsorption rate.

In order to explain pseudo-first-order kinetics, adsorption rate constants (k) and sorption capacities (q_e) were calculated for each adsorbent and metal. It was not possible to calculate pseudo-second-order rate constants since the pseudo-second-order equation did not fit experimental data. Summary of the results is reported in Table 10.

Metal	Biochar	K (h^{-1})	Q_e (mg/g)	R^2
Ni	PW	0.5 ± 0.1	9.1 ± 0.6	0.97
	CM	0.14 ± 0.01	44.9 ± 0.8	0.99
	CW	0.32 ± 0.07	2.5 ± 0.2	0.94
Cu	PW	0.33 ± 0.06	19 ± 1	0.97
	CM	0.5 ± 0.1	38.7 ± 1.8	0.96
	CW	12 ± 6	0.28 ± 0.01	0.75
Pb	PW	0.18 ± 0.05	38.7 ± 2.3	0.96
	CM	0.274 ± 0.002	165.6 ± 0.2	0.99
	CW	0.47 ± 0.15	0.262 ± 0.008	0.89

Table 10 – Pseudo-first-order constants determined from adsorption kinetics of copper, nickel and lead sorption by conifer, poplar and chicken manure biochars.

The calculated correlation coefficients (R^2) for metal sorption by CM and PW char are consistent and closer to unity for pseudo-first-order kinetic model. Thus, the adsorption kinetics of all the metals on PW and CM biochars are favorably approximated by this model. Conversely, the calculated R^2 for metal sorption on CW char surface was lower, especially for copper and lead. Actually, the sorption of each metal onto conifer char surface (blue line) was almost negligible (Fig. 21). This behavior can be explained by CW chemical characteristics. Indeed, from the relaxometric analysis, conifer char resulted to be quite hydrophobic (Fig. 20). Indeed, it has weak interaction with water due to its surface composition (mainly macropores) (Fig. 19c) and the deficiency of functional groups able to bind ions. Because of its lack of adsorption, CW biochar was not investigated for more sorption experiments. Conversely, CM char (red line) was the most effective in removing metal ions from water (maximum Q_e for each metal), followed by PW char (black line).

5.3.6 Qualitative metals adsorption

The experimental equilibrium results were fitted by Freundlich, Langmuir, Redlich-Peterson and Toth isotherm models (Figs. 22 and 23). From isotherm data, a two-step mechanism can be hypothesized. During the first step, at lower metal concentrations, the adsorption follows an exponential behavior. The metal ions rapidly occupy the available binding sites on the adsorbent surface. Then, as the concentration of metal increases, the adsorption sites become saturated and the isotherm curve reaches the asymptote.

The rate of the first step and the overall adsorbent sorption efficiency depend upon its capacity (number of available sites), its specificity (due to its physicochemical nature) and the affinity between metal ion and char surface (Sud et al., 2008).

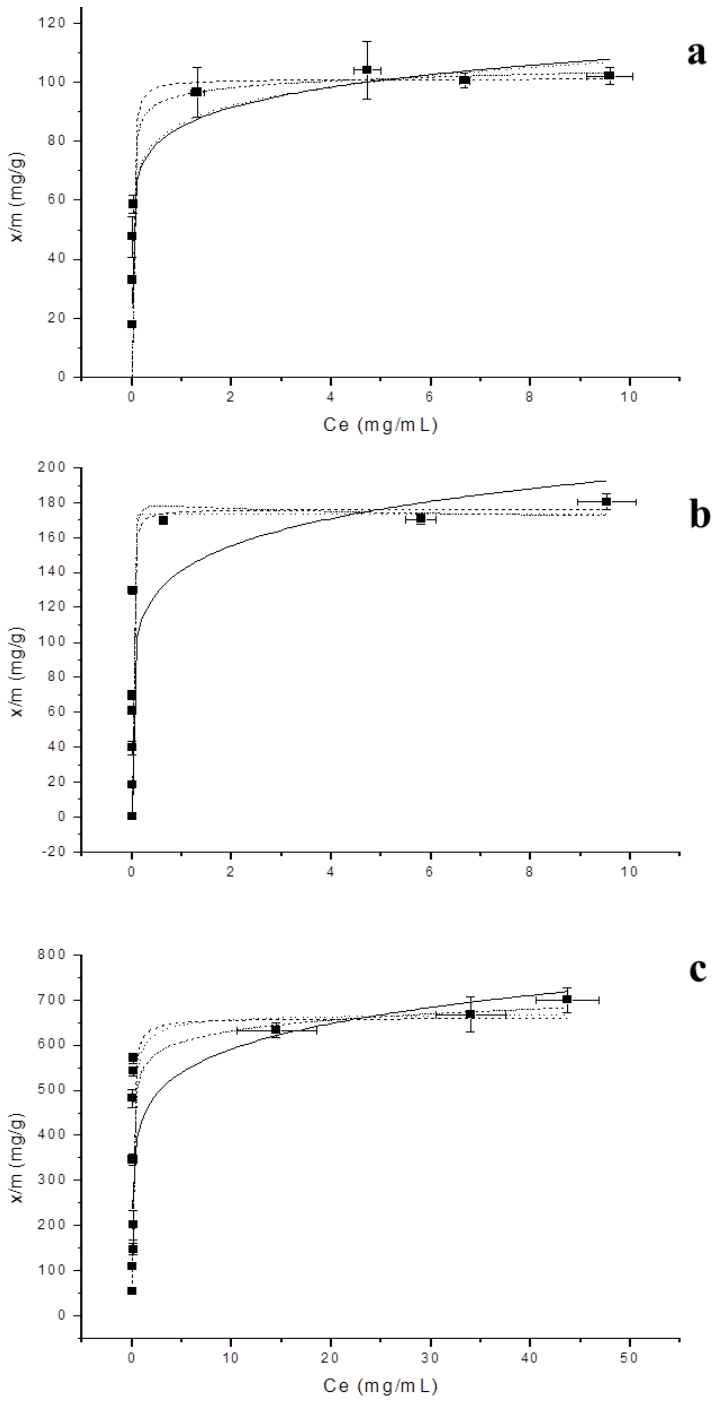

Figure 22 - Freundlich (solid line), Langmuir (dash line), Redlich-Peterson (short dash dot line), and Toth (dot line) isotherm models applied on nickel (a), copper (b), and lead (c) adsorption data on chicken manure char.

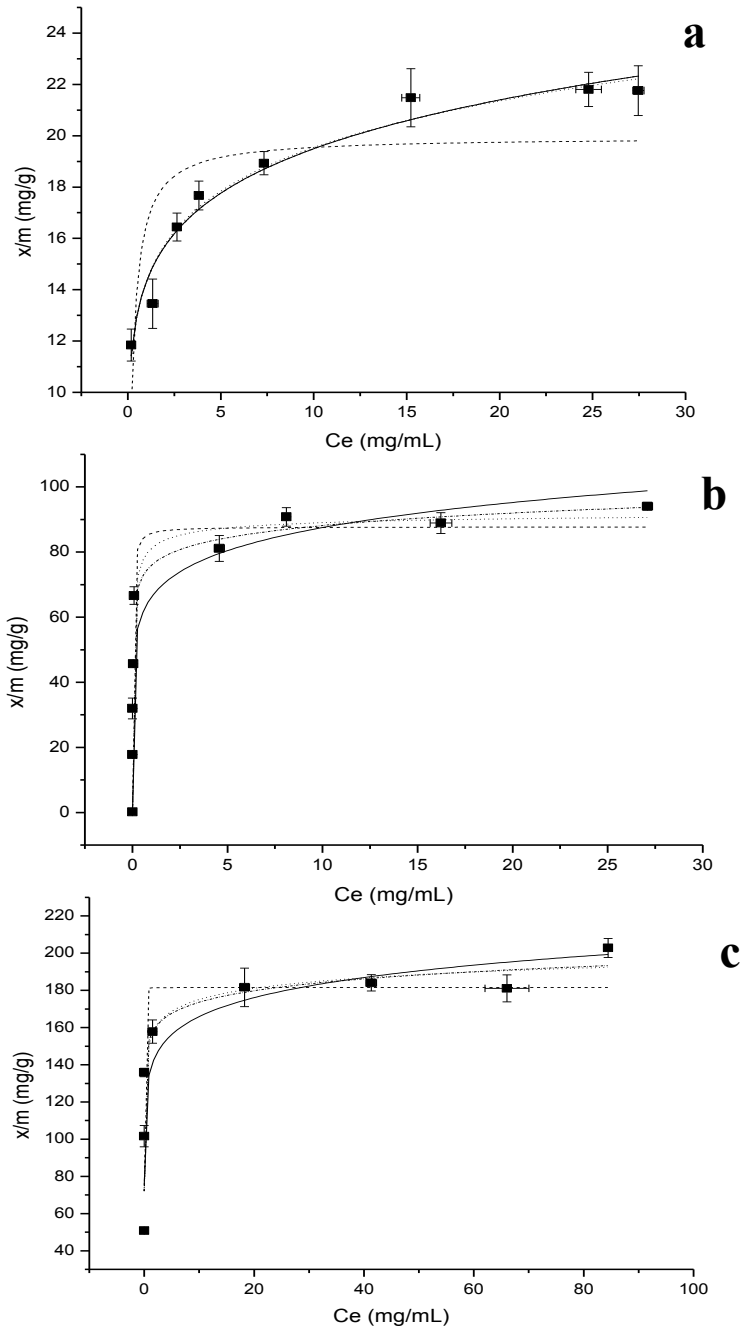

Figure 23 - Freundlich (solid line), Langmuir (dash line), Redlich-Peterson (Short dash dot line), and Toth (Dot line) isotherm models applied on nickel (a), copper (b), and lead (c) adsorption data on poplar char.

The isotherm parameters for copper, nickel and lead adsorption on poplar and chicken manure biochar surface are reported on Table 11.

		Chicken Manure			Poplar		
		Cu	**Ni**	**Pb**	**Cu**	**Ni**	**Pb**
Freundlich	R^2	0.79	**0.96**	0.64	0.92	**0.96**	**0.73**
	χ^2	1014	**50**	24132	92	**0.6**	**664**
	k	141	85	436	66	14	130
	n	7	10	8	8	8	10
Langmuir	R^2	0.93	0.8	**0.71**	0.95	0.58	0.65
	χ^2	342	239	**19004**	55	5.4	842
	a	18794	6416	8267	3765	107	2320
	b	106	63	13	43	5.5	12
Toth	R^2	**0.93**	0.95	0.69	**0.98**	0.95	0.62
	χ^2	**332**	58	20775	**26**	0.7	1798
	A	174	5813	674	93	575	225
	B	$1.1*10^{-4}$	0.1	0.1	0.07	0.16	0.12
	d	2	0.02	0.7	0.49	0.04	0.25
Redlich-Peterson	R^2	0.92	0.77	0.69	0.98	0.89	0.62
	χ^2	392	283	20385	24	1.5	1797
	A	17608	8121	13014	8312	8404	8100
	B	98	84	23	108	582	57
	p	1	1	0.9	0.9	0.8	0.9

Table 11 - Isotherm constants for copper, nickel and lead adsorption on poplar and chicken manure biochar surfaces.

Copper adsorption data on both CM and PW char surfaces are better fitted by Toth isotherm (higher R^2 and lower χ^2) (Tab. 11), whereas the parameter set for the Langmuir isotherm provides the second closest fit over all the error methods. For d=1, Toth isotherm reduces to Langmuir equation. Conversely,

more this parameter is lower than unity, more heterogeneous is the system, approximating Freundlich model. When the lateral interactions between the adsorbed molecules are greater than the adsorptive potential, d is greater than unity (Toth, 2002).

For the adsorption on PW and CM char, d assumes respectively the values 0.49 and 2 (Tab. 11). Therefore, copper adsorption on PW surface approximates Langmuir model which predicts a monolayer adsorption onto a surface with a finite number of identical sites. However, the Cu-PW adsorption isotherm also partially follows Freundlich model indicating that Cu adsorption on PW surface is more heterogeneous. Since PW char has a high affinity for water, it can be hypothesized that water adsorption on PW active sites could interfere with cations adsorption. Some hydrophilic centers located in PW porous structure could increase its affinity for water leading to a water clustering that can block some micropores. This mechanism was already studied by Terzyk (2003) who refers to it as "solvent effect".

Vice versa, on CM char, the interactions between adsorbed ions prevail over the surface adsorptive potential (d=2). This deviation from pure Langmuir behavior can be explained by considering that a copper ion bound to CM char surface can in turn interact with other copper ions through a mechanism mediated by inner sphere water molecules. In other words, the Cu(II) absorbed on CM surface interacts with water molecules. These, in turn, are able to interact with other Cu(II) ions present in the solution, leading to the formation of alternating layers Cu(II)-H_2O-Cu(II) on CM char surface. This mechanism can also explain the highest adsorption potential of CM char compared to PW char ($A_{CM}>A_{PW}$) (Tab. 11). Indeed, the parameter A in Toth equation represents the maximum amount of absorbable solute.

Data in Table 11 show that Freundlich model well describes Ni(II) adsorption on both adsorbents, indicating a non-ideal sorption of this metal on char heterogeneous surface, as well as a multilayer sorption mechanism. This

heterogeneity may arise from the presence of different functional groups on adsorbent surface and/or from various adsorbent-adsorbate interactions (Hameed and El-Khaiary, 2008). The value of the Freundlich parameter n, falling in the range 1–10, indicates favorable adsorption (Treybal, 1981), whereas higher is the K value, higher is char adsorption capacity.

For CM and PW adsorbent, the value of n was found to be respectively 10 and 8, and the k values were 85 and 14 (Tab. 11). Thus, both adsorbents have a good adsorption capacity, but CM has the highest adsorption potential compared to PW char.

For lead equilibrium data, Langmuir isotherm produced the best fit for CM, and Freundlich model provided the closest fit for PW char. But, considering the magnitude of both R^2 and χ^2 values, none of the equations applied appears to produce a reasonable model for lead sorption in all the systems. Further studies are needed to find a best fit equation.

5.3.7 Quantitative metals adsorption

Figure 24 shows the maximum amount of metal adsorbed on char surfaces after 24 hours. Both CM and PW biochars were effective in adsorbing heavy metals from the aqueous solutions.

Char sorption capacity strongly depended on metal ion type, showing the following trend for greater removal from solution: Ni<Cu<Pb (Fig. 24). The same sorption capacity order has already been reported on different adsorbent, i.e. modified coconut coir (Baes et al., 1996), peat (Ho et al., 2001) and broiler litter-derived biochars (Uchimiya et al., 2010). Conversely, Abollino et al. (2003) reported the opposite trend (Pb<Cu<Ni) on Na-montmorillonite.

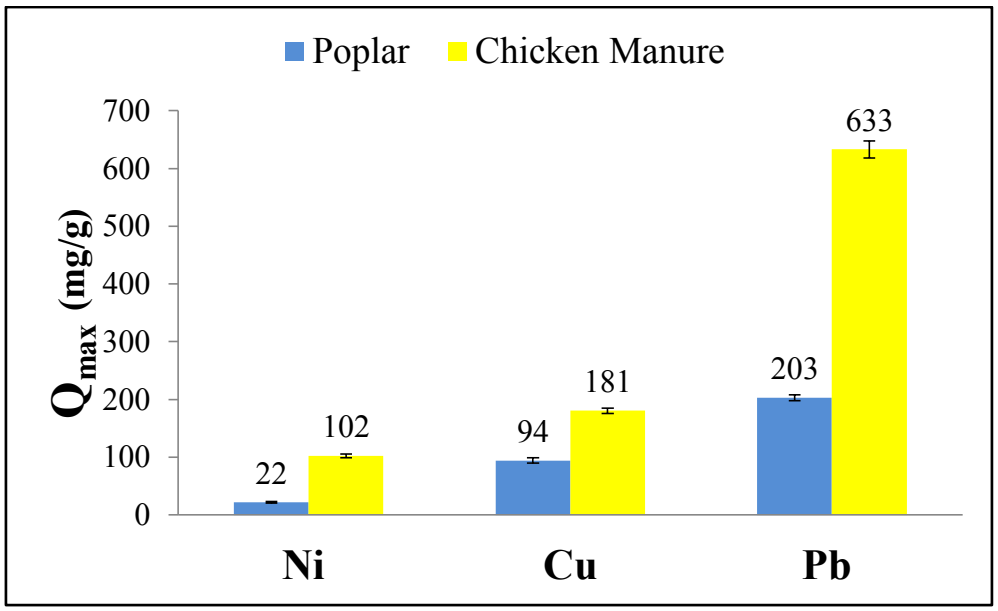

Figure 24 - Maximum amount of metal adsorbed (expressed as mg g^{-1}) on char surface after 24 hours.

The adsorption order can be explained by the different ionic radius of the metal ions (LeGeros and Legeros, 1984; Abollino et al., 2003), by their hydrated radius, hydration energy and electronegativity, as reported by other studies (Seco et al., 1997; Mobasherpour et al., 2011). Indeed, lead has a higher electronegativity compared to copper and nickel, which favors electrostatic and inner sphere surface complexation reactions.

In addition, char surfaces contain hard Lewis bases, such as N or P groups, with an available pair of electrons, either unshared or in a π-orbital, which interact preferentially with hard acid ions. Pb^{2+}, as well as Cu^{2+}, is a borderline hard Lewis acid whereas Ni^{2+} is a soft Lewis acid (Mobasherpour et al., 2011). Unlike soft acid atoms, hard acid atoms do not contain unshared pairs of electrons in their valence shells nevertheless they have an available orbital (Alfarra et al., 2004). Hard Lewis bases (e.g., nitrogen and phosphate groups on char surfaces) tend to donate their available pair of electrons to hard Lewis acids (i.e., lead atoms) to form a Lewis adduct. This can explain the highest affinity of char surface for lead.

Comparing the two different biochars, CM had a higher adsorption potential for every metal considered (Fig. 24). Indeed, it uptaked five times more nickel (102 vs. 22mg g^{-1}), the double of copper (181 vs. 94mg g^{-1}) and three times more lead (633 vs. 203mg g^{-1}) than PW char.

CM char also adsorbed more nickel than other adsorbent, such as activated carbon (Rao et al., 2002), cone biomass of *Thuja orientalis* (Malkoc, 2006) and nano hydroxyapatite (Mobasherpour et al., 2011). Even for lead and copper ions, the CM adsorption potential proved to be higher than those observed for natural Moroccan stevensite (Benhammou et al., 2005), grafted silica (Chiron et al., 2003), apricot stones activated carbon (Kobya et al., 2005), sugarcane bagasse (Inyanga et al., 2011), dairy manure char and its activated carbon (Cao et al., 2009; Cao and Harris, 2010). Only nano hydroxyapatite seems to uptake more lead (up to 1000 mg g^{-1}) (Mobasherpour et al., 2011).

Adsorption capacity depends on several surface characteristics, such as surface functional groups, surface charge, hydrophilicity, and porosity (Mobasherpour et al., 2011). In our study, the porosity seems not to be the primary determinant of adsorption capacity, since $SA_{PW}>SA_{CM}$ (Tab. 8). The higher affinity of all the metals for CM (compared to PW) can be rather explained by the presence on CM char surface of a higher amount of specific functional groups, such as basic nitrogen groups, phosphate and mineral impurities (Tab. 8), able to bind cations.

With specific regard to lead, our results support those obtained by Cao et al. (2009) who found that dairy-manure biochars had a greater capacity for Pb sorption, compared to a commercially available wood-derived activated carbon. Indeed, despite its lower surface area, manure char retained up to 6 times more lead than the activated carbon. One of the mechanisms suggested by the authors was that manure biochar reduced Pb mobility by the precipitation of insoluble Pb-phosphates. In fact, P tends to react with metals

to form insoluble metal phosphate minerals (e.g., pyromorphite $Pb_5(PO_4)_3Cl$, Ksp approximately 10^{-80}) (Cao et al., 2002). It is possible to hypothesize the same mechanism for CM char, as a result of its high P content.

5.4 Conclusions

The present paper reports the CPMAS ^{13}C NMR characterization and FFC NMR Relaxometry investigation of chicken manure, poplar and conifer wood biochars and an evaluation of their remediation application in heavy metals sorption (Cu, Ni and Pb) from aqueous solutions.

Notwithstanding the different nature of the biomasses and the process parameters used for biochar production, CPMAS ^{13}C NMR spectroscopy revealed a substantial structural similarity among the examined chars. Indeed, all the biochar examined resulted composed mainly by aromatic moieties. However, their physicochemical characterization revealed the presence of dissimilar properties in different chars. For example, a higher amount of nitrogen, phosphate and minerals, but a lower surface area, were found in manure- compared to wood-chars. These differences determined the occurrence of different char surface-water interactions, as encountered by applying FFC NMR relaxometry on water-saturated chars. The higher efficiency of water binding poplar char surface was explained by its porous structure, rich in small-sized pores. On the contrary, large pore sizes appeared to be representative of conifer char.

Chicken manure char-water interactions depended more on its chemical composition rather than on physical restrictions. In fact, the presence of specific surface groups (i.e., nitrogen compounds, phosphate and minerals) confer to chicken manure biochar positive properties, for example enhancing its water retention capacity.

Adsorption studies revealed that biochar metal sorption from aqueous solutions occurs through a two-step mechanism involving an initial rapid

uptake phase followed by the achievement of equilibrium after 24 hours. Biochar sorption capacity strongly depended on the metal ion type, showing the following trend for greater removal from solution: Ni<Cu<Pb. This order was explained by the higher electronegativity of lead compared to copper and nickel ions, that favors electrostatic and inner sphere surface complexation reactions.

The sorption of each metal by conifer char was negligible. This behavior was explained by its surface physicochemical characteristics, i.e. hydrophobicity, prevalence of macropores and lack of functional groups able to bind ions. Conversely, despite its lower surface area, chicken manure biochar was the most effective in removing metal ions from water since it uptaked five times more nickel (102 vs. 22 mg g^{-1}), the double of copper (181 vs. 94 mg g^{-1}) and three times more lead (633 vs. 203 mg g^{-1}) than poplar char. Chicken manure highest remediation potential depends on the presence of a higher amount of specific surface functional groups, such as basic nitrogen groups (e.g., pyridine), phosphate and minerals (such metal oxides) that serve as adsorption sites for heavy metal cations.

Copper adsorption data on both chicken manure and poplar char surface were better fitted by Toth isotherm. The evaluation of Toth parameters revealed that copper adsorption on poplar surface is heterogeneous.

PW char has a high affinity for water, thus water adsorption on active sites could effectively block some micropores and interfere with cations adsorption (solvent effect). Besides on chicken manure char, the interactions between adsorbed ions prevail over the surface adsorptive potential. This leads to the formation of alternating layers Cu(II)-H_2O-Cu(II) on char surface, explaining the highest adsorption potential of chicken manure char compared to poplar one.

Freundlich model well describes Ni(II) adsorption for both adsorbents indicating a non-ideal sorption of this metal on an heterogeneous surface as

well as a multilayer sorption. Contrariwise, considering the magnitude of both R^2 and χ^2 values, none of the equations applied appears to produce a reasonable model for sorption of lead in all the systems. Since metals absorption by biochars involves both physical and chemical mechanisms, further studies should be addressed to explain it.

Resuming, different chars have different physicochemical characteristics so they should be addressed to different uses. For example, conifer char should not be used for remediation since it is not effective in removing inorganic metals from aqueous solutions. Conversely, chicken manure-derived biochar has the potential to be an effective heavy metal adsorbent for application in environmental remediation, probably due to the presence of specific functional groups on its surface able to interact with cations. Finally, thanks to its great microporous structure, poplar char could effectively enhance soil water and nutrients retention. Thus, its application to soils may lead to important agronomic benefits.

Overall, turning abundant agricultural waste products (e.g., crop residues, animal manure) into materials that can absorb contaminants or enhance soil properties can have important environmental implications for improving waste management and protecting the environment.

References

Abdullah MA, Chiang L, Nadeem M (2009) Comparative evaluation of adsorption kinetics and isotherms of a natural product removal by Amberlite polymeric adsorbents. Chem Eng J 146:370–376

Abollino O, Aceto M, Malandrino M, Sarzanini C, Mentasti E (2003) Adsorption of heavy metals on Na-montmorillonite. Effect of pH and organic substances. Water Res 37(7):1619–1627

Aksu Z, Tezer S (2005) Biosorption of reactive dyes on the green alga *Chlorella vulgaris*. Process Biochem 40:1347–1361

Alfarra A, Frackowiack E, Béguin F (2004) The HSAB concept as a meant to interpret the adsorption of metal ions onto activated carbons. Appl Surf Sci 228:84-92

Anoardo E, Galli G, Ferrante G (2001) Fast-field-cycling NMR: applications and instrumentation. Appl Magn Reson 20:365–404

Antal MJ, Grønli M (2003) The Art, Science, and Technology of Charcoal Production. Ind Eng Chem Res 42(8):1619-1640

Arthur CL, Pawliszyn J (1990) Solid phase microextraction with thermal desorption using fused silica optical fibers. Anal Chem 62(19):2145–2148

Ascough PL, Bird MI, Wormald P, Snape CE, Apperley D (2008) Influence of production variables and starting material on charcoal stable isotopic and molecular characteristics. Geochim Cosmochim Ac 72(24):6090-6102

Baes AU, Umali SJP, Mercado RL (1996) Ion exchange and adsorption of some heavy metals in a modified coconut coir cation exchanger, Water Sci Technol 34:193–200

Bandosz TJ, Ania CO (2006) Chapter 4. Surface chemistry of activated carbons and its characterization. In: Bandosz TJ (ed.) Interface Science and Technology, Elsevier 7:159-229.

Basu P. (2010) - Biomass gasification and pyrolysis : practical design and theory. Elsevier. 365 pp.

Beesley L, Moreno-Jimenez E, Gomez-Eyles JL (2010),Effects of biochar and green waste compost amendments on mobility, bioavailability and toxicity of inorganic and organic contaminants in a multi-element polluted soil. Environ Pollut 158:2282–2287

Benhammou A, Yaacoubi A, Nibou L, Tanouti B (2005) Adsorption of metal ions onto Moroccan stevensite: kinetic and isotherm studies. J Colloid Interf Sci 282:320–326

Borgia GC, Brown RJS, Fantazzini P (1998) Uniform-penalty inversion of multiexponential decay data. J Magn Reson 132:65–77

Borgia GC, Brown RJS, Fantazzini P (2000) Uniform-penalty inversion of multiexponential decay data: II. Data spacing, T_2 data, systematic data errors, and diagnostics. J Magn Reson 147:273–285

Brown R (2009) Biochar Production Technology. In: Lehmann J, Joseph S (eds) Biochar for Environmental Management: Science and Technology. Earthscan, London

Callaghan PT, Coy A (1994) PGSE NMR and molecular translational motion in porous media. In: Tycho R (ed) Nuclear magnetic resonance probes of molecula dynamics. Kluwer Academic Publishers, Dordrecht NL

Cao X, Ma LQ, Chen M, Singh SP, Harris WG (2002) Impacts of phosphate amendments on lead biogeochemistry at a contaminated site. Environ Sci Technol 36:5296–5304

Cao X, Ma L, Gao B, Harris W (2009) Dairy-Manure Derived Biochar Effectively Sorbs Lead and Atrazine. Environ Sci Technol, 43:3285–3291

Cao X, Harris W (2010) Properties of dairy-manure-derived biochar pertinent to its potential use in remediation. Bioresource Technol 101:5222–5228

Chen JP, Yoon JT, Yiacoumi S(2003) Effects of chemical and physical properties of influent on copper sorption onto activated carbon fixed-bed columns. Carbon 41:1635–1644

Chen JY, Zhu DQ, Sun C (2007) Effect of heavy metals on the sorption of hydrophobic organic compounds to wood charcoal. Environ Sci Technol 41:2536–2541

Chiron N, Guilet R, Deydier E (2003) Adsorption of Cu(II) and Pb(II) onto a grafted silica: isotherms and kinetic models. Water Research 37:3079–3086

Cho H, Oh D, Kim K (2005) A study on removal characteristics of heavy metals form aqueous solution by fly ash. J Hazard Mater B 127:187–195

Conte P, Marsala V, De Pasquale C, Bubici S, Valagussa M, Pozzi A, Alonzo G (2013) Nature of water-biochar interface interactions. GCB Bioenergy 5: 116-121

Czimczik CI, Preston CM, Schmidt MWI, Werner RA, Schulze ED (2002) Effect of charring on mass, organic carbon, and stable carbon isotope composition of wood. Org Geochem 33:1207–1223

De Pasquale C, Marsala V, Berns AE, Valagussa M, Pozzi A, Alonzo G, Conte P (2012) Fast field cycling NMR relaxometry characterization of biochars obtained from an industrial thermochemical process. J Soil Sedim 12(8):1211-1221

Demirbas A (2004) Effects of temperature and particle size on bio-char yield from pyrolysis of agricultural residues. J Anal Appl Pyrol 72(2):243-248

Dunn KJ, Bergman DJ, Latorraca GA (2002) Handbook of geographic exploration-seismic exploration: nuclear magnetic resonance petrophysical and logging applications. Elsevier, Oxford

Erlich C, Björnbom E, Bolado D, Giner M, Fransson TH (2006) Pyrolysis and gasification of pellets from sugar cane bagasse and wood. Fuel 85(10-11):1535-1540

Fellet G, Marchiol L, Delle Vedove G, Peressotti A (2011) Application of biochar on mine tailings: effects and perspectives for land reclamation. Chemosphere 83:1262-1297

Ferrante G, Sykora S (2005) Technical aspects of fast field cycling. Adv Inorg Chem 57:405–470

Franz M, Arafat HA, Pinto NG (2000) Effect of chemical surface heterogeneity on the adsorption mechanism of dissolved aromatics on activated carbon. Carbon 38:1807–1819

Freitas JCC, Bonagamba TJ, Emmerich FG (1999) 13C High-resolution solid-state NMR study of peat carbonization. Energ Fuel 13:53–59

Fushimi C, Araki K, Yamaguchi Y, Tsutsumi A (2003) Effect of Heating Rate on Steam Gasification of Biomass. 2. Thermogravimetric-Mass Spectrometric (TG-MS) Analysis of Gas Evolution. Ind Eng Chem Res 42:3929-3936

Gardea-Torresdey JL, Hejazi M, Tiemann KJ, Parsons JG, Duarte-Gardea M, Henning J (2002) Use of Hop (*Humulus lupulus*) agricultural by-products for the reduction of aqueous lead (II) environmental health hazards. J Hazard Mater 91:95–112

Garg UK, Kaur MP, Garg VK, Sud D (2007) Removal of hexavalent Cr from aqueous solutions by agricultural waste biomass. J Hazard Mater 140:60–68

Gaskin JW, Steiner C, Harris K, Das KC, Bibens B (2008) Effect of low-temperature pyrolysis conditions on biochar for agricultural use. T Asabe 51:2061–2069

Gaur VK, Gupta SK, Pandey SD, Gopal K, Misra V (2005) Distribution of heavy metals in sediment and water of river Gomti. Environ Monit Assess 102:419–433

Gundale MJ, DeLuca TH (2006) Temperature and source material influence ecological attributes of Ponderosa pine and Douglas-fir charcoal. For Ecol Manag 231:86–93

Hameed BH, El-Khaiary MI (2008) Kinetics and equilibrium studies of malachite green adsorption on rice straw-derived char. J Hazard Mater 153:701–708

Hartley W, Lepp NW (2008) Effect of in situ soil amendments on arsenic uptake in successive harvest of ryegrass (*Lolium perenne Elka*) grown in amended As-polluted soils, Environ Pollut 156:1030–1040

Ho YS, McKay G (2000) The kinetics of sorption of divalent metal ions onto *Sphagnum Moss* peat. Wat Res 34(3):735-742

Ho YS, Porter JF, Mckay G (2001) Equilibrium isotherm studies for the sorption of divalent metal ions onto peat: copper, nickel and lead single component systems. Hong Kong University of Science and Technology.

Inyanga M, Gao B, Ding W, Pullammanappallil P, Zimmerman AR, Cao X (2011) Enhanced Lead Sorption by Biochar Derived from Anaerobically Digested Sugarcane Bagasse. Separ Sci Technol, 46(12):1950-1956

Karami N, Clemente R, Moreno-Jiménez E, Lepp NW, Beesley L (2011) Efficiency of green waste compost and biochar soil amendments for reducing lead and copper mobility and uptake to ryegrass. J Hazard Mater 19: 41–48

Kimmich R, Anoardo E (2004) Field-cycling NMR relaxometry. Prog Nucl Magn Reson Spectrosc 44:257–320

Kobya M, Demirbas E, Senturk E, Ince M (2005) Adsorption of heavy metal ions from aqueous solutions by activated carbon prepared from apricot stone. Bioresource Technol 96:1518–1521

Knicker H (2011) Pyrogenic organic matter in soil: its origin and occurrence, its chemistry and survival in soil environments. Quat Int 243(2):251–263

Krull ES, Baldock JA, Skjemstad JO, Smernik RJ (2009) Characteristics of biochar: Organo-chemical properties. In: Lehmann J, Joseph S (eds) Biochar for Environmental Management, Science and Technology, London: Earthscan

Kumpiene J, Lagerkvist A, Maurice C (2008) Stabilization of As, Cr, Cu, Pb and Zn in soil using amendments–A review, Waste Manage 28:215–225

Langmuir I (1918) The adsorption of gases on plane surfaces of glass, mica and platinum, J Am Chem Soc 40:1361–1403

Lee Y, Park J, Ryu C, Gang KS, Yang W, Park YK, Jung J, Hyun S (2013) Comparison of biochar properties from biomass residues produced by slow pyrolysis at 500°C. Bioresource Technol 148:196–201

LeGeros RZ, Legeros JP (1984) Phosphate minerals in human tissues. In: Nriagu JO, Moore PB (eds), Phosphate Minerals. Springer, Berlin, 351-385

Lehmann J (2007) Bio-energy in the black. Front Ecol Environ 5:381–387

Lima IM, Marshall WE (2005) Granular activated carbons from broiler manure: physical, chemical and adsorptive properties. Bioresource Technol 96:699–706

Lu C, Liu C (2006) Removal of nickel (II) from aqueous solution by carbon nanotubes, J Chem Technol Biotechnol 81:1932–1940

Machida M, Yamazaki R, Aikawa M, Tatsumoto H (2005) Role of minerals in carbonaceous adsorbents for removal of Pb(II) ions from aqueous solution. Sep Purif Technol 46:88–94

Machida M, Mochimaru T, Tatsumoto H (2006) Lead(II) adsorption onto the graphene layer of carbonaceous materials in aqueous solution. Carbon 44:2681–2688

Malkoc E (2006) Ni(II) removal from aqueous solutions using cone biomass of *Thuja orientalis*. J Hazard Mater 137:899–908

McBeath AV, Smernik RJ (2009) Variation in the degree of aromatic condensation of chars. Org Geochem 40:1161–1168

Mobasherpour I, Salahi E, Pazouki M (2011) Comparative of the removal of Pb^{2+}, Cd^{2+} and Ni^{2+} by nano crystallite hydroxyapatite from aqueous solutions: Adsorption isotherm study. Arab J Chem
doi:10.1016/j.arabjc.2010.12.022

Montes-Moràn MA, Suàrez D, Menéndez JA, Fuente E (2004) On the nature of basic sites on carbon surfaces: An overview. Carbon 42:1219–1225

Namgay T, Singh B, Singh BP (2010) Influence of biochar application to soil on the availability of As, Cd, Cu, Pb, and Zn to maize (*Zea mays* L.). Aust J Soil Res 48:638-647

Olsen SR, Cole CV, Watanabe FS, Dean LA (1954) Estimation of Available Phosphorus in Soils by Extraction with Sodium Bicarbonate. U.S. Department of Agriculture Circular No. 939. Banderis, A. D., D. H. Barter and K. Anderson. Agricultural and Advisor

Pan X, Wang J, Zhang D (2009) Sorption of cobalt to bone char: Kinetics, competitive sorption and mechanism. Desalination 249:609–614

Park D, Yun YS, Lim SR, Park JM (2006) Kinetic analysis and mathematical modeling of Cr(VI) removal in a differential reactor packed with ecklonia biomass. J Microbiol Biotechnol 16:1720–1727

Pohlmeier A, Haber-Pohlmeier S, Stapf S (2009) A fast field cycling nuclear magnetic resonance relaxometry study of natural soils. Vadose Zone J 8:735-742

Proctor A, Toro-Vazquez JF (1996) The Freundlich isotherm in studying adsorption in oil processing. J Am Oil Chem Soc 73:1627–1633

Randall JM, Hautala E, Waiss Jr AC (1974) Removal and recycling of heavy metal ions from mining and industrial waste streams with agricultutral by-products. In: Proceedings of the Fourth Mineral Waste Utilization Symposium. Chicago.

Redlich O, Peterson DL (1959) A useful adsorption isotherm. J Phys Chem 63:1024–1026

Rao M, Parwate AV, Bhole AG (2002) Removal of Cr^{6+} and Ni^{2+} from aqueous solution using bagasse and fly ash. Waste Manage 22:821–830

Salt DE, Blaylock M, Kumar NPBA, Dushenkov V, Ensley BD, Chet I, Raskin I (1995) Phytoremediation: a novel strategy for the removal of toxic metals from the environment using plants. Biotechnol13:468–474

Schmidt IK, Williams DL, Tietema A, Gundersen P, Beier C, Emmett BA, Estiarte M (2004) Soil solution chemistry and element fluxes in three European heathlands and their responses to warming and drought. Ecosystems 7:638-649

Schure MR, Soltys PA, Natusch DFS, Mauney T (1985) Surface area and porosity of coal fly ash. Environ Sci Technol 19:82–86

Seco A, Marzal P, Gabaldon C, Ferrer J (1997) Adsorption of Heavy Metals from Aqueous Solutions onto Activated Carbon in Single Cu and Ni Systems and in Binary Cu-Ni, Cu-Cd and Cu-Zn Systems. J Chem Technol Biotechnol 68:23-30

Seredych M, Hulicova-Jorcakova D, Lu GQ, Bandosz TJ (2008) Surface functional groups of carbons and the effects of their chemical character, density and accessibility to ions on electrochemical performance. Carbon 46: 1475-1488

Sharma DC, Forster CF (1993) Removal of hexavalent chromium using sphagnum moss peat. Water Research 27(7):1201–1208

Shinogi Y, Kanri Y (2003) Pyrolysis of plant, animal and human waste: physical and chemical characterization of the pyrolytic products. Bioresource Technol, 90(3):241-247

Sohi SP, Krull E, Lopez-Capel E, Bol R (2010) A review of biochar and its use and function in soil. Adv Agron 105:47-82

Stöhr B, Boehm HP, Schlögl R (1991) Enhancement of the catalytic activity of activated carbons in oxidation reactions by thermal treatment with ammonia or hydrogen cyanide and observation of a superoxide species as a possible intermediate. Carbon 29:707-720

Sud D, Mahajan G, Kaur MP (2008) Agricultural waste material as potential adsorbent for sequestering heavy metal ions from aqueous solutions – A review. Bioresource Technol 99:6017–6027

Suen SY (1996) A comparison of isotherm and kinetic models for binary-solute adsorption to affinity membranes. J Chem Technol Biotechnol, 65:249–257

Taiz L, Zeiger E (2002) Fisiologia Vegetale. Piccin eds.

Tchobanoglous G, Burton FL (1991) Wastewater Engineering: Treatment, Disposal and Reuse. 3rd ed. New York, Metcalf and Eddy, McGraw-Hill, 11:740–741

Terzyk AP (2003) Further insights into the role of carbon surface functionalities in the mechanism of phenol adsorption. J Colloid Interf Sci 268:301–329

Toth J (2002) Adsorption. Theory, Modelling, and Analysis, Dekker, New York

Treybal RE (1981) Mass-Transfer Operations, 3rd ed. McGraw-Hill, Tokyo.

Uchimiya M, Lima IM, Klasson KT, Chang S, Wartelle LH, Rodgers JE (2010) Immobilization of Heavy Metal Ions (CuII, CdII, NiII, and PbII) by Broiler Litter-Derived Biochars in Water and Soil. J Agric Food Chem 58:5538–5544

Uchimiya M, Wartelle LH, Klasson KT, Fortier CA, Lima IM (2011) Influence of pyrolysis temperature on biochar property and function as a heavy metal sorbent in soil. J Agr Food Chem 59:2501–2510

Uras Ű (2011) Biochar from vacuum pyrolysis of agricultural residues : characterisation and its applications. Thesis. Master of science in chemical engineering – University of Stellenbosch.

Vassilev SV, Baxter D, Andersen LK, Vassileva CG (2010) An overview of the chemical composition of biomass. Fuel 89(5):913–933

Volesky B, Holan ZR (1995) Review: biosorption of heavy metals. Biotechnol Progr 11:235–250

Yadav S, Tyagi DK, Yadav OP (2011) Equilibrium and kinetic studies on adsorption of aniline blue from aqueous solution onto rice husk carbon. Int J Chem Res 2(3):59-64

CHAPTER 6 : GENERAL CONCLUSIONS

Biochar production processes as well as its various applications can provide numerous benefits to both environment and economy. However, biochar characteristics and properties are greatly affected by the original feedstock, the pyrolysis process and its parameters (mainly process temperature and residence time). These factors are particularly important in determining the nature of the final product and, consequently, its potential value in terms of carbon sequestration, agronomic performance and/or environmental remediation.

The understanding of the physicochemical properties of this valuable product, and how these vary depending on pyrolysis conditions, is of paramount importance in order to address biochars of different nature to more focused and aware uses. Only in this way, it would be possible to obtain the aforementioned benefits and to avoid environmental damages.

The aim of this work was twofold.

The first part focused on the changes occurring in the chemical properties and in the physical structure of biochar produced from poultry manure when it is obtained at different pyrolysis temperatures and heating times, and how these changes can influence char agronomic or remediation potential.

CPMAS ^{13}C NMR characterization and thermal investigation of poultry manure and its char derivatives obtained at 350, 450 and 600°C for charring times of 30, 60, 90 and 120 minutes were performed.

All the results revealed that char chemical nature is affected more by production temperature than by production time. Indeed, poultry manure char composition at each temperature remained more or less unchanged as heating time was gradually switched from 30 to 120 min.

The chars obtained at 350 and 450°C contained both aromatic and alkyl domains whereas only aromatic systems were present after charring at 600°C. Unexpectedly, the aromatic domains in the latter char revealed a lower thermal stability as compared to the former two. In fact, whereas aromatics in 350 and 450°C PM chars degraded at 460°C, those in the 600°C PM char were destroyed at a lower temperature (414°C). This result was explained by hypothesizing that the alkyl domains in chars produced at 350 and 450°C were mainly displaced on the surface of a rigid aromatic core. For this reason, the thermal destruction of the original aromatic core was retrieved only after the complete degradation of the products developed from the original alkyl systems. Alkyl removal by poultry manure charring at 600°C left unprotected the aromatic domain, thereby allowing the thermal degradation of the aromatic systems at a lower temperature than that measured for PM chars produced at the two lowest temperatures (350 and 450°C).

Fast field cycling-NMR relaxometry investigation was performed to examine the physical features of biochar samples produced at different pyrolysis conditions and how these characteristics affect biochar interaction with water. As aforementioned, chemical analysis such as elemental and metal content, CPMAS ^{13}C NMR spectrometry and thermogravimetry (TGA) revealed that char chemical nature is affected more by production temperature than by production time. Conversely, the differences in char physical properties were found to be produced both by pyrolysis temperature and residence time. In particular, residence time has a major effect at the lowest charring temperature used (350°C). Vice versa, above 450°C, the pyrolysis temperature has a major influence in char structuring.

NMR results suggest a reduction of biochar affinity for water as pyrolysis temperature or charring time increases. This reduction was explained by: 1) the loss of acidic functional groups on poultry manure char surface (e.g.,

phenolic, lactone and carboxylic group) able to interact with water protons, 2) the increase in char hydrophobicity (due to their reduced organic matter content) and 3) the increase in biochar pores size with charring temperature or muffle residence time.

All the results considered, the last explanation resulted to be the most reliable and convincing since the loss of strong interaction between water and biochar surface most likely depends on an increase in the pores size with pyrolysis temperature.

The combination of ^{1}H-T_1 and T_2 NMR relaxometry provided more informations on the nature of the surface of porous media with respect to the analytical techniques used previously. The combination of several techniques provided good basis for the comprehension of complex systems making it essential for the complete characterization of the char as a porous medium.

The second part of the study investigated the potential of three different kinds of biochars, produced from poultry manure (pyrolyzed at 500°C for 120min), conifer and poplar wood residues (gasified up to 1200°C), as adsorbents for inorganic contaminants for wastewater treatment.

Each char was first characterized by CPMAS ^{13}C NMR and FFC NMR Relaxometry and then applied in heavy metals remediation (Cu, Ni and Pb) from aqueous solutions.

Notwithstanding the different nature of the biomasses and the process parameters used for biochar production, CPMAS ^{13}C NMR spectroscopy revealed a substantial structural similarity among the chars. Indeed, all the biochar examined resulted composed mainly by aromatic moieties. However, their physicochemical characterization revealed some differences: a higher amount of nitrogen, phosphate and minerals, but a lower surface area, in manure- than in wood-chars.

The differences in the physical structure and chemical composition of the examined biochars determined the occurrence of different char surface-water interactions, as encountered by applying FFC NMR relaxometry on water-saturated chars. In particular, poplar char surface interacted with water with high efficiency due to its porous structure, rich in small-sized pores. Conversely, large pore sizes appeared to be representative of conifer char and determined the presence of weak interactions with water.

Chicken manure char-water interactions were determined more by char chemical composition rather than physical restrictions. In fact, the presence of specific surface groups (i.e., nitrogen compounds, phosphate and minerals) confer to chicken manure biochar positive properties, for example enhancing its water retention capacity.

Adsorption studies results showed that biochar metal sorption from aqueous solutions occurs through a two-step mechanism involving an initial rapid uptake phase followed by the achievement of equilibrium after 24 hours.

Biochar sorption capacity strongly depended on the metal ion type, showing the following trend for greater removal from solution: Ni<Cu<Pb. This order was explained by the higher electronegativity of lead compared to copper and nickel ions, that favors electrostatic and inner sphere surface complexation reactions.

The sorption of each metal by conifer char was negligible due to its surface physicochemical characteristics, i.e. hydrophobicity, prevalence of macropores and lack of functional groups able to bind ions. Conversely, despite its lower surface area, chicken manure biochar was the most effective in removing metal ions from water since it uptaked five times more nickel (102 vs. 22 mg g^{-1}), the double of copper (181 vs. 94 mg g^{-1}) and three times more lead (633 vs. 203 mg g^{-1}) than poplar char.

Chicken manure highest remediation potential was related to the presence of a higher amount of specific surface functional groups, such as basic nitrogen

groups (e.g., pyridine), phosphate and minerals (such as ash and metal oxides) that serve as adsorption sites for heavy metal cations.

Copper adsorption data on both chicken manure and poplar char surface were better fitted by Toth isotherm. The evaluation of Toth parameters revealed that copper adsorption on poplar surface is heterogeneous. Since poplar char has a high affinity for water, water adsorption on active sites could effectively block some micropores and interfere with cations adsorption (solvent effect). Besides on chicken manure char, the interactions between adsorbed ions prevail over the surface adsorptive potential. This leads to the formation of alternating layers Cu(II)-H_2O-Cu(II) on char surface, explaining the highest adsorption potential of chicken manure char compared to poplar one.

Freundlich model well describes Ni(II) uptake for both adsorbents indicating a non-ideal sorption of this metal on heterogeneous surfaces as well as a multilayer sorption. Contrariwise, considering the magnitude of both R^2 and χ^2 values, none of the equations applied appears to produce a reasonable model for sorption of lead in all the systems.

Since metals absorption by biochars involves both physical and chemical mechanisms, further studies should be addressed to explain it.

Resuming, different chars have different physicochemical characteristics so they should be addressed to different uses. For example, conifer char should not be used for remediation since it is not effective in removing inorganic metals from aqueous solutions. Conversely, chicken manure-derived biochar has the potential to be an effective heavy metal adsorbent for application in environmental remediation, probably due to the presence of specific functional groups on its surface able to interact with cations. Finally, thanks to its great microporous structure, poplar char could effectively enhance soil water and nutrients retention. Thus, its application to soils may lead to important agronomic benefits.

All the results obtained in this work appear promising and should be followed in a near future by further studies on the effect of pyrolysis conditions on the physicochemical properties of biochar from various feedstock. The understanding of these effects will allow the selection of the appropriate combination of original biomass and process temperature in order to produce a 'designed' biochar for specific environmental/agricultural applications.

Moreover, further investigations on adsorption equilibrium, kinetics and thermodynamics are required to optimize biochar remediation potential, and desorption studies are needed in order to avoid negative environmental effects.

Overall, turning abundant agricultural waste products (e.g., crop residues, animal manure) into materials that can absorb contaminants or enhance soil properties can have environmental implications for improving waste management and protecting the environment.